2010-12-01

High Flow Air Sampling for Field Detection Using Gas Chromatography-Mass Spectrometry

Jacolin Ann Murray
Brigham Young University - Provo

High Flow Air Sampling for Field Detection Using

Gas Chromatography-Mass Spectrometry

Jacolin Ann Murray

A dissertation submitted to the faculty of
Brigham Young University
in partial fulfillment of the requirements for the degree of

Doctor of Philosophy

Milton L. Lee
David V. Dearden
Steven R. Goates
Delbert J. Eatough
H. Dennis Tolley

Department of Chemistry and Biochemistry

Brigham Young University

April 2011

ABSTRACT

High Flow Air Sampling for Field Detection Using

Gas Chromatography-Mass Spectrometry

Jacolin Ann Murray

Department of Chemistry and Biochemistry

Doctor of Philosophy

The ability to rapidly detect and identify hazardous analytes in the field has become increasingly important. One of the most important analytical detection methods in the field is gas chromatography-mass spectrometry (GC-MS). In this work, a hand-portable GC-MS system is described that contains a miniature toroidal ion trap mass analyzer and a low thermal mass GC. The system is self-contained within the dimensions of 47 x 36 x 18 cm and weighs less than 13 kg. Because the instrument has a small footprint, it was used as the detector for an automated near-real-time permeation testing system. In permeation testing, materials that are used to make individual protective equipment such as gloves, masks, boots, and suits are exposed to hazardous analytes to determine how long the equipment can be worn safely. The system described herein could test five samples simultaneously. A multi-position valve rotated among the various sample streams and delivered time aliquots into the MS for quantitation. Current field air sampling techniques suffer from long desorption times, high pressure drops, artifact formation and water retention. These disadvantages can be avoided by concentrating the analytes in short open tubular traps containing thick films. There are several advantages to using polymer coated capillaries as traps, including fast desorption, inertness and low flow restriction. An air sampling trap was constructed utilizing open tubular traps for the concentration of semi-volatile organic compounds. The system consisted of multiple capillary traps bundled together, providing high sample flow rates. The analytes were desorbed from the multi-capillary bundle and refocused in a secondary trap. The simultaneous focusing and separation effect of a trap subjected to a negative temperature gradient was also explored. In this configuration, analytes were focused because the front of the peak was at a lower temperature than the rear of the peak and, hence, moved slower. In addition to the focusing effect, analytes with different volatilities focused at different temperatures within the gradient, allowing for separation.

Keywords: gas chromatography-mass spectrometry, toroidal ion trap, permeation testing, air sampling, open tubular traps, multi-capillary trap, negative temperature gradient, toxic industrial chemicals, chemical warfare agents

Table of Contents

List of Abbreviations viii

List of Symbols xi

1 Introduction 1

1.1 Portable GC-MS 2

1.1.1 Vehicle-portable GC-MS systems 2

1.1.2 Man-portable GC-MS systems 4

1.2 Air Sampling Techniques 6

1.2.1 Concentration by adsorption 9

1.2.2 Concentration by absorption 20

1.2.3 Open tubular traps 23

1.2.4 Denuders 27

1.2.5 Microtraps 28

1.2.6 Equilibrium sorption 29

1.2.7 Solid phase microextraction 30

1.2.8 Cold trapping 33

1.2.9 Sorbent cold trapping 35

1.2.10 On-line sampling techniques 35

1.2.11 Sample flow rate considerations 36

1.3 Considerations When Coupling Concentration Techniques to Capillary GC 36

1.4 Dissertation Overview 38

1.5 References 39

2 Hand-portable Gas Chromatograph-Toroidal Ion Trap Mass Spectrometer (GC-TMS) for Detection of Hazardous Compounds in Harsh Environments 48
2.1 Introduction 48
2.2 Experimental 51
2.2.1 GC-TMS instrumentation 51
2.2.2 Mass analyzer 54
2.2.3 Vacuum system 55
2.2.4 Low thermal mass GC 55
2.2.5 SPME and SPME holder 57
2.2.6 Low thermal mass injector 59
2.2.7 Data analysis 59
2.2.8 Chemicals and standards 60
2.2.9 Sampling methodology 60
2.3 Results and Discussion 60
2.3.1 Mass calibration 60
2.3.2 Mass spectral resolution 61
2.3.3 Detection limits 62
2.3.4 Analysis of chemical warfare agents 64
2.3.5 Analysis of EPA Method 624 volatile halocarbon compounds 64
2.4 Conclusions 66
2.5 Acknowledgement 67
2.6 References 67
3 System for Testing Near-Real-Time Chemical Permeation Rates Through Materials 72

3.1 Introduction 72
3.2 Experimental Section 77
3.2.1 Near-real-time permeation test system 77
3.2.2 Swatch test cell fixture 77
3.2.3 Switching valves and temperature controlled transfer line manifold 78
3.2.4 Toroidal ion trap mass spectrometer 79
3.2.5 Calibration system 80
3.2.6 System software 80
3.2.7 Materials 81
3.2.8 Test procedure 81
3.3 Results and Discussion 82
3.3.1 Calibration 82
3.3.2 Test cell fixture 83
3.3.3 Permeation curves 85
3.4 Conclusions 92
3.5 Acknowledgments 93
3.6 References 93
4 Trapping at High Flows Using Multi-Capillary Open Tubular Traps 95
4.1 Introduction 95
4.2 Experimental 96
4.2.1 Preparation of sol-gel coated capillary traps 96
4.2.2 Preparation of polymer-coated capillary traps 97
4.2.3 Commercially available coated capillary traps 98

4.2.4 Determination of breakthrough times by frontal chromatography 99
4.2.5 Characterization of open tubular traps by elution chromatography..... 101
4.2.6 Preparation of multi-capillary bundle 101
4.2.7 Secondary traps 102
4.2.8 2-Trap system..... 104
4.3 Results and Discussion 108
4.3.1 Trap characterization methods 108
4.3.2 Sorbents in open tubular traps..... 110
4.3.3 Multi-capillary open tubular traps 125
4.3.4 Secondary traps 127
4.3.5 High flow rate sampling and focusing 131
4.4 Conclusions 134
4.5 References 135
5 Simultaneous Sampling, Focusing and Separation of a Continuous Sample of Semi-Volatile Organic Compounds in a Negative Temperature Gradient..... 138
5.1 Introduction..... 138
5.2 Experimental Section 139
5.2.1 Construction of thermal gradient devices 139
5.2.2 Preparation of sol-gel columns/traps 142
5.2.3 Sample introduction 143
5.2.4 Analytical equipment 144
5.3 Results and Discussion 144
5.4 Conclusions 151

5.5 References 152
6 Conclusions and Suggested Work 153
6.1 Conclusions 153
6.2 Suggested Work 155
6.2.1 Swatch permeation testing 155
6.2.2 Water sorption in open tubular traps 156
6.2.3 Multi-phase open tubular traps 157
6.2.4 Interfacing high flow open tubular air sampling to portable GC-MS 158
6.2.5 On-line sampling using a negative temperature gradient 160
6.3 References 162

List of Abbreviations

ASTM	American Society for Testing and Materials
C10	Decane
C11	Undecane
C12	Dodecane
C13	Tridecane
C14	Tetradecane
CBMS	Chemical biological mass spectrometer
CWA	Chemical warfare agent
DEP	Diethyl Phthalate
DMMP	Dimethyl methylphosphonate
FID	Flame ionization detector
FPD	Flame photometric detector
FTICR	Fourier transform ion cyclotron resonance
GB	Sarin
GC	Gas chromatography
GD	Soman
GF	Cyclosarin
GC-MS	Gas chromatography-mass spectrometry
GUI	Graphical user interface
FWHM	Full-width half-maximum
HD	Sulfur mustard

i.d.	Internal diameter
IDLH	Immediate danger to life and health
IMS	Ion mobility spectrometry
IPE	Individual protective equipment
IR	Infrared spectroscopy
LCD	Liquid crystal display
MES	Methyl salicylate
MINICAMS	Miniature continuous air monitoring system
MS	Mass spectrometry
NFPA	National Fire Protection Association
PDMS	Polydimethylsiloxane
PDMS-DVB	Polydimethylsiloxane-divinylbenzene
PEG	Poly(ethylene glycol)
PID	Photoionization detector
PLOT	Porous layer open tubular
PTFE	Polytetrafluoroethylene
RF	Radio frequency
RTD	Resistive thermal device
SAW	Surface acoustic wave
SEM	Scanning electron microscopy
Semi-VOC	Semi-volatile organic compounds
SPME	Solid phase microextraction
TCD	Thermal conductivity detector

TEP	Triethyl Phosphate
TICs	Toxic industrial compounds
TMS	Toroidal ion trap mass spectrometer
TOF	Time-of-flight
TWA	Time weighed average
VOC	Volatile organic compounds

List of Symbols

a	Internal diameter
b	Amplitude of wave
b_0	Amplitude of wave at time 0
C	Concentration
C_0	Inlet concentration
C_M	Concentration in the mobile phase
C_S	Concentration in the stationary phase
D	Diffusion coefficient
D_{AB}	Diffusion coefficient of analyte A in gas B
d_f	Film thickness
k	Capacity factor
K	Partition (distribution) coefficient
K_{fs}	SPME fiber coating/sample matrix distribution coefficient
K_V	Rate constant
L	Length of trap
M_A	Molecular mass of analyte A
M_B	Molecular mass of analyte B
m_{sorbed}	Mass sorbed in a trap
N	Number of theoretical plates
n	Number of moles
P	Pressure

Q	Flow rate
r	Internal radius of trap
SD	Standard deviation
t	Time
t_R	Retention time
T	Temperature
t_B	Breakthrough time
u	Average linear velocity
V_0	Dead volume
V_b	Breakthrough volume
V_f	SPME fiber coating volume
V_R	Retention volume
V_s	Volume of sample
V_{sp}	Volume of the stationary phase
w	Peak width
W	Weight (of sorbent)
W_e	Adsorption capacity of a trap
β	Phase ratio
γ	Surface tension
η	Viscosity
ρ_b	Bulk density
Σv_A	Sum of atomic volume increments for analyte A
Σv_B	Sum of atomic volume increments for analyte

1 Introduction

Recent technology has enabled the development of miniaturized analytical detection equipment, permitting analysis and detection in the field. There are several applications that find portable instrumentation and, particularly, portable gas chromatography-mass spectrometry (GC-MS) useful, which can include emergency response, forensics, environmental, and process control applications.[1-2] In many of these applications, it is beneficial that analysis takes place immediately in the field. For example, in forensics applications, investigators may be overwhelmed with potential evidence and unsure of what types of samples to collect. However, with field detection equipment, investigators can quickly determine potential threats and more confidently collect samples.[3] It is also useful to quickly identify unknown contaminants in order to treat those who may have been exposed in a timely manner and to facilitate cleanup while protecting emergency personnel. For environmental applications, several analyses can be performed to identify what and when analytes were present to determine when certain events took place.[3] Field detection can increase sample throughput and decrease the cost per analysis for many process control applications.[4]

While there are several types of portable detectors available for field detection, GC-MS remains one of the most important tools available. MS alone can be used to identify unknown compounds from their characteristic fragmentation patterns; however, for complex mixtures, compound identification by MS alone can be challenging. MS coupled with a separation technique such as GC can provide two-dimensional analysis, which provides significantly greater power for identification of compounds in complex mixtures. Because of the power of GC-MS, the technique is frequently used for positive identification of unknown volatile and semi-volatile

organic compounds. It is the approved method for the identification of chemical warfare agents in the field.[5]

One of the most important applications for field detection is the determination of volatile organic compounds (VOCs) and semi-volatile organic compounds (semi-VOCs) in the air. These analytes can be inhaled, which can pose an immediate health danger. Thus, it is important to quickly detect trace levels of hazardous compounds such as toxic industrial chemicals (TICs), including phosgene and cyanogen chloride, and chemical warfare agents, such as sarin, soman, mustard and VX. Because these target analytes are toxic at trace levels, collection and concentration methods are necessary for field detection. Furthermore, all of these methods must be fast, easy to perform, reliable, and compatible with personal protective equipment.

1.1 Portable GC-MS

Portable GC-MS systems can be classified as either vehicle-portable or man-portable. Vehicle-portable GC-MS systems can be transported in land vehicles, planes, helicopters, and boats, and are typically used in portable laboratories. Man-portable GC-MS systems can be carried and used by one individual and can be used directly in the field where samples are collected.

1.1.1 Vehicle-portable GC-MS systems

Developments of small benchtop GC-MS instruments in the 1970's led way to the development of vehicle-portable instrumentation.[6] Many researchers used current technology available in these benchtop instruments and adapted them to the field. Typically, these instruments are used in fixed mobile laboratories and, after initial transport of the equipment and

startup, they are not usually moved until analysis is completed. As long as there is a stable power source available, little modifications are required to the original benchtop instrumentation.

Various vehicle-portable GC-MS systems have been commercialized, most of which contain quadrupole mass analyzers.[1, 4] One such system was introduced in 1993 and has dimensions of 55 x 45 x 35 cm and weighs 45 kg. The instrument uses electron ionization and covers a mass range of 1-640 daltons.[4] GC modules can be equipped with a wide range of columns and sample introduction systems including liquid injection, thermal desorption, and purge and trap.[4] Another similar vehicle-portable GC-MS system has dimensions of 35 x 53 x 83 cm and weighs 60 kg. It has both electron impact and chemical ionization capability, and has a mass range of 1-640 Daltons with 1 Dalton resolution.[4] It uses an oven-based GC to allow for temperature programming and several different sample introduction methods, including liquid injection through a split/splitless injector, thermal desorption, direct air sampling (without GC), air sampling by sorbent trapping, and purge-and-trap.[4] Both of these instruments have been used in many applications, including analysis of dangerous analytes and VOCs in air, water, and soil samples, and also in identification of hazardous chemicals from clandestine labs.[2, 4, 7]

Some vehicle-portable instruments have been classified as roving GC-MS systems, with which several samples can be taken rapidly for mapping chemical trends.[6] McClennen et al. described a system for which a commercially available MS was placed in the bed of a battery-powered truck (to avoid car exhaust contamination) to construct detailed VOC gradients through a large area, which sampling methods based on averaging cannot accomplish.[8] Analysis speeds of approximately 1 sample/s were achieved with the system.

There have also been a few vehicle-portable MS systems designed specifically for battlefield detection of chemical and biological agents. The first system used to detect chemical

agents in the field was introduced in the 1980's.[9] This system was designed to detect persistent chemical agents on the ground. The MS contained a quadrupole mass analyzer with electron ionization. The weight of the mass spectrometer was 177 kg. The system was placed inside a vehicle, and the ground was sampled using a double wheel sampling system that consisted of two silicone sampling wheels. One wheel sampled the ground for approximately 20 s as the vehicle moved while the other wheel was being analyzed. After sampling, the wheel was introduced to a heated probe that was extruded from the vehicle to where the analytes were desorbed from the wheel and introduced into the MS system through a membrane transfer line.[9] A MS that could detect both chemical and biological agents was developed that was based on an ion trap mass analyzer with electron ionization.[9] The system, which weighed 117 kg used fatty acids and other biomarkers to detect bacterial threats. The instrument was comprised of 3 modules: biosampler module, sample introduction module and mass spectrometer module. The biosampler module consisted of an impactor and particle concentrator and was only used for sampling biological agents. The sample introduction module contained switching valves that allowed samples to be introduced into the biosampler module for sampling biological agents, through a heated transfer line for sampling chemical agents, and through a transfer line from a double wheel sampling system to measure persistent chemical agents on the ground.[9]

1.1.2 Man-portable GC-MS systems

Although vehicle portable instruments allow for sampling in the field, man-portable instruments are still needed for situations where vehicle-portable instruments are not accessible. In these cases, a GC-MS system that can be carried and operated by one man is desirable. There have been a number of reports on miniaturization of mass analyzers. These include miniaturization of time-of-flight (TOF),[10-11] quadrupoles,[12] magnetic sector,[13-14] Fourier

transform ion cyclotron resonance (FTICR),[15] and cylindrical,[16-18] rectilinear, [19-21] and toroidal [22-24] ion traps. There have also been advancements in the miniaturization of GC.[25-29] Although these reports focus on miniaturization of key components, there are relatively few reports on miniaturization of all components (GC, mass analyzer, vacuum system, electronics, carrier supply, etc.) for the development of a truly man-portable GC-MS system. Despite this fact, there are systems that are commercially available.[30-34]

A widely used man-portable GC-MS system has been described in detail by Smith et al. for detection of chemical agents.[35] The overall system has dimensions of 46 x 43 x 18 cm and weighs 16 kg with battery. It contains a quadrupole MS detector with electron ionization, and provides a mass range of 1-300 Daltons. The system contains a resistively heated, low thermal mass analytical column that is capable of performing column temperature ramps up to 30°C/min. An air sample is loaded inside a sample loop by an internal sampling pump. Analytes can also be concentrated on sorbent material to improve detection. The power consumption is 30 W using a 24 V battery, and GC-MS analysis times are around 15 min. Smith et al. compared the performance of this man-portable system to that of a vehicle-portable system and determined that the vehicle-portable instrument provided faster analysis times and greater variety in sample introduction methods.[35]

In 2001, Diaz et al. described a portable double-focusing sector MS for gas analysis and monitoring applications. The design of the system was compact because of the superimposed magnetic field that was placed perpendicular to the electric field, limiting the need for using separate electric and magnetic sectors in tandem, as in many laboratory double-focusing systems. This instrument uses a 1.1 Tesla NdFeB permanent magnet and a lithographically defined electric sector. The system weighs a total of 18 lbs and has a mass range of 200 Daltons. The

system does not have a GC. It has been used to monitor volcanic gas emissions and leaks in the fuel systems of space shuttles.[13]

Gao et al. introduced a miniature rectilinear ion trap system, which provides a simple geometry, but offers high trapping capacity. [19] The analyzer has unit mass resolution with a mass range of 500 Daltons. The entire system has dimensions of 32 x 22 x 19 cm and weighs 10 kg including batteries. The maximum power of the system is less than 70 W. A membrane inlet is typically used for sample introduction; however, in one report, 9 TICs were concentrated using a sorption trap.[36] The device does not contain a GC, however, it does have tandem MS capability. Applications with this instrument include continuous monitoring of air and solution samples.

Geear et al. introduced a method using microelectromechanical systems to construct quadrupole mass spectrometers containing quadrupole rods of 500 μm in diameter and 30 mm in length that could provide unit mass resolution and high mass range (400 Daltons).[12] This technology led to a commercialized portable GC-MS system with dimensions of 38 x 27 x 18 cm, weighing 14 kg. Sample introduction methods for this system include solid phase microextraction (SPME), syringe, and membrane inlet.[37]

1.2 Air Sampling Techniques

Traditional air sampling methods for VOCs and semi-VOCs consist of either whole air sampling or preconcentration techniques. Whole air sampling consists of collecting a volume of air in a container. The most common devices for the collection of whole air samples are polymer bags (i.e., Tedlar and Teflon) and stainless steel canisters.[38-41] Advantages of collecting whole air samples are that multiple analyses can be performed with one sample, there is no concern with sample breakthrough, and there is less of a concern for trapping moisture compared to

preconcentration techniques.[40-43] Disadvantages to whole air sampling include meeting the stringent requirements for container cleanliness and surface passivation, handling bulky sampling equipment in the field, shipping containers to the laboratory where they must be stored properly before analysis, and accepting lower sensitivity compared to preconcentration techniques.[40-41, 43]

Preconcentration sampling techniques allow for sampling of large volumes of air while concentrating analytes. The most common preconcentration techniques are cryotraps and sorbent traps. Analytes are concentrated either by freezing at cryogenic temperatures (cryotraps) or by sorption in packing materials (solid sorbent traps). Desorption of analytes is accomplished for both approaches by quickly heating the trap. Desorption in solid sorbent traps can also be accomplished by solvent extraction. Preconcentration sampling techniques allow for a larger volume of gas to be sampled compared to whole air sampling, which permits detection of trace analytes.[44] Disadvantages of preconcentration techniques include complications from trapping water, the possibility of sample breakthrough, and possible production of artifacts when sorbents are used.[40, 43] Cryotraps have an advantage over sorbents in that lower desorption temperatures can be used compared to sorbent traps, which could be important for analysis of labile compounds and elimination of artifact formation. However, methods to generate cold temperatures are required, which may be difficult to implement in the field.

Preconcentration sampling techniques can be utilized in either the active (dynamic) or passive (diffusion) mode. In the active mode, air is forced through the collection medium usually with a pump, whereas in the diffusion mode, analytes are allowed to freely migrate into the collection medium by diffusion. Diffusion samplers include diffusion through a diffusion barrier or permeation through a membrane.[40, 45-46] Active sampling allows for grab sampling (i.e.,

obtaining a sample over a short time period), which is generally used to monitor changes in concentrations of analytes in the air. Passive sampling usually provides averaging over a long sampling time, since it involves a low air flow through the collection device. Thus, the mode of sampling depends on the application.

Since the main objective of the work reported in this dissertation was to develop methods for rapidly concentrating trace analytes from air or gas streams, the following discussion is focused on dynamic concentration techniques that are amendable to the field. Figure 1.1 classifies the types of dynamic concentration methods, which can be operated in either exhaustive or equilibrium modes. Ideally, in exhaustive sampling, all of the analytes are trapped and concentrated; there is no sample breakthrough. To characterize traps for exhaustive sampling, often the breakthrough time and/or the breakthrough volume is reported. The breakthrough time (or volume) is defined in the literature as the time (or volume) when 1-5% of the original concentration in the gas (e.g., air) breaks through the trap.[47] It is the breakthrough time that determines the maximum length of time or volume that can be sampled with the trap. The safe sampling time or volume is usually reported in the literature to be 2/3 of the breakthrough time or volume, which ensures that there can be no sample breakthrough.[48] Most air sampling applications prefer exhaustive sampling. In equilibrium sampling, the sample is introduced into the trap until each analyte is in equilibrium with the sorbent trapping material. Unlike exhaustive sampling, not all analyte is trapped. The concentration, however, can be determined by the amount of analyte that is trapped. A more detailed discussion of equilibrium trapping is given later. Both equilibrium and exhaustive sampling can be performed during sorbent trapping; however, when cryogens are used, only exhaustive sampling is performed.

Analytes can be trapped in sorbents by two mechanisms, adsorption or absorption. Adsorption occurs when analytes are trapped on the surface of the adsorbent. In absorption, analytes partition into a polymer material. The term "sorbent" is used as a general term in this dissertation for both adsorption and absorption mechanisms.

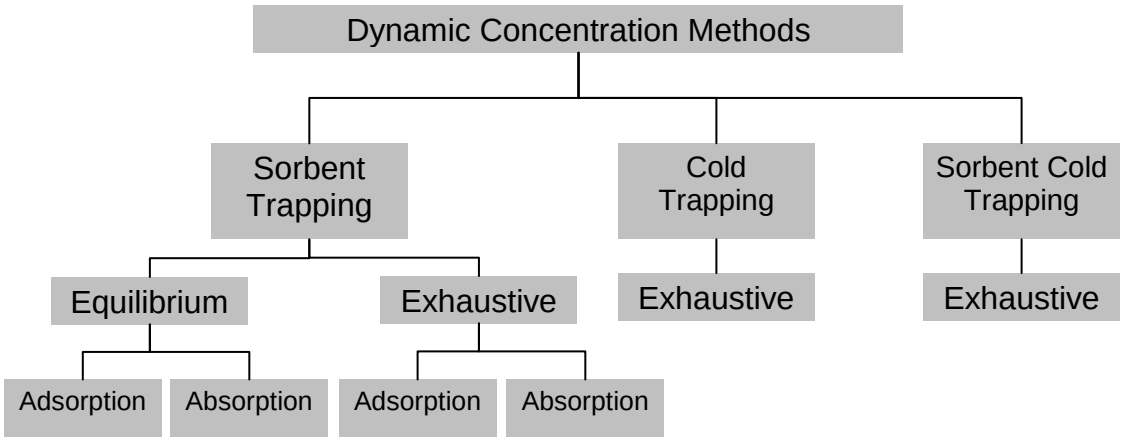

Figure 1.1. Classification of dynamic concentration methods.

1.2.1 Concentration by adsorption

Adsorption is a surface phenomenon, during which analytes are attracted to the surface of the adsorbent by forces that can include dispersion, induction, electrostatic, hydrogen bonding, charge transfer, covalent bonding, and ion exchange.[49] Adsorption can be classified as chemical or physical adsorption. Chemical adsorption occurs when a bond is formed between the analyte and the sorbent, while physical adsorption occurs without the formation of a chemical bond; van der Waals forces are typically responsible for physical adsorption. In most cases for air sampling applications, physical adsorption is used, for which adsorption and desorption rates are fast.

Adsorption isotherms are used to characterize the adsorption process between an analyte and an adsorbent. The adsorption isotherm describes the equilibrium distribution between adsorbed and nonadsorbed analyte. The shape of the isotherm can be used to describe the adsorption process. Brunauer described 5 types of isotherms, of which two are shown in Figure 1.2.[50] Type I (Figure 1.2A) occurs when a single layer of analyte is adsorbed on the surface, and little more can be adsorbed after the monolayer is formed. A type II isotherm (Figure 1.2B) occurs when additional layers are adsorbed onto the surface after the monolayer is formed. There are other types of isotherms that are not shown, and there are mathematical models describing the isotherms. Many simple adsorption systems have isotherms similar to that shown in Figure 1.2A.

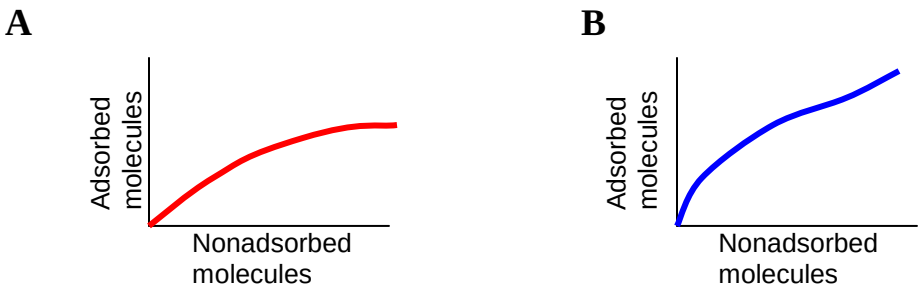

Figure 1.2. (A) Type I and (B) type II isotherms as described by Brunauer.[50]

There are several models that describe breakthrough for different operating parameters. One model is the Wheeler model which is described by Equation 1.1

$$t_B = \frac{W_e}{C_0 Q}\left[W - \frac{\rho_b Q}{K_v} \ln\left(\frac{C_0 - C}{C} \right) \right] \qquad (1.1)$$

where t_B is the breakthrough time , W_e is the adsorption capacity (mg/mg), C_0 is the inlet concentration (mg/mL), C is the concentration (mg/mL) eluting out of the trap (a fraction of C_0), Q is the flow rate (mL/min), W is the weight of the adsorbent (g), ρ_b is the bulk density of the packed bed (g/mL), and K_V is the rate constant (min^{-1}).[51-53] The model described in Equation 1.1 is only an approximation, for which high deviations occur at high concentrations.[51-52] As can be seen from Equation 1.1, the breakthrough time is concentration dependent. Breakthrough will occur at shorter times for higher concentrations. The breakthrough time is also indirectly proportional to the flow. High flow rates permit shorter sampling times, however, they also reduce the breakthrough time.

The amount adsorbed also depends on surface area of the adsorbent. Usually, sorbents with higher surface areas will adsorb more analyte. However, not all of the surface area is available for adsorption. Analytes may not fit into pores within the sorbent. The temperature also affects the amount that is adsorbed onto the sorbent. Higher temperatures shift the equilibrium so that there is a higher concentration of nonadsorbed analytes. At high temperatures, there is little or no adsorption. The presence of other analytes also affects the amount of a particular analyte adsorbed. Other analytes can compete for adsorption sites, and displacement of the less retained analytes is possible.[54]

Applications of adsorbent tubes. Active sampling using solid adsorbent tubes followed by thermal desorption is one of the most widely used air sampling techniques for the analysis of VOCs and semi-VOCs. Several official methods specify this technique including EPA TO-17 (Determination of Volatile Organic Compounds in Ambient Air Using Active Sampling onto Sorbent Tubes), ASTM D-6196 (Standard Practice for Selection of Sorbents and Pumped Sampling/Thermal Desorption Analysis Procedures for Volatile Organic Compounds in Air),

NIOSH 2549 (Volatile Organic Compounds) and ISO 16017 (Indoor, Ambient and Workplace Air –Sampling and Analysis of Volatile Organic Compounds by Sorbent Tube/Thermal Desorption/Capillary Gas Chromatography).[55] The flow rates used for these methods range from 10-200 mL/min, and the total volume sampled is typically 1-10 L. Solid sorbent tubes have even been standardized to 3.5 in. x 0.25 in. o.d., and many commercially available instruments are available for automated desorption of analytes from these tubes.

Solid adsorbents. There is a wide range of adsorbents that are commercially available. The most common adsorbents are porous polymers, activated carbon, graphitized carbon, and carbon molecular sieves. Table 1.1 lists the properties of some of the sorbents that are available. Porous polymers can be prepared from polymerization and cross-linking of various single or mixed monomers. One of the most widely used and characterized porous polymer sorbents is Tenax, which is a polymer of 2,6-diphenyl-*p*-phenylene oxide. One of the reasons Tenax is widely used is because of its high temperature stability (approximately 400°C), which allows for collecting a wide range of analytes and provides good recovery for semi-VOCs.[56] Tenax also demonstrates low water retention, which is useful in limiting the adsorption of water from high humidity air samples. However, Tenax has been reported to react with certain compounds including ozone, nitrogen dioxide, nitrogen oxide, sulfur dioxide, sulfuric acid and chlorine.[57] The artifacts that can be formed from the reaction of these compounds with Tenax include phenol, benzaldehyde, acetophenone, decanal, dibutylphthalate, 2,6-diphenyl-*p*-quinone and 2,6-diphenylhydroquinone.[58-59] There are 3 types of Tenax listed in Table 1. Tenax TA shows reduced column bleed compared to Tenax GC, and Tenax GR contains 23% graphitized carbon for trapping more volatile analytes.[40] Chromosorb represents another set (8 types) of porous polymer adsorbents. Some of them are listed in Table 1.1. Chromosorb 106, for example, is a

polystyrene polymer. It has a greater sample capacity compared to Tenax, is unaffected by ozone, and is highly hydrophobic. However, it has a much lower temperature limit compared to Tenax, which can restrict its use.[56] Table 1.1 also lists several sorbents from the Porapak and HayeSep series, which are usually interchangeable.[40] The Amberlite XAD resins are non-ionic macroreticular resins. They adsorb analytes through hydrophobic and hydrophilic interactions.[40]

Table 1.1. Common solid sorbents and their properties.[40, 44, 55-56]

Sorbent	Composition	Surface Area (m^2/g)	Sorbent Mean Size (Å)	Temperature Limit (°C)
		Porous polymers		
Tenax				
Tenax GC	Poly (2,6-diphenyl-p-phenylene oxide)	19-30	720	450
Tenax TA	Poly (2,6-diphenyl-p-phenylene oxide)	35		300
Tenax GR	Poly (2,6-diphenyl-p-phenylene oxide) +23% graphitized carbon	35		350
Chromosorb				
Chromosorb 101	Styrene-divinylbenzene	350	3500	275
Chromosorb 102	Styrene-divinylbenzene	300-400	90	250
Chromosorb 103	Cross-linked polystyrene	350		275
Chromosorb 104	Acrylonitrile-divinylbenzene	100-200		250
Chromosorb 105	Polyaromatic	600-700	500	250
Chromosorb 106	polystyrene	700-800		225
Chromosorb 107	Polyacrylic ester	400-500		225
Chromosorb 108	Cross-linked acrylic ester	100-200		225
Porapak				
Porapak N	Polyvinylpyrrolidone	225-350	120	190
Porapak P	Styrene-divinylbenzene	100-200	150	250

Table 1 (cont.)

Sorbent	Composition	Surface Area (m^2/g)	Sorbent Mean Size (Å)	Temperature Limit (°C)
Porapak Q	Ethylvinylbenzene-divinylbenzene	500-600	75	250
Porapak R	Polyvinylpyrrolidone	450-600	76	250
Porapak S	Polyvinylpyridine	300-450	76	250
Porapak T	Ethylene glycol dimethyl adipate	250-350		190
HayeSep				
Hayesep A	Divinylbenzene – ethylene glycol dimethacrylate	526		165
Hayesep D	Divinylbenzene	795		290
HayeSep Q	Divinylbenzene	582		275
HayeSep R	Divinylbenzene-N-vinyl-2-pyrrolidone	344		250
HayeSep S	Divinylbenzene-4-vinyl-pyridine	583		250
Amberlite Resins				
XAD-2	Styrene-divinylbenzene	300		200
XAD-4	Styrene-divinylbenzene	750		150
XAD-7	Polymethacrylate resin	450		150
XAD-8	Polymethyl-metharcylate	140		150
Activated Carbon				
Coconut-based	Carbon	800-1000	20	220
Petroleum-based	Carbon	800-1000	18-20	
Graphitized Carbon Blacks				
Carbotrap				
Carbotrap	Graphitized carbon black	100	3000	400
Carbotrap C	Graphitized carbon black	10	2000	400
Carbopack				
Carbopack B	Graphitized carbon black	100		>400
Carbopack C	Graphitized carbon black	10		>400

Table 1. (Cont.)

Sorbent	Composition	Surface Area (m^2/g)	Sorbent Mean Size (Å)	Temperature Limit (°C)
Carbopack F	Graphitized carbon black	5		>400
Carbon Molecular Sieves				
Carbosieve				
Carbosieve G	Graphitized carbon black	910		225
Carbosieve S-III	Graphitized carbon black	820	15-40	400
Carboxen				
Carboxen 563	Graphitized carbon black	510		400
Carboxen 564	Graphitized carbon black	400		400
Carboxen 569	Graphitized carbon black	485		400
Carboxen 1000	Graphitized carbon black	1200		400
Carboxen 1004	Graphitized carbon black	1100		225

Activated carbon sorbents are prepared from low temperature oxidation of charcoal. They have high surface areas containing polar functional groups and can withstand high temperatures. However, they suffer from high water retention and irreversible adsorption.[40] As a result of these limitations, graphitized carbon blacks were developed. The graphitization process eliminates specific adsorption sites and limits the formation of hydrogen bonds.[55] This prevents adsorption of small polar analytes such as water. It has been found that certain analytes such as terpenes and chlorinated hydrocarbons are unstable when adsorbed on these sorbents.[56] Carbon molecular sieves are another class of sorbents which contain micro pores for the adsorption of small molecules. These adsorbents are prepared from carbon-containing materials such as anthracite and mineral coal, which are converted into soot by pyrolysis methods in the absence of oxygen. Depending on the preparation method, sorbents of different particle sizes and with different pore

sizes can be prepared.[60] Carbosieves and Carboxens are classified as carbon molecular sieves as listed in Table 1.1.

A single adsorbent cannot trap all analytes. Multi-bed traps have been used to sample analytes covering a wide volatility range. Typically, in multi-bed traps, 2 or 3 adsorbents are packed in series separated by metallic mesh or glass wool. The adsorbents are arranged by increasing retention capability. As the analytes are introduced into the multi-bed trap, heavier analytes are retained on the weak adsorbent, while the more volatile analytes break through the weak adsorbent and are trapped on subsequent stronger adsorbents. As a result, the flow must be reversed during desorption to prevent the heavier analytes from entering stronger sorbent sections that could result in irreversible adsorption. Figure 1.3 shows a schematic of a multi-bed sorbent trap.

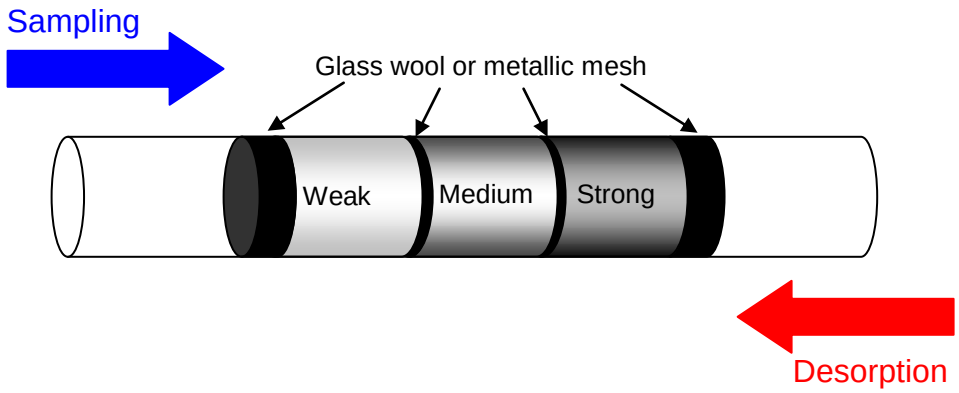

Figure 1.3. Multi-bed sampling tube consisting of 3 adsorbents with weak, medium, and strong adsorption strengths. During sampling, the analytes are introduced into the sorbent bed in the direction of increasing sorbent strength. The flow is reversed during desorption.

New adsorbents are continuously being explored. Wu et al. synthesized a mesoporous silica with pore sizes of 29 Å for trapping VOCs from air.[61] The new sorbent showed good retention of C_8-C_{12}; smaller analytes were less retained. Temperatures of only 150°C were

required to efficiently desorb the analytes, which were much lower than for carbon molecular sieves. Carbon nanotubes have recently been explored as adsorbent materials for trapping analytes. Li et al. examined the use of purified multi-walled carbon nanotubes as adsorbents for trapping VOCs.[62] With particles ranging from 60-80 mesh and with a surface area of 98 m^2/g, carbon nanotubes showed 2-3 times the breakthrough volumes compared to some commercially available carbon molecular sieve adsorbents. Furthermore, the authors showed that the carbon nanotubes were not affected by humidity. Hussain et al. also demonstrated good retention using carbon nanotubes.[63] In addition, they showed that carbon nanotubes have excellent desorption properties as demonstrated by the resultant narrow bandwidths. Carbon nanotubes can agglomerate, which can decrease permeability. To overcome this problem, Wang et al. deposited multi-walled carbon nanotubes on the exterior surface of porous silica gel particles.[64]

***Water retention in adsorbents*.** Sampling from air requires the ability to sample under high humidity conditions. Water vapor adsorption can decrease the capacity for other analytes. In addition, a large water background can cause retention shifts in GC and can be problematic for many detectors, including MS. Some adsorbents adsorb more water than others. Gawlowski et al. examined several solid adsorbents for the retention of water at 20°C in 95% relative humidity (RH).[65] The results can be seen in Table 1.2.

As can be seen in Table 1.2, activated carbon shows the highest retention of water, followed by the carbon molecular sieves. The porous polymers have the lowest retention of water. The adsorbent can be chosen to limit the amount of water that is adsorbed; however, the analytes and sampling conditions must be considered. Another approach is to limit the time and flow during sampling to limit the amount of water that is adsorbed. Again, this approach may not be feasible as it reduces the total amount of analyte that can be concentrated. Water can be

reduced by passing the sample through a trap containing a drying agent such as K_2CO_3, Na_2CO_3, and $Mg(ClO_4)_2$ before introducing it into the trap.[66-67] However, there can be analyte losses in the drying trap. In a recent publication, Pettersson and Roeraade used a short packed precolumn of anhydrous lithium chloride to remove water from aqueous samples. The water was strongly retained, however, polar and nonpolar VOCs had low retention. The analytes were transferred to an analytical column for separation and detection. The lithium chloride precolumn was then back-flushed to remove the water.[68] This method showed good potential without analyte losses, even for polar analytes.

Table 1.2. Maximum mass of water adsorbed on adsorbents at 20°C and 95% RH.[65]

Adsorbent	Air flow (mL/min)	Mass of adsorbed water (mg/g)
Carbosieve S-III	50	343
Carbosieve S-III	100	330
Carboxen 569	50	207
Carboxen 569	100	194
Carboxen 1000	100	450
Active Carbon	50	690
Porapak T	50	110
Porapak N	50	115
Chromosorb 108	50	65
Chromosorb 106	50	<5
Tenax GC	50	<5
Carbotrap C	50	<5

An ion exchange membrane (Nafion) has also been used to selectively remove water from sample streams.[69-70] Nafion tubes remove water by the use of a perfluorinated ion-exchange resin. It is the high water complexing properties of sulfonic acid groups that are responsible for the ion-exchange properties of Nafion, while the perfluorinated backbone makes the material highly resistive to chemical attack. However, analytes such as alcohols, ketones, organic acids and aldehydes can be lost when passed over a Nafion membrane.[70] In addition, Nafion

membranes cannot be heated to high temperatures, which prevents their use with semi-VOCs. Other methods have been used to separate water from the sample, such as selectively freezing the water or selectively desorbing the analytes.

Helmig and Vierling predicted that water can be prevented from adsorbing on carbon molecular sieves by slightly heating the trap to reduce the relative humidity (RH), since the amount of water adsorbed depends on the RH.[66] It was shown in similar adsorbents that if the RH exceeds 90%, up to a 10-fold decrease in the safe sampling volume can be observed.[71] Gawrys et al. attributed the amount of water adsorbed in carbon molecular sieves to the adsorption mechanism.[72] At low RH, water is adsorbed at polar centers of the adsorbent, which contain a small number of functional groups such as carboxylic, hydroxylic, and phenolic. For high RH, water vapor is condensed inside the pores, which can occur below the saturation point due to the strong adsorption fields inside the micropores. Hence, by decreasing the RH below a critical value that is dependent on the adsorbent, the amount of water adsorbed can be decreased. This can be done by increasing the temperature of the trap. Increasing the trap temperature reduces the safe sampling volume only 2-fold, while sampling at high RH can decrease it by 10-fold.[72]

Gawlowski et al. demonstrated that water adsorbed on sorbents of Tenax, Chromosorb 106, and Carbotraps B and C can be eliminated by a dry purge of only 300 mL before thermal desorption, even after sampling from air with relative humidity as high as 95%.[73] Adsorbed water can also be purged from carbon molecular sieves, but larger purging volumes are required. There is a risk of loosing VOCs using a dry purge.

1.2.2 Concentration by absorption

Absorption is based on solubility rather than on surface interactions as in adsorption. In absorption, analytes dissolve into a homogeneous, non-porous, gum-like liquid that behaves similar to organic solvents. Absorption only occurs when the temperature is above the glass transition point of the phase. Below this temperature, adsorption mechanisms dominate.[57] There are only a few materials that meet this requirement for temperatures that are required for sampling and desorption. The most common material used is polydimethylsiloxane (PDMS). PDMS has been well characterized in the literature and is one of the most widely used stationary phases in GC. Some advantages of PDMS include high inertness and temperature stability. The structure of PDMS is shown in Figure 1.4. Some of the methyl groups of PDMS can be substituted with more polar groups, such as phenyl and cyanopropyl, to make it more polar to favor absorption of polar analytes. Polyacrylates can also be used for absorption of more polar analytes.

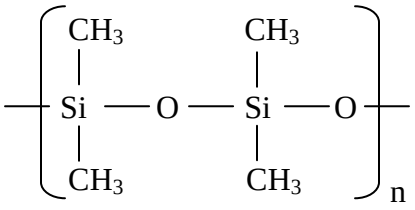

Figure 1.4. Structure of polydimethylsiloxane.

The partition (or distribution) coefficient (K) is often used to determine the affinity of an analyte for an absorbing phase. In chromatography, it is defined as

$$K = \frac{C_S}{C_M} \tag{1.2}$$

Where C_S is the concentration of the analyte in the stationary phase (the concentration that is absorbed) and C_M is the concentration in the mobile phase (or the amount that is not absorbed). Analytes with a high partition coefficient will favor the absorption phase. Unlike adsorption, most absorption processes have a linear isotherm, i.e., the absorption of an analyte is not concentration dependent (unless the phase becomes saturated). The partition coefficient does not change with sample concentration. As a result, breakthrough volumes can be easily determined and can even be calculated from chromatographic data found in the literature, eliminating the need to determine them directly for analytes at different concentrations.[74] The breakthrough volume can be determined using the following equation

$$V_b = V_R\left(1 - \frac{2}{\sqrt{N}}\right) \tag{1.3}$$

where V_b is the breakthrough volume, V_R is the retention volume and N is the number of theoretical plates.[47, 75]

Lovkvist and Jonsson developed a model to determine breakthrough volumes for traps with theoretical plates less than 9, at which point chromatographic methods deviate.[76] The breakthrough volume (V_b) at 5% is given by Equation 1.4

$$V_b = V_0 \times (1+k) \times \left(0.9025 + \frac{5.360}{N} + \frac{4.603}{N^2}\right)^{-\frac{1}{2}} \tag{1.4}$$

where V_0 is the trap dead volume, k is the capacity factor, and N is the number of theoretical plates.

An advantage of absorbents is that they generally are not affected by competitive effects of different analytes. Since absorption is based on solubility, displacement of one analyte by another is not observed. Hence, the presence of multiple analytes does not affect the absorption of a particular analyte. The main disadvantage of absorption materials is that they have a lower sample capacity compared to adsorbents.

***Water in absorption*.** Polysiloxanes are excellent for trapping VOCs and semi-VOCs because of strong dispersion interactions, while the solubility of water in polysiloxanes is very low, leading to an extremely low partition coefficient. When sampling high humidity gas streams using PDMS as packing material or as coatings in open tubular traps, the water vapor essentially passes directly through the capillary with very little retention. On the other hand, organic compounds with much higher volatilities than water are effectively trapped in the polymer film. Table 1.3 shows retention indices for water and a number of other analytes on a PDMS gas chromatographic stationary phase.

Use of absorbents in packed beds. Because of the advantages of absorbents, there have been a number of reports describing the use of packed absorbent traps to enrich vapors.[74, 78-80] Baltussen et al. characterized a packed bed of PDMS particles for concentrating gaseous samples. They demonstrated that breakthrough volumes can be predicted from retention index data obtained in the literature and from theoretical equations. The authors also demonstrated that PDMS packing materials showed good thermal stability even after 200 runs. PDMS was also compared to common adsorbents such as Tenax and Carbotrap.[78] PDMS produced lower background compared to other adsorbents. Even though PDMS is nonpolar, it showed adequate

trapping of polar analytes and, over a wide range of analytes, PDMS performed better than the adsorbents. The inertness of PDMS was demonstrated in another publication by Baltussen et al. for the concentration of sulfur compounds.[79] It was observed that several artifacts were formed from the Tenax and Carbotrap adsorbents, and permanent adsorption was observed for heavier compounds. The use of PDMS as a packing material eliminated these problems.

Table 1.3. Retention indices for water and other analytes on a PDMS gas chromatographic stationary phase.[77]

Analyte	Retention Index
Water	327
Acetone	470
Methylene Chloride	560
Carbon Disulfide	564
Benzene	650
Toluene	751
Sarin	789
Nitrobenzene	1100
VX	1667

1.2.3 Open tubular traps

Open tubular traps using typical thick-film GC columns have been used for concentrating analytes in air.[81-87] Advantages of coated capillary traps compared to traditional packed traps include increase in quantitative reliability, low resistance to gas sample flow (i.e., large gas volumes can be sampled in reasonable time, which improves detection), and good transfer between the trap and the analytical column.

To ensure that analytes are trapped in the open tubular trap, the gas phase analyte molecules must have sufficient time to diffuse to the walls where they can interact with the coating, and the absorption/adsorption interactions must be sufficient enough to provide adequate trapping. The minimum length of an open tubular trap to allow 99% of the analytes to diffuse to

the walls can be calculated from Equation 1.5.[51] The model developed for these calculations assumes a laminar profile, steady state absorption in the stationary phase, and a stationary phase that is far from being saturated.

$$L = \frac{1.2 \times u \times r^2}{D} \qquad (1.5)$$

In this equation, L is the length of the capillary, r is the internal radius, u is the average linear velocity of the fluid, and D is the diffusion coefficient of the analyte in the mobile phase (air). The diffusion coefficient of an analyte can be estimated using the Fuller-Schettler-Giddings equation (Equation 1.6)

$$D_{AB} = \frac{0.001\, T^{1.75} \sqrt{\frac{1}{M_A} + \frac{1}{M_B}}}{P\left[\left(\sum v_A\right)^{1/3} + \left(\sum v_B\right)^{1/3}\right]^2} \qquad (1.6)$$

where D_{AB} is the diffusion coefficient of analyte A in gas B in units of cm^2/s, T is the temperature in K, M_A and M_B are the molecular masses of the analyte (A) and the gas (B), respectively, P is the pressure in units of atm, and Σv_A and Σv_B are the sums of the atomic volume increments for the analyte (A) and the gas (B), respectively.[88] The atomic volume increments can be found in the literature. Because diffusion of gases is fast, traps of only short lengths are necessary to allow the analytes to diffuse to the walls. For example, a trap length of only 0.075 cm is needed to trap toluene ($D = 0.085\ cm^2/s$) at a flow rate of 1 mL/min, and 7.5 cm is needed for a flow rate of 100 mL/min. It should be noted that the radius in Equation 1.5

cancels when converting linear velocity to volumetric flow rate in the example above. The strength of the interaction between the analyte and sorbent then becomes the most important factor in determining the trap dimensions.

The first reports of open tubular traps were for trapping fractions from a GC column in order to re-chromatograph the fractions on another column.[89-90] However, it wasn't until 1985, when capillaries with thick stationary phase films were used for headspace and air sampling applications. Grob and Habich compared capillary traps that were coated with a thick polymer film (absorption based) to capillaries in which the walls were coated with charcoal particles (adsorption based).[81] While the adsorption based open tubular traps provided higher capacity, the absorption based traps provided fast desorption and inertness, and did not exhibit any analyte displacement.

Bicchi et al. used longer traps to increase the retention of compounds.[83-84, 91] In their work involving the analysis of living plants, breakthrough volumes increased from 1.2 mL to 30-100 mL by changing the trap dimensions from 0.24-0.5 m x 0.32 mm i.d. to 3 m x 0.53 mm i.d. However, with the longer traps, a refocusing step was necessary to narrow the bands.

Blomberg and Roeraade developed a technique to coat capillaries in which films up to 100 μm thick could be prepared to increase the retention on open tubular traps.[92] To achieve high film thicknesses, the authors immediately immobilized the PDMS stationary phase by moving the capillary being coated into an oven during the coating process to cross-link the polymer. In another publication, the authors demonstrated that by using 2 m x 0.7 mm i.d. x 80 μm film thickness traps, a phase ratio of 1.44 could be achieved, which is 20-100 times lower than reported by previous workers, leading to breakthrough volumes of 13 mL for pentane and 11,107 mL for dodecane.[85]

In recent years, capillary traps have greatly increased in popularity. A patent by Overton encompasses trapping, refocusing and separation in a single capillary.[93] In this design, the capillary behaves like a trap when the sample is introduced at ambient temperature. The analytes are focused into a narrow band when the first section of the capillary (the longer section) is heated and the second section is maintained at ambient temperature. The analytes are desorbed from the first section and refocused in the second section. Once the analytes are refocused and the first section of the capillary is allowed to return to ambient temperature, the carrier gas is reversed and the whole capillary is heated by a temperature ramp, during which the analytes are separated. Multiple capillaries can be used with different stationary phases for the analysis of a larger range of analytes.

Another method to increase retention on open tubular traps is to increase the surface area of the stationary phase. Porous layer open tubular (PLOT) columns provide high sample capacity due to large surface area, and are generally used for separation of light gases. PLOT columns have also been used as traps. Gordin and Amirav used 15 mm x 0.53 mm i.d. short PLOT columns for headspace sampling.[86] The trap was connected to a battery operated pump that sampled at 10-60 mL/min in the field. After sampling, the trap was taken back to the laboratory, desorbed and analyzed.

In a recent publication, Bonn et al. prepared open tubular traps consisting of multiple phases to increase the retention of more polar analytes.[87] Liquid and solid poly(ethylene glycol) (PEG) were mixed with a thick PDMS film. For some polar analytes, there was up to 10-fold increase in retention with only 7.5% PEG in the PDMS polymer.

Bundling multiple capillaries in parallel is another method to increase the capacity of open tubular traps. Originally, multi-capillary columns have been used in high speed

chromatography applications to increase sample capacity. [94] Multi-capillary devices have also found uses for air sampling applications. Lane et al. constructed an annular denuder for the collection of semi-volatile organic compounds that consisted of 6 concentric glass tubes with stationary phase coated on both sides of each of the glass tubes.[95] This allowed an air flow of 16.7 L/min through the system. Krieger and Hites constructed a 25 cm long denuder that consisted of 120 fused silica capillaries cut from a single capillary column coated with a 5 μm film of PDMS.[96] Using multi-capillaries increased the total flow rate of the denuder while keeping the flows through individual capillaries low. Ortner and Rohwer also bundled multiple capillaries to increase the capacity of their open tubular traps.[97] The authors constructed multichannel air sampling traps consisting of 3-8 silicone tubes.

1.2.4 Denuders

Open tubular traps have also been used in denuders for atmospheric analysis.[96, 98] It is often useful to know the concentration of VOCs or Semi-VOCs that are both in the vapor phase and associated with particles in the air. Denuders are used to separate the vapor phase from the particles. A diffusion denuder consists of a tube in which the interior wall is coated with a material to collect the analytes (essentially an open tubular column used in GC). As the sample is introduced into the denuder, analytes in the gas phase have time to diffuse to the walls of the denuder where they are collected. The diffusion of particles is much slower and, therefore, they pass through the denuder without interacting with the walls. The analytes in the gas phase can be desorbed and analyzed. The particles that pass through the denuder can be collected on a filter.

1.2.5 Microtraps

It is difficult to interface a high volume trap to a capillary GC system. Oftentimes, a split is required to decrease the flow rate for the GC system. Splitting the flow, however, increases the detection limits of the system. Because of interfacing problems, the trend in sorbent trapping is to use micro-traps, which consist of a small section (~5 cm) of analytical column (320 μm-530 μm i.d.) packed with sorbent.[40, 43] Feng and Mitra showed that the larger the i.d. of the trap, the wider the bandwidth due to slower desorption.[99] The low thermal mass of these traps allows for fast heating and cooling which can be easily adapted for field or on-line air monitoring. Injections are made into the GC by thermal pulses of the microtrap. Since only a small amount of packing material is available for trapping, the sorbent must have a high sample capacity. Microtraps can handle limited sampling flow rates, and they have limited total sample capacities.

Frank and Frank showed that a microtrap with a single packing material directly coupled to a GC system provides narrow bandwidths for analytes that have a narrow boiling point range (within 100°C of each other).[100] For samples containing a wide volatility range, a multibed microtrap can be used, with a back-flush mode.

A series of publications by Mitra et al. demonstrated the usefulness of microtraps used in on-line continuous monitoring applications.[101-104] Large volumes of air can be sampled through the microtrap and trace analytes can be concentrated and injected in narrow bands into a GC. Because the microtraps can be heated and cooled within seconds, short analysis times can be accomplished.

Because of the low capacity of microtraps, ways to improve retention have been addressed. O'Doherty et al. chilled a Carboxen-filled microtrap to temperatures down to -50°C using a commercially available chiller (no cryogenics) to trap very volatile

chlorofluorocarbons.[105] Feng and Mitra used a 2-stage microtrap to increase volume breakthrough.[99] The first trap was a larger diameter trap containing a greater amount of packing material. The second trap was a smaller trap that was used to focus the analytes in a sharp band.

1.2.6 Equilibrium sorption

For extremely volatile compounds, it is difficult to obtain 100% trapping efficiency on solid sorbents. A method called equilibrium sorptive enrichment was developed to solve this problem.[106-108] In this method, the sample is continuously purged through a sorptive trap until all analytes in the sample are in equilibrium with the sorptive material. This allows for the analysis of all analytes, including those that tend to break through the sorptive material quickly. It also prevents competition binding since all analytes are in equilibrium. However, this technique is limited to samples that have a constant concentration over the sampling time. To facilitate fast equilibrium, a weak sorption material is often preferred. This is in contrast to exhaustive sampling in which a strong sorbent material is desired to prevent fast breakthrough. For this reason, open tubular traps are frequently used for this application. Although not all of the analyte is trapped by this method, the inlet concentration, C_0, of an analyte in the sample can still be determined as demonstrated in Equation 1.7 for an absorption based mechanism.

$$C_0 = \frac{m_{sorbed}}{V_R} = \frac{m_{sorbed}}{V_0 \times \left(1 + \frac{K}{\beta}\right)} \approx \frac{m_{sorbed}}{V_{sp} \times K} \quad for\ K >> 1 \qquad (1.7)$$

where m_{sorbed} is the sorbed amount of the compound, V_R is the retention volume of the trap, V_0 is the dead volume of the trap, V_{sp} is the volume of the stationary phase in the trap, K is the

equilibrium constant, and β is the phase ratio.[108] The equilibrium constant can be determined experimentally, or estimated from retention indices obtained from the literature.[74]

Packed beds and open tubular traps have both been used in equilibrium sorption. Usually, absorption based techniques have been applied, but the technique is also amendable to adsorbents.

1.2.7 Solid phase microextraction

Solid phase microextraction (SPME) is a convenient technique for the analysis of VOCs and semi-VOCs in air. After the introduction of SPME by Pawliszyn in 1990, it quickly became a popular solvent-free extraction method that combined extraction and concentration into a single step.[109] SPME consists of a solid support, usually a fused silica fiber, on which a sorptive polymer coating is applied. The coated fiber is then introduced directly into a matrix such as air, an aqueous sample, or headspace of a container where the analytes that have an affinity for the coating are absorbed/adsorbed. The analytes are subsequently desorbed from the fiber in an injection port of a GC or GC-MS system for analysis.[110] There are several coatings that are commercially available from Supelco (Bellefonte, PA) that are based either on absorption or adsorption of analytes. SPME has been successfully applied in many areas, including environmental, food, flavor, fragrance, pheromone, pharmaceutical, clinical, forensic, and reaction monitoring.[110-113]

Sampling modes with SPME include direct sampling in which the SPME fiber is placed directly in an aqueous solution, headspace sampling in which the SPME fiber is placed in the headspace above a sample, or in air analysis in which the SPME fiber is placed in either static air or in an air stream. Quantitation in SPME is based on an equilibrium process in which the analyte comes to equilibrium with the SPME fiber coating and the other phases in the system.[112]

The concentration of a sample can be determined from the amount of analyte that is absorbed into the SPME phase. Equation 1.8 shows this relationship for the case of direct equilibrium sampling with an absorption-based SPME fiber, where n is the number of moles extracted by the SPME fiber, K_{fs} is a fiber coating/sample matrix distribution constant, V_f is the fiber coating volume, V_s is the sample volume, and C_0 is the initial concentration of a given analyte in the system.[110, 112, 114]

$$n = \frac{K_{fs} V_f V_s C_0}{K_{fs} V_f + V_s} \qquad (1.8)$$

As seen from equation 1.8, there is a linear relationship between the amount of analyte absorbed by the SPME fiber and the initial concentration in the sample. Furthermore, equation 1.8 can be simplified if the volume of the sample is large (i.e. $V_s >> K_{fs}V_f$) as shown in equation 1.9.[110, 112, 114]

$$n = K_{fs} V_f C_0 \qquad (1.9)$$

It is not required to know the volume of the sample to calculate the initial concentration in that sample, just as long as $V_s >> K_{fs}V_f$. Thus, SPME can be used to sample undefined volumes of sample such as air.

The general methods by which air sampling can be accomplished with SPME include static sampling (collecting air in a bulb or polymer bag, then sampling with SPME), dynamic sampling (sampling with air moving across the SPME), and time weighted average (TWA) sampling (the fiber is kept in the protective sheath while analytes diffuse through the small

opening of the protective sheath). Figure 1.5 shows the methods of air sampling that can be achieved with SPME.

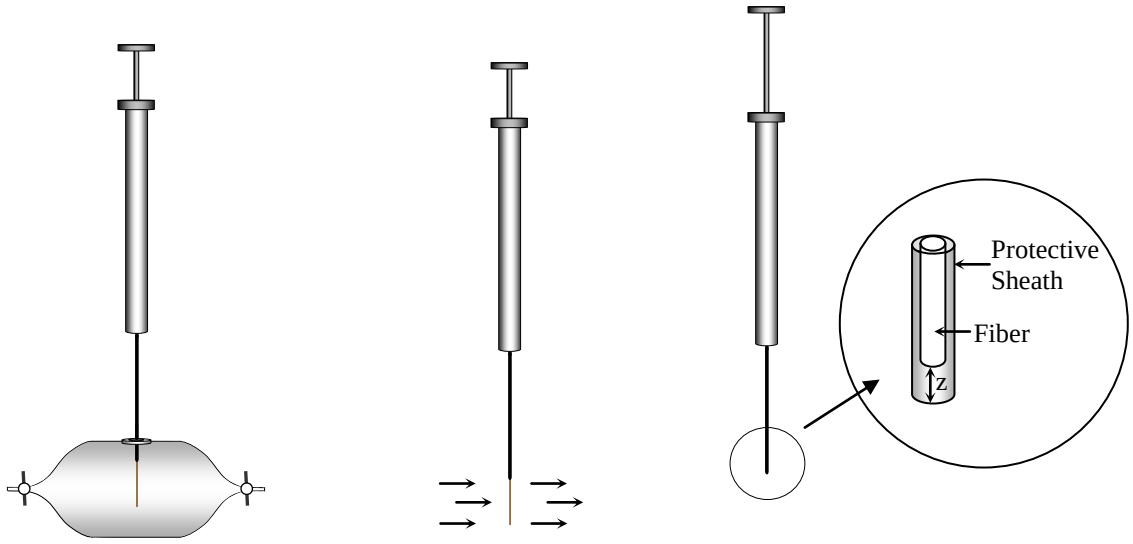

(A) Static sampling (B) Dynamic sampling (C) TWA sampling

Figure 1.5. SPME air sampling methods.

In sampling air with SPME, the rate limiting step for the absorption/adsorption of analytes by the SPME fiber is the diffusion of analytes through a static boundary layer that surrounds the fiber. This boundary layer can be decreased by dynamically flowing air across the SPME fiber (dynamic sampling).[114-115] This allows for equilibrium to be established much quicker than in static air conditions. Many research groups have focused their attention on creating portable dynamic air sampling units for field applications.[116-120] Augusto et al. devised a portable dynamic air sampling device from a commercially available hair dryer by disabling the heating coil and reversing the flow in order to prevent contamination from the blower.[116] The average air flow velocity of this system was 1.5 m/s. Augusto et al. also reported another

portable dynamic air sampling device that consisted of Teflon spacers sandwiched between stainless steel sheets, with flow established with an air pump.[116] Hook et al. was able to achieve detection limits of sarin, a chemical agent, at half of the "immediate danger to life and health" (IDLH) level of 0.20 mg/m^3 by use of a portable SPME air sampling device.[118]

To increase the amount of analyte that is sorbed by SPME, the surface area and length of the solid support can be increased. Ciucanu reported a helical shaped SPME fiber. The helical shape allowed for a longer length to be coated with the sorptive material.[121] The helical SPME device was also applied to focus analytes from a membrane inlet system.[122] Ramsey et al. developed a high surface area SPME device for rapid field analyses.[123] The device consisted of a wire coated with Carboxen/PDMS that was sandwiched between two glass tubes used for high flow sampling. The analytes were then desorbed and focused on a microtrap and analyzed with field detection equipment.

1.2.8 Cold trapping

Cryotraps are often used to concentrate VOCs. Usually a tube is immersed in a cryogenic liquid and the VOCs are condensed. Cryogens such as liquid nitrogen are used to achieve temperatures as low as -196°C. Glass beads are often used to improve trapping efficiency. The advantages of using cryotraps as opposed to sorbent trapping is the elimination of thermal degradation of temperature-sensitive analytes due to the ability to desorb at moderate temperatures. The lack of solid sorbents also eliminates artifact formation and the need for sorbent conditioning and replacement. Many volatile sulfur compounds must be concentrated in sorbent traps.[40] Water content is problematic since water can be trapped and transferred to the MS. In smaller traps, the formation of ice can block the trap. Traps containing drying agent or a Nafion membrane can be used upstream from the cryotrap to prevent concentration of water.

Two cryotraps can be used in series to help eliminate the transfer of water to the detector. This is accomplished by heating the first trap slowly, which decreases the amount of water that is transferred to the second trap.[124] Cryogenic liquids, however, are not convenient to use in the field. Pressurized liquid CO_2 is more amendable to field use and can be carried in small pressurized cylinders. The liquid can be sprayed directly onto the trap, allowing it to cool to temperatures as low as -78°C.[125] Li and Andrews used a carbon dioxide cooled cryotrap for fast GC applications.[126]

There are commercially available refrigerator systems that can achieve subambient temperatures. For example, a single-stage, closed cycle Freon refrigerator can cool to -50°C.[127] Farwell et al. used a commercially available immersion cooler to achieve temperatures as low as -80°C.[128] Although using such refrigerator systems eliminates the need for cryogenic liquids, they are expensive and large, and they require a significant amount of power to cool to low temperatures.

Using thermoelectric heat pumps, or Peltier coolers, is a way (without cryogenics) for achieving subambient temperatures. Peltier coolers are small devices consisting of two dissimilar metals that, when current is applied, pump heat from one side of the device to the other side. Colder temperatures can be achieved by applying more current and removing heat from the hot side of the cooler. As a result, a heat sink is usually placed on the heated side of the cooler to remove heat. Peltier coolers are small and are well suited for field use, however, they do consume a lot of power. Bertman et al. described a cryogen free device with which they were able to trap analytes at -100°C using a stack of Peltier coolers and a Freon refrigerator to cool the heat sink of the Peltier coolers.[127] With the Freon single stage refrigerator system at 50 W of power, the trap was able to achieve -50°C; however, with the addition of 3 Peltier coolers

stacked one on top of the other, temperatures of -100°C were achieved for the trapping of organic nitrates.

Vortex coolers have also been used for cryotrapping applications.[129] A vortex tube is a heating and cooling device with no moving parts and only requiring a supply of compressed air. Due to the vortex movement of the high pressure air (30-100 psi) that is introduced into the vortex tube and the conservation of angular momentum, hot air exits one side of the tube while cold air exits the other.[130] The typical cold temperature limit of these devices is -40°C and the high temperature limit is 190°C. The maximum temperature difference between the hot and cold ends is typically 140-160°C.[130] Although the vortex tube itself is portable, it does require substantial amounts of compressed air.

1.2.9 Sorbent cold trapping

Although there is little use of cryotraps in the field, a common practice is sorbent trapping at reduced temperatures to increase the capacity of the sorbents. There have been reports for trapping very volatile analytes.[131-133] There have also been reports for increasing the capacity of microtraps to allow injection of narrow bands in an analytical column.[105, 134] Any of the cooling approaches discussed thus far can be used to cool the trap, but Peltier coolers are most often used due to their small size.[135-136]

1.2.10 On-line sampling techniques

While many field air sampling applications only require periodic analysis (which can be performed either off-line or on-line), there are applications where real-time or near-real-time analysis is needed, such as in environmental sampling. In these cases, automated air analysis is needed. Several of the methods discussed this far can be incorporated in on-line field sampling.

One of the most common approaches is the use of sorbent traps. For automation, valves are used to allow both sample and desorption gas through the sorbent trap with software controlling valve positions and timing.[137] Microtraps have also been used for on-line sampling techniques, mainly because of the narrow desorption bands that can be injected into the GC system without the need for refocusing.[101-104]

1.2.11 Sample flow rate considerations

Concentrating trace analytes in air at high flow rates decreases the amount of time that is needed to collect the amount necessary to meet the desired detection limits. Sampling for short times becomes increasingly important when analyzing hazardous analytes. For example, only a concentration of 10 ppt of VX (a nerve agent) can cause symptoms. If a minimum of 1 ng is need to quantify VX, then approximately 9 L of air must be sampled. If a flow of 100 mL/min is used (typically flow rates for air sampling methods using sorbent tubes), then 90 min sampling time is required in order to collect the amount needed for detection. This may be too long to determine if there is a threat. However, if 5 L/min is sampled using a high flow rate sampler, then less than 2 min is needed. For TWA levels (time weighted average), up to 100 L of air must be collected. Unfortunately, sampling at high flow rates decreases the breakthrough time. Hence there is a need for high retention and high flow rate concentration techniques.

1.3 Considerations When Coupling Concentration Techniques to Capillary GC

Coupling concentration techniques to capillary GC instrumentation may seem straightforward, but several critical aspects should be considered, including the respective flow rates of the trap and the column, the bandwidths leaving the trap, and the sample amounts that

are introduced into the column. Optimum flows for capillary GC columns are low, and when MS is used for detection, the flow is limited to approximately 1 mL/min. Depending on the concentration method (i.e., trap), the flow rate from the trap may be larger than this. If, for example, a solid adsorbent trap with an i.d. of 3 mm is used, flow rates up to 20 mL/min may be needed to effectively transfer analytes from the trap to the column in a narrow band.[138] If a low flow rate is used to desorb the analytes (i.e., that used in the analytical column), incomplete transfer of the analyte may result, even with long desorption times.[81] Lower flow rates from the concentrator also contribute to wider bandwidths introduced into the GC column. Since peaks experience diffusion during the chromatographic process, it is important that the initial bandwidth be as narrow as possible to maintain good chromatographic resolution. Typically, the concentrating trap has a much higher sample capacity compared to the capillary GC column. Column overloading can occur if too much analyte is introduced into the analytical column, which results in peak distortion, broadening, and retention time shifts.

A split installed between the trap and the column can be used to allow only a portion of the total flow from the concentrator to enter the analytical column. Higher desorption flow rates from the trap can be used to increase transfer efficiency and decrease peak width. The split can also help to prevent overloading of the column with high sample amounts. However, for trace analysis, incorporating a split decreases the much needed sensitivity. A secondary trap with dimensions closer to the analytical column can be used to focus the analytes from the first trap. This secondary trap can be a cold trap, sorbent trap (microtrap), or a combination of both. With a secondary trap, slower desorption flow rates from the first trap can be used, since the analytes are focused on the secondary trap. However, if the second trap is connected directly to the column, the slow desorption flow rates from the first trap may prevent complete transfer of the analytes.

The best method of incorporating a secondary trap is to separate it from the column (through a valve). In this way, the flow rate that is desired to desorb analytes from the first trap can be used, and sufficient retention capability of the second trap can be maintained.

Reducing the size of the trap eliminates much of the interfacing issues, since the trap has similar dimensions as the analytical column, and requires similar flow rates. Since microtraps are smaller, they are faster to heat and, as a result, produce narrower peaks that may not need to be refocused.

There have been reports of focusing analytes using a negative temperature gradient.[139-143] In a negative gradient system, the temperature of the trap varies along the length, with colder temperature at the end of the trap. In a negative temperature gradient, the front end of an analyte peak is at a lower temperature than the rear end of the peak and, as a result, it moves slower then the rear end, which focuses the analyte. This focusing effect is important when sampling from a large volume of air.

1.4 Dissertation Overview

In this chapter, background information on portable GC-MS instrumentation and air sampling techniques were presented. Air sampling considerations and interfacing to capillary GC were included. The following chapters describe my efforts in developing new vapor sampling methods for future use with a hand-portable GC-MS system. Chapter 2 describes the performance testing of an early model of a hand-portable GC-MS based on a resistively heated GC and a toroidal ion trap MS. Chapter 3 describes a swatch test permeation system that used the portable MS for detection. The swatch test permeation system allowed for the detection of TICs that penetrate through protective barriers, such as clothes, gloves and masks. Chapter 4 discusses

high flow air sampling using multi-capillary traps in parallel. Chapter 5 describes a method in which analytes in air can be sampled, separated and focused in a capillary with a negative temperature gradient. Finally, Chapter 6 presents some suggestions for future development of air sampling techniques.

1.5 References

1. Santos, F. J.; Galceran, M. T., Modern Developments in Gas Chromatography-Mass Spectrometry-Based Environmental Analysis. *J. Chromatogr. A* **2003,** *1000*, 125-151.
2. Eckenrode, B. A., The Application of an Integrated Multifunctional Field-Portable GC/MS System. *Field Anal. Chem. Technol.* **1998,** *2*, 3-20.
3. Eckenrode, B. A., Environmental and Forensic Applications of Field-Portable GC-MS: An Overview. *J. Am. Soc. Mass Spectrom.* **2001,** *12*, 683-693.
4. McDonald, W. C.; Erickson, M. D.; Abraham, B. M.; Robbat, A., Jr., Developments and Applications of Field Mass Spectrometers. *Environ. Sci. Technol.* **1994,** *28*, 336A-343A.
5. Hill, H. H. j.; Martin, S. J., Conventional Analtyical Methods for Chemical Warefare Agents. *Pure Application Chemistry* **2002,** *74*, 2281-2291.
6. Meuzelaar, H. L. C.; Dworzanski, J. P.; Arnold, N. S.; McClennen, W. H.; Wager, D. J., Advances in Field-Portable Mobile GC/MS Instrumentation. *Field Anal. Chem. Technol.* **2000,** *4*, 3-13.
7. Smith, P. A.; Sng, M. T.; Eckenrode, B. A.; Leow, S. Y.; Koch, D.; Erickson, R. P.; Lepage, C. R. J.; Hook, G. L., Towards Smaller and Faster Gas Chromatography-Mass Spectrometry Systems for Field Chemical Detection. *J. Chromatogr. A* **2005,** *1067*, 285-294.
8. McClennen, W. H.; Vaughn, C. L.; Cole, P. A.; Sheya, S. N.; Wager, D. J.; Mott, T. J.; Dworzanski, J. P.; Arnold, N. S.; Meuzelaar, H. L. C., Roving GC/MS: Mapping VOC Gradients and Trends in Space and Time. *Field Anal. Chem. Technol.* **1996,** *1*, 109-116.
9. Griest, W. H.; Lammert, S. A., The Development of the Block II Chemical Biological Mass Spectrometer. In *Identification of Microorganisms by Mass Spectrometry*, Wilkins, C. L.; Lay, J. O. J., Eds. John Wiley & Sons: Hoboken, NJ, 2006; Vol. 169, pp 61-89.
10. Syage, J. A.; Hanning-Lee, M. A.; Hanold, K. A., A Man Portable Photoionization Time-of-Flight Mass Spectrometer. *Field Anal. Chem. Tech.* **2000,** *4*, 204-215.
11. Syage, J. A.; Nies, B. J.; Evans, M. D.; Hanold, K. A., Field-Portable, High-Speed GC/TOFMS. *J. Am. Soc. Mass Spectrom.* **2001,** *12*, 648-655.
12. Geear, M.; Syms, R. R. A.; Wright, S.; Holmes, A. S., Monolithic MEMs Quadrupole Mass Spectrometers by Deep Silicon Etching. *J. Microelectromech. Syst.* **2005,** *14*, 1156-1166.
13. Diaz, J. A.; Giese, C. F.; Gentry, W. R., Portable Double-Focusing Mass-Spectrometer System for Field Gas Monitoring. *Field Anal. Chem. Tech.* **2001,** *5*, 156-167.

14. Diaz, J. A.; Daley, P.; Miles, R.; Rohrs, H.; Polla, D., Integration Test of a Miniature ExB Mass Spectrometer with a Gas Chromatography for Development of a Low -Cost Portable, Chemical-Detection System. *Trends Anal. Chem.* **2004,** *23*, 314-321.
15. Rimkus, W. V.; Davis, D. V.; Gallaher, K. In *Transportable Miniature FTMS for Anlaysis of Corrosives and Chemical Warfare Agents*, Proceedings of the 4th Workshop on Harsh-Environment MS, St. Petersburg Beach, FL, St. Petersburg Beach, FL, 2003.
16. Patterson, G. E.; Guymon, A. J.; Riter, L. S.; Everly, M.; Griep-Raming, J.; Laughlin, B. C.; Ouyang, Z.; Cooks, R. G., Miniature Cylindrical Ion Traps Mass Spectrometer. *Anal. Chem.* **2002,** *74*, 6145-6153.
17. Blain, M. G.; Giter, L. S.; Cruz, D.; Austin, D. E.; Wu, G.; Plass, W. R.; Cooks, R. G., Towards the Hand-Held Mass Spectrometer: Design Considerations, Simulation, and Fabrication of Micrometer-Scaled Cylindrical Ion Traps. *Int. J. Mass Spectrom.* **2004,** *236*, 91-104.
18. Riter, L. S.; Peng, Y.; Noll, R. J.; Patterson, G. E.; Aggerhholm, T.; Cooks, R. G., Analytical Performance of a Miniature Cylindrical Ion Trap Mass Spectrometer. *Anal. Chem.* **2002,** *74*, 6154-6162.
19. Gao, L.; Song, Q.; Patterson, G. E.; Cooks, R. G.; Ouyang, Z., Handheld Rectilinear Ion Trap Mass Spectrometer. *Anal. Chem.* **2006,** *78*, 5994-6002.
20. Ouyang, Z.; Wu, G.; Song, Y.; Li, H.; Plass, W. R.; Cooks, R. G., Rectilinear Ion Trap: Concepts, Calculations, and Analytical Performance of a New Mass Analyzer. *Anal. Chem.* **2004,** *76*, 4595-4605.
21. Fico, M.; Yu, M.; Ouyang, Z.; Cooks, R. G.; Chappell, W. J., Miniaturization and Geometry Optimization of a Polymer-Based Rectilinear Ion Trap. *Anal. Chem.* **2007,** *79*, 8076-8082.
22. Lammert, S. A.; Rockwood, A. A.; Wang, M.; Lee, M. L.; Lee, E. D.; Tolley, S. E.; Oliphant, J. R.; Jones, J. L.; Waite, R. W., Miniature Toroidal Radio Frequency Ion Trap Mass Analyzer. *J. Am. Soc. Mass Spectrom.* **2006,** *17*, 916-922.
23. Austin, D. E.; Wang, M.; Tolley, S. E.; Maas, J. D.; Hawkins, A. R.; Rockwood, A. L.; Tolley, H. D.; Lee, E. D.; Lee, M. L., Halo Ion Trap Mass Spectrometer. *Anal. Chem.* **2007,** *79*, 2927-2932.
24. Contreras, J. A.; Murray, J. A.; Tolley, S. E.; Oliphant, J. L.; Tolley, H. D.; Lammert, S. A.; Lee, E. D.; Later, D. W.; Lee, M. L., Hand-Portable Gas Chromatograph-Toroidal Ion Trap Mass Spectrometer (GC-TMS) for Detection of Hazardous Compounds. *J. Am. Soc. Mass Spectrom.* **2008,** *19*, 1425-1434.
25. Mustacich, R.; Everson, J.; Richards, J., Fast GC. Thinking Outside the Box. *Am. Lab.* **2003,** *27*, 38-41.
26. Sloan, K. M.; Mustacich, R. V.; Eckenrode, B. A., Development and Evaluation of a Low Thermal Mass Gas Chromatograph for Rapid Forensic GC-MS Analyses. *Field Anal. Chem. Technol.* **2001,** *5*, 288-301.
27. Lambertus, G.; Sensenig, K.; Potkay, J.; Agah, M.; Scheuering, S.; Dorman, K. W. F.; Sacks, R., Design, Fabrication, and Evaluation of Microfabricated Columns for Gas Chromatography. *Anal. Chem.* **2004,** *76*, 2629-2637.
28. Zampolli, S.; Elmi, I.; Sturmann, J.; Nicoletti, S.; Dori, L.; Cardinali, G. C., Selectivity Enhancement of Metal Oxide Gas Sensors Using a Micromachined Gas Chromatographic Column. *Sens. Actuators B.* **2005,** *105*, 400-406.

29. Overton, E. B.; Carney, K. R.; Roques, N.; Dharmasena, H. P., Fast GC Instrumentation and Analysis for Field Applications. *Field Anal. Chem. Tech.* **2001,** *5*, 97-105.
30. Bruker. http://www.bdal.de/cbrn-detection/chemical-detection/e2m.html.
31. Griffin Analytical. http://www.Griffinanalytical.Com/Griffin400.html.
32. Inficon. http://www.inficonchemicalidentificationsystems.com
33. Microsaic. http://www.microsaic.com.
34. Torion, www.torion.com.
35. Smith, P. A.; Koch, D.; Hook, G. L.; Erickson, R. P.; Jackson Lepage, C. R.; Wyatt, H. D. M.; Betsinger, G.; Eckenrode, B. A., Detection of Gas-Phase Chemical Warfare Agents Using Field-Portable Gas Chromatography-Mass Spectrometry Systems: Instrument and Sampling Strategy Considerations. *Trends Anal. Chem.* **2004,** *23*, 296-306.
36. Keil, A.; Hernandez-Soto, H.; Noll, R. J.; Fico, M.; Gao, L.; Ouyang, Z.; Cooks, R. G., Monitoring of Toxic Compounds in Air Using a Handheld Rectilinear Ion Trap Mass Spectrometer. *Anal. Chem.* **2008,** *80*, 734-741.
37. New & Notable at Pittcon 2006: Instrumentation and More. *Chem. Eng. News* **2006,** *84*, 62-67.
38. Hess-Kosa, K., *Indoor Air Quality: Sampling Methodologies*. Lewis Publishers: Boca Raton, Fl, 2002; p 300.
39. Wang , Y.; Raihala, T. S.; Jackman, A. P.; S t . J ohn, R., Use of Tedlar Bags in VOC Testing and Storage: Evidence of Significant VOC Losses. *Environ. Sci. Technol.* **1996,** *30*, 3115-3117.
40. Camel, V.; Caude, M., Trace Enrichment Methods for the Determination of Organic Pollutants in Ambient Air. *J. Chromatogr. A* **1995,** *710*, 3-19.
41. Dewulf, J.; Huybrechts, T.; Van Langenhove, H., Developments in the Analysis of Volatile Halogenated Compounds. *Trends Anal. Chem.* **2006,** *25*, 300-309.
42. Haas, K.; Feldmann, J., Sampling of Trace Volatile Metal(Loid) Compounds in Ambient Air Using Polymer Bags: A Convenient Method. *Anal. Chem.* **2000,** *72*, 4205-4211.
43. Dewulf, J.; Van Langenhove, H., Anthropogenic Volatile Organic Compounds in Ambient Air and Natural Waters: A Review on Recent Developments of Analytical Methodology, Performance and Interpretation of Field Measurements. *J. Chromatogr. A* **1999,** *843*, 163-177.
44. Kumar, A.; Viden, I., Volatile Organic Compounds: Sampling Methods and Their Worldwide Profile in Ambient Air. *Environ. Monit. Assess* **2007,** *131*, 301-321.
45. Namiesnik, J.; Zabiegala, B.; Kot-Wasik, A.; Partyka, M.; Wasik, A., Passive Sampling and/or Extraction Techniques in Environmental Analysis: A Review. *Anal. Bioanal. Chem.* **2005,** *381*, 279-301.
46. Gorecki, T.; Namiesnik, J., Passive Sampling. *Trends Anal. Chem.* **2002,** *21*, 276-291.
47. Bielicka-Daszkiewicz, K.; Voelkel, A., Theoretical and Experimental Methods of Determination of the Breakthrough Volume of SPE Sorbents. *Talanta* **2009,** *80*, 614-621.
48. Environmental Protection Agency. Compendium Method TO-17: Determination of Volatile Organic Compounds in Ambient Air Using Active Sampling onto Sorbent Tubes. Cincinnati, OH, 1999.
49. Snyder, L. R., *Principles of Adsorption Chromatography: The Separation of Nonionic Organic Compounds*. Marcel Dekker: New York, 1968; Vol. 3.

50. Brunauer, S., *The Adsorption of Gases and Vapors*. Princeton University Press: Princeton, NJ, 1945; Vol. 1.
51. Zellers, E. T.; Morishita, M.; Cai, Q. Y., Evaluating Porous-Layer Open-Tubular Capillaries as Vapor Preconcentrators in a Microanalytical System. *Sens. Actuators B* **2000,** *B67*, 244-253.
52. Yoon, Y. H.; Nelson, J. H., Application of Gas-Adsorption Kinetics .1. A Theoretical-Model for Respirator Cartridge Service Life. *Am. Ind. Hyg. Assoc. J.* **1984,** *45*, 509-516.
53. Wheeler, A.; Robell, A. J., Performance of Fixed-Bed Catalytic Reactors with Poison in the Feed. *J. Catal.* **1969,** *13*, 299-305.
54. Wight, G. D., *Fundamentals of Air Sampling*. Lewis Publishers: Boca Raton, 1994.
55. Ras, M. R.; Borrull, F.; Marce, R. M., Sampling and Preconcentration Techniques for Determination of Volatile Organic Compounds in Air Samples. *Trends Anal. Chem.* **2009,** *28*, 347-361.
56. Harper, M., Sorbent Trapping of Volatile Organic Compounds from Air. *J. Chromatogr. A* **2000,** *885*, 129-151.
57. Baltussen, H. A. New Concepts in Sorption Based Sample Preparation for Chromatography. Technische Universiteit Eindhoven, Eindhoven, Netherlands, 2000.
58. Pellizzari, E.; Demian, B.; Krost, K., Sampling of Organic Compounds in the Presence of Reactive Inorganic Gases with Tenax Gc. *Anal. Chem.* **1984,** *56*, 793-798.
59. Clausen, P. A.; Wolkoff, P., Degradation Products of Tenax TA Formed During Sampling and Thermal Desorption Analysis: Indicators of Reactive Species Indoors. *Atmos. Environ.* **1997,** *31*, 715-725.
60. Kettrup, A., *Analysis of Hazardous Substances in Air*. Weinheim, Federal Republic of Germany, 1993; Vol. 2, p 3-12.
61. Wu, T.-M.; Wu, G.-R.; Kao, H.-M.; Wang, J.-L., Using Mesoporous Silica MCM-41 for In-Line Enrichment of Atmospheric Volatile Organic Compounds. *J. Chromatogr. A* **2006,** *1105*, 168-175.
62. Li, Q.-L.; Yuan, D.-X.; Lin, Q.-M., Evaluation of Multi-Walled Carbon Nanotubes as an Adsorbent for Trapping Volatile Organic Compounds from Environmental Samples. *J. Chromatogr. A* **2004,** *1026*, 283-288.
63. Hussain, C. M.; Saridara, C.; Mitra, S., Microtrapping Characteristics of Single and Multi-Walled Carbon Nanotubes. *J. Chromatogr. A* **2008,** *1185*, 161-166.
64. Wang, L.; Liu, J.; Zhao, P.; Ning, Z.; Fan, H., Novel Adsorbent Based on Multi-Walled Carbon Nanotubes Bonding on the External Surface of Porous Silica Gel Particulates for Trapping Volatile Organic Compounds. *J. Chromatogr. A* **2010,** *1217*, 5741-5745.
65. Gawlowski, J.; Gierczak, T.; Jezo, A.; Niedzielski, J., Adsorption of Water Vapour in the Solid Sorbents Used for the Sampling of Volatile Organic Compounds. *Analyst* **1999,** *124*, 1553-1558.
66. Helmig, D.; Vierling, L., Water-Adsorption Capacity of the Solid Adsorbents Tenax-TA, Tenax-GR, Carbotrap, Carbotrap-C, Carbosieve-SIII, and Carboxen-569 and Water Management-Techniques for the Atmospheric Sampling of Volatile Organic Trace Gases. *Anal. Chem.* **1995,** *67*, 4380-4386.
67. Westberg, H. H.; Rasmussen, R. A.; Holdren, M., Gas Chromatographic Analysis of Ambient Air for Light Hydrocarbons Using a Chemically Bonded Stationary Phase. *Anal. Chem.* **1974,** *46*, 1852-1854.

68. Pettersson, J.; Roeraade, J., Method for Analysis of Polar Volatile Trace Components in Aqueous Samples by Gas Chromatography. *Anal. Chem.* **2005,** *77*, 3365-3371.
69. Janicki, W.; Wolska, L.; Wardecki, W.; Namiesnik, J., Simple Device for Permeation Removal of Water Vapour from Purge Gases in the Determination of Volatile Organic Compounds in Aqueous Samples. *J. Chromatogr. A* **1993,** *654*, 279-285.
70. Burns, W. F.; Tingey, D. T.; Evans, R. C.; Bates, E. H., Problems with a Nafion Membrane Dryer for Drying Chromatographic Samples. *J. Chromatogr.* **1983,** *269*, 1-9.
71. Woolfenden, E., Monitoring VOCs in Air Using Sorbent Tubes Followed by Thermal Desorption-Capillary GC Analysis: Summary of Data and Practical Guidelines. *J. Air Waste Manage. Assoc.* **1997,** *47*, 20-36.
72. Gawrys, M.; Fastyn, P.; Gawlowski, J.; Gierczak, T.; Niedzielski, J., Prevention of Water Vapour Adsorption by Carbon Molecular Sieves in Sampling Humid Gases. *J. Chromatogr. A* **2001,** *933*, 107-116.
73. Gawlowski, J.; Gierczak, T.; Pietruszynska, E.; Gawrys, M.; Niedzielski, J., Dry Purge for the Removal of Water from the Solid Sorbents Used to Sample Volatile Organic Compounds from the Atmospheric Air. *Analyst* **2000,** *125*, 2112-2117.
74. Baltussen, E.; Janssen, H. G.; Sandra, P.; Cramers, C. A., A New Method for Sorptive Enrichment of Gaseous Samples. Application in Air Analysis and Natural Gas Characterization. *J. High Resolut. Chromatogr.* **1997,** *20*, 385-393.
75. Raymond, A.; Guiochon, G., Use of Graphitized Carbon Black as a Trapping Material for Organic Compounds in Light Gases Before a Gas-Chromatographic Analysis. *J. Chromatogr. Sci.* **1975,** *13*, 173-177.
76. Lovkvist, P.; Jonsson, J. A., Capacity of Sampling and Preconcentration Columns with a Low Number of Theoretical Plates. *Anal. Chem.* **1987,** *59*, 819-821.
77. National Institue of Standards and Technology. Webbook. http://webbook.nist.gov/chemistry/
78. Baltussen, E.; David, F.; Sandra, P.; Janssen, H.-G.; Cramers, C. A., Sorption Tubes Packed with Polydimethylsiloxane. A New and Promising Technique for the Preconcentration of Volatiles and Semivolatiles from Air and Gaseous Samples. *J. High Resolut. Chromatogr.* **1998,** *21*, 332-340.
79. Baltussen, E.; David, F.; Sandra, P.; Cramers, C., On the Performance and Inertness of Different Materials Used for the Enrichment of Sulfur Compounds from Air and Gaseous Samples. *J. Chromatogr. A* **1999,** *864*, 345-350.
80. Baltussen, E.; Den Boer, A.; Sandra, P.; Janssen, H. G.; Cramers, C., Monitoring of Nicotine in Air Using Sorptive Enrichment on Polydimethylsiloxane and TD-CGC-NPD. *Chromatographia* **1999,** *49*, 520-524.
81. Grob, K.; Habich, A., Headspace Gas Analysis: The Role and the Design of Concentration Traps Specifically Suitable for Capillary Gas Chromatography. *J. Chromatogr.* **1985,** *321*, 45-58.
82. Burger, B. V.; Munro, Z., Headspace Gas Analysis. Quantitative Trapping and Thermal Desorption of Volatiles Using Fused-Silica Open Tubular Capillary Traps. *J. Chromatogr.* **1986,** *370*, 449-64.
83. Bicchi, C.; D'Amato, A.; David, F.; Sandra, P., Capturing of Volatiles Emitted by Living Plants by Means of Thick Film Open Tubular Traps. *J. High. Resolut. Chromatogr.* **1989,** *12*, 316-321.

84. Bicchi, C.; D'Amato, A.; David, F.; Sandra, P., Direct Capture of Volatiles Emitted by Living Plants. Part II. *Flavour Frag. J.* **1988,** *3*, 143-153.
85. Blomberg, S.; Roeraade, J., Preparative Capillary Gas Chromatography. II. Fraction Collection on Traps Coated with a Very Thick Film of Immobilized Stationary Phase. *J. Chromatogr.* **1987,** *394*, 443-453.
86. Gordin, A.; Amirav, A., Snifprobe: New Method and Device for Vapor and Gas Sampling. *J. Chromatogr. A* **2000,** *903*, 155-172.
87. Bonn, J.; Redeby, J.; Roeraade, J., Mixed Sorbent Phases for Thick Film Open Tubular Traps. *J. Chromatogr. Sci.* **2009,** *47*, 297-303.
88. Ettre, L. S.; Hinshaw, J. V., *Basic Relationships of Gas Chromatography*. 1993 ed.; Advanstar Communications: Cleveland, OH, 1993; p 45-46.
89. Cronin, D. A., Simple Quantitative Method for Trapping and Transfer of Low Concentration Gas Chromatographic Fractions Suitable for Use with Small Diameter Glass Column Systems. *J. Chromatogr.* **1970,** *52*, 375-83.
90. Sandra, P.; Saeed, T.; Redant, G.; Godefroot, M.; Verstappe, M.; Verzele, M., Odor Evaluation, Fraction Collection and Preparative Scale Separations with Glass Capillary Columns. *HRC & CC* **1980,** *3*, 107-114.
91. Bicchi, C.; D'Amato, A.; David, F.; Sandra, P., Direct Capture of Volatiles Emitted by Living Plants. *Flavour Frag. J.* **1987,** *2*, 49-54.
92. Blomberg, S.; Roeraade, J., A Technique for Coating Capillary Columns with a Very Thick Film of Crosslinked Stationary Phase for Gas Chromatography. *HRC & CC* **1988,** *11*, 457-61.
93. Overton, E. B. Chromatograph with Column Extraction. 98-US9165 9850129, 19980505., 1998.
94. Belov, Y. P.; Ulyanova, M. M.; Sidelnikov, V. N., Multicapillary Columns for Chromatography. *Am. Lab.* **2005,** *37*, 42-46.
95. Lane, D. A.; Johnson, N. D.; Barton, S. C.; Thomas, G. H. S.; Schroeder, W. H., Development and Evalutiaon of a Novel Gas and Particle Sampler for Semivolatile Chlorinated Organic Compounds in Ambient Air. *Environ. Sci. Technol.* **1988,** *22*, 941-947.
96. Krieger, M. S.; Hites, R. A., Diffusion Denuder for the Collection of Semivolatile Organic Compounds. *Environ. Sci. Technol.* **1992,** *26*, 1551-1555.
97. Ortner, E. K.; Rower, E. R., Trace Analysis of Semi-Volatile Organic Air Pollutants Using Thick Film Silicone Rubber Traps with Capillary Gas Chromatography. *J. High Resolut. Chromatogr.* **1996,** *19*, 339-344.
98. Kloskowski, A.; Pilarczyk, M.; Namiesnik, J., Denudation - A Convenient Method of Isolation and Enrichment of Analytes. *Critical Reviews in Analytical Chemistry* **2002,** *32*, 301-335.
99. Feng, C.; Mitra, S., Two-Stage Microtrap as an Injection Device for Continuous Online Gas Chromatographic Monitoring. *J. Chromatogr. A* **1998,** *805*, 169-176.
100. Frank, W.; Frank, H., The Micro-Trap: An Alternative to Cryofocussing in Capillary Gas Chromatography. *Chromatographia* **1990,** *29*, 571-574.
101. Mitra, S.; Yun, C., Continuous Gas Chromatographic Monitoring of Low Concentration Sample Streams Using an on-Line Microtrap. *J. Chromatogr.* **1993,** *648*, 415-421.

102. Mitra, S.; Lai, A., A Sequential Valve-Microtrap Injection System for Continuous, Online Gas Chromatographic Analysis at Trace Levels. *J. Chromatogr. Sci.* **1995,** *33*, 285-289.
103. Mitra, S.; Xu, Y. H.; Chen, W.; Lai, A., Characteristics of Microtrap-Based Injection Systems for Continuous Monitoring of Volatile Organic Compounds by Gas Chromatography. *J. Chromatogr. A* **1996,** *727*, 111-118.
104. Mitra, S.; Feng, C.; Zhang, L.; Ho, W.; McAllister, G., Microtrap Interface for on-Line Mass Spectrometric Monitoring of Air Emissions. *J. Mass Spectrom.* **1999,** *34*, 478-485.
105. O'Doherty, S. J.; Simmonds, P. G.; Nickless, G., Analysis of Replacement Chlorofluorocarbons Using Carboxen Microtraps for Isolation and Preconcentration in Gas Chromatography-Mass Spectrometry. *J. Chromatogr. A* **1993,** *657*, 123-129.
106. Tuan, H. P.; Janssen, H.; Cramers, C. A., Novel Preconcentration Technique for on-Line Coupling to High-Speed Narrow-Bore Capillary Gas Chromatography: Sample Enrichment by Equilibrium (Ab)Sorption I. Principles and Theoretical Aspects. *J. Chromatogr. A.* **1997,** *791*, 177-185.
107. Tuan, H. P.; Janseen, H.; Cramers, C. A.; Mussche, P.; J., L.; Wilson, N.; Handley, A., Novel Preconcentration Technique for on-Line Coupling to High-Speed Narrow-Bore Capillary Gas Chromatography: Sample Enrichment by Equilibrium (Ab)Sorption II. Coupling to a Portable Micro Gas Chromatograph. *J. Chromatogr. A* **1997,** *791*, 187-195.
108. Baltussen, E.; David, F.; Sandra, P.; Janseen, H.; Cramers, C., Equilibrium Sorptive Enrichment on Poly(Dimethylsiloxane) Particles for Trace Analysis of Volatile Compounds in Gaseous Samples. *Anal. Chem.* **1999,** *71*, 5193-5198.
109. Arthur, C. L.; Pawliszyn, J., Solid Phase Microextraction with Thermal Desorption Using Fused Silica Optical Fibers. *Anal. Chem.* **1990,** *62*, 2145-2148.
110. Zhang, Z.; Yang, M. J.; Pawliszyn, J., Solid Phase Microextraction. *Anal. Chem.* **1994,** *66*, 844A-853A.
111. Alpendurada, M. D. F., Solid-Phase Microextraction: A Promising Technique for Sample Preparation in Environmental Analysis. *J. Chromatogr. A* **2000,** *889*, 3-14.
112. Pawliszyn, J., *Application of Solid Phase Microextraction*. Royal Society of Chemistry: Letchworth, Hertfordshire, UK, 1999; p 655.
113. Wercinski, S. A. S., *Solid Phase Microextraction: A Practical Guide*. Marcel Dekker, Inc.: New York, 1999; p 257.
114. Lord, H.; Pawliszyn, J., Evolution of Solid-Phase Microextraction Technology. *J. Chromatogr. A* **2000,** *885*, 153-193.
115. Koziel, J. A.; Jia, M.; Pawliszyn, J., Air Sampling with Porous Solid-Phase Microextraction Fibers. *Anal. Chem.* **2000,** *72*, 5178-5186.
116. Augusto, F.; Koziel, J. A.; Pawliszyn, J., Design and Validation of Portable SPME Devices for Rapid Field Air Sampling and Diffusion-Based Calibration. *Anal. Chem.* **2001,** *73*, 481-486.
117. Razote, E.; Jeon, I.; Maghirang, R.; Chobpattana, W., Dynamic Air Sampling of Volatile Organic Compounds Using Solid Phase Microextraction. *J. Environ. Sci. Health, B* **2002,** *37*, 365-378.
118. Hook, G. L.; Lepage, C. J.; Miller, S. I.; Smith, P. A., Dynamic Solid Phase Microextraction for Sampling of Airborne Sarin with Gas Chromatography-Mass Spectrometry for Rapid Field Detection and Quantifiation. *J. Sep. Sci.* **2004,** *27*, 1017-1022.

119. Yassaa, N.; Williams, J., Analysis of Enantiomeric and Non-Enantiomeric Monoterpenes in Plant Emissions Using Portable Dynamic Air Sampling/Solid-Phase Microextraction (PDAS-SPME) and Chiral Gas Chromatography/Mass Spectrometry. *Atmos. Environ.* **2005,** *39*, 4875-4884.
120. Isetun, S.; Nilsson, U., Dynamic Field Sampling of Airborne Organophosphate Triesters Using Solid-Phase Microextraction under Equilibrium and Non-Equilibrium Conditions. *Analyst* **2005,** *130*, 94-98.
121. Ciucanu, I., Helical Sorbent for Fast Sorption and Desorption in Solid-Phase Microextraction-Gas Chromatographic Analysis. *Anal. Chem.* **2002,** *74*, 5501-5506.
122. Ciucanu, I.; Caprita, A.; Chiriac, A.; Barna, R., Helical Sorbent Microtrap for Continuous Sampling by a Membrane and Trap Interface for on-Line Gas Chromatographic Monitoring of Volatile Organic Compounds. *Anal. Chem.* **2003,** *75*, 736-741.
123. Ramsey, S. A.; Mustacich, R. V.; Smith, P. A.; Hook, G. L.; Eckenrode, B. A., Directly Heated High Surface Area Solid Phase Microextraction Sampler for Rapid Field Forensic Analyses. *Anal. Chem.* **2009,** *81*, 8724-8733.
124. Greenberg, J. P.; Lee, B.; Helmig, D.; Zimmerman, P. R., Fully Automated Gas Chromatograph-Flame Ionization Detector System for the in Situ Determination of Atmospheric Non-Methane Hydrocarbons at Low Parts Per Trillion Concentration. *J. Chromatogr. A* **1994,** *676*, 389-398.
125. Contreras, J. A. Axial Temperature Gradients in Gas Chromatography. Brigham Young University, Provo, UT, 2010.
126. Li, W. C.; Andrews, A. R. J., A Modified Inlet System for High-Speed Gas Chromatography Using Inert Metal Tubing with a Carbon Dioxide Cooled Cryotrap. *J. High Resolut. Chromatogr.* **1996,** *19*, 492-496.
127. Bertman, S. B.; Buhr, M. P.; Roberts, J. M., Automated Cryogenic Trapping Technique for Capillary GC Analysis of Atmospheric Trace Compounds Requiring No Expendable Cryogens: Application to the Measurement of Organic Nitrates. *Anal. Chem.* **1993,** *65*, 2944-6.
128. Farwell, S. O.; Verwolf, A.; Cai, Z.; Smith, P.; Roy, W., Design and Performance of an Integrated Analytical Swatch Testing System. *Instrum Sci. Technol.* **2008,** *36*, 577-597.
129. Bruno, T. J., Application of the Vortex Tube in Chemical Analysis. Part 2. Applications. *Am. Lab.* **1993,** *25*, 16, 18, 20-24.
130. Bruno, T. J., Applications of the Vortex Tube in Chemical Analysis. Part 1. Introductory Principles. *Am. Lab.* **1993,** *25*, 15-20.
131. De Greef, J.; De Proft, M.; De Winter, F., Gas Chromatographic Determination of Ethylene in Large Air Volumes at the Fractional Parts-Per-Billion Level. *Anal. Chem.* **1976,** *48*, 38-41.
132. Kivi-Etelaetalo, E.; Kostiainen, O.; Kokko, M., Analysis of Volatile Organic Compounds in Air Using Retention Indices Together with a Simple Thermal Desorption and Cold Trap Method. *J. Chromatogr. A* **1997,** *787*, 205-214.
133. Bouche, M.-P. L. A.; Lambert, W. E.; Van Bocxlaer, J. F. P.; Piette, M. H.; De Leenheer, A. P., Quantitative Determination of N-Propane, Iso-Butane, and N-Butane by Headspace GC-MS in Intoxications by Inhalation of Lighter Fluid. *J. Anal. Toxicol.* **2002,** *26*, 35-42.
134. Ciccioli, P.; Brancaleoni, E.; Mabilia, R.; Cecinato, A., Simple Laboratory-Made System for the Determination of C2-C7 Hydrocarbons Relevant to Photochemical Smog Pollution. *J. Chromatogr., A* **1997,** *777*, 267-274.

135. PerkinElmer. http://www.perkinelmer.com
136. Markes. http://www.Markes.Com/Instrumentation/Default.Aspx.
137. Qin, Y.; Walk, T.; Gary, R.; Yao, X.; Elles, S., C2-10 Nonmethane Hydrocarbons Measured in Dallas, USA - Seasonal Trends and Diurnal Characteristics. *Atmos. Environ.* **2007,** *41*, 6018-6032.
138. Hinshaw, J. V., Thermal Desorption Sampling. *LC-GC* **2000,** *18*, 940-949.
139. Kaiser, R., Reversion Gas Chromatography: A Method for Determination of Traces of Volatile Substances in Gas in the ppb. Range. *Fresenius' Z. Anal. Chem.* **1968,** *236*, 168-170.
140. Kaiser, R. E., Enriching Volatile Compounds by a Temperature Gradient Tube. *Anal. Chem.* **1973,** *45*, 965-967.
141. Drozd, J.; Novak, J.; Rijks, J. A., Quantitative and Qualitative Head-Space Analysis of Parts Per Billion Amounts of Hydrocarbons in Water. A Study of Model Systems by Capillary-Column Gas Chromatography with Splitless Sample Injection. *J. Chromatogr.* **1978,** *158*, 471-482.
142. Rijks, J. A.; Drozd, J.; Novak, J., Versatile All-Glass Splitless Sample-Introduction System for Trace Analysis by Capillary Gas Chromatography. *J. Chromatogr.* **1979,** *186*, 167-181.
143. Reglero, G.; Herraiz, T.; Herraiz, M., Direct Headspace Sampling with on-Column Thermal Focusing in Capillary Gas Chromatography. *J. Chromatogr. Sci.* **1990,** *28*, 221-224.

2 Hand-portable Gas Chromatograph-Toroidal Ion Trap Mass Spectrometer (GC-TMS) for Detection of Hazardous Compounds in Harsh Environments *

2.1 Introduction

When exposure to hazardous compounds, such as chemical warfare agents (CWAs) and toxic industrial chemicals (TICs), is a concern, the ability to rapidly detect and accurately identify such chemicals in harsh environments is of great utility. There is a need for field-portable, selective, and sensitive detectors for military and emergency first-responder operations and for on-site environmental contamination measurement, to mention only a couple of key applications. The development of field-portable devices directed towards fast, on-site analysis is one of the most active research areas in analytical chemistry.

Currently, several approaches for detection of CWAs and TICs are utilized by military personnel, first responders, and environmental scientists. They include dye solubility (detection paper), enzymatic reaction, gas-solid phase reaction, surface acoustic wave (SAW), flame photometry (FPD), and ion mobility spectrometry (IMS).[1-4] These detectors, although small and relatively easy to use in the field, offer only limited chemical specificity and sensitivity, and they are prone to false positive responses.[3] They typically can confirm only what is already believed to be present, but cannot provide information about other possible harmful agents.[1,5]

* Published as:
Contreras, J. A.; Murray, J. A.; Tolley, S. E.; Oliphant, J. L.; Tolley, H. D.; Lammert, S. A.; Lee, E. D.; Later, D. W.; Lee, M. L., Hand-Portable Gas Chromatograph-Toroidal Ion Trap Mass Spectrometer (GC-TMS) for Detection of Hazardous Compounds. *J. Am. Soc. Mass Spectrom.* **2008,** *19*, 1425-1434.

Combining results obtained from several individual analytical techniques has been shown to be particularly advantageous for detection of possible chemical threats.[6] MS alone can be used to identify unknown compounds from their characteristic fragmentation patterns, however, for complex mixtures, compound identification by MS alone can be challenging. MS coupled with a separation technique such as gas chromatography (GC) can provide two-dimensional analysis, which provides significantly greater power for identification of compounds in complex mixtures. Analytical advantages of high sensitivity, high selectivity, and rapid response time make GC-MS a preferred detection technique for CWAs and TICs.[7] GC-MS remains the standard for positive identification of unknown volatile and semi-volatile organic compounds, and the preferred instrumentation for field detection and verification of chemical agents.[1,8, 9]

Major efforts have been made to miniaturize capillary GC[10-14] and most MS analyzers, including time-of-flight (TOF),[15-17] quadrupole,[18] magnetic sector,[17-19] Fourier transform ion cyclotron resonance (FTICR),[20] and cylindrical,[21-23] rectilinear,[24-26] and toroidal[27,28] ion traps. Most of these reports have concentrated on miniaturizing the GC column or the mass analyzer. However, few groups have focused on miniaturizing other system components such as vacuum pumps, electronics and consumable items required for truly portable (i.e., totally self-contained) GC-MS systems.[19,24,29,30] Even so, a number of so-called portable systems have been commercialized.[9,24,29-36] The most widely used portable GC-MS system by military and first responder personnel, for example, suffers from several limitations: the analysis time for a sample is about 15 min,[32,36] which is quite slow for field applications that require immediate response; the use of a membrane sample inlet limits the range of analytes that can be introduced into the system;[38] the getter vacuum pump in this system has a finite lifetime (30 days at 8 h/day

operation) and must be replaced at the manufacturer's facility; and field-portability requires taking along the support platform, which weighs about as much as the GC-MS system.

The high demand for portable GC-MS is driving further efforts to develop systems that are even smaller and more rugged, with the goal of producing a truly hand-portable GC-MS system. Among the different types of mass analyzers, ion traps are ideal candidates for miniaturization because of their simplicity, high sensitivity, relatively high operating pressure, and less stringent ion optic element alignment compared to other types of MS analyzers.[39] Furthermore, ion traps provide potential for tandem MS operation in a portable MS format. Lower power consumption can be achieved by reducing the trapping volume radial dimension. One limitation to miniaturizing ion traps is reduction in ion storage capacity. However, this reduction can be ameliorated by trapping ions in a toroidal geometry.[27,28,39]

Power reduction and short analysis time are the main challenges for the GC component of portable GC-MS. Microchip based GC has certainly demonstrated both reduced analysis time and reduced power consumption, however, it has proven difficult to evenly coat the separation channels and to connect them to injection systems and detectors, and their separation performance has not yet matched the high efficiency of conventional fused silica capillary columns.[12] Another approach has been to use low thermal mass GC that relies on resistively heating the capillary column instead of using a bulky convection oven.[11,14,40-42] Resistive heating provides high heating and cooling efficiency and speed. These qualities make low thermal mass GC ideal for fast analysis with minimum power consumption.

Two major challenges of any field analysis method is the collection and subsequent transfer of a sample to the analytical system. Many of the current CWA and TIC detectors rely on vapor detection. This is a problem for detection of less volatile CWAs and TICs, particularly

at low environmental temperatures where vapor pressures of the target analytes are greatly reduced. Solid phase micro extraction (SPME) offers a convenient method for sampling gaseous, liquid and dissolved solid samples, concentrating the analytes, and transferring them to the injection port of a GC-MS. SPME theory, methodologies, and applications can be found elsewhere.[43-45] There are a number of reports that validate the use of SPME for the analysis of CWAs in air, water and soil.[46-51] These studies include the analysis of hydrogen cyanide,[46] VX,[50,52] sarin,[48-50] soman,[50] tabun,[50] and mustard.[51] There have also been reports describing the detection of precursor chemicals and degradation products of CWAs using SPME.[52-55]

In this paper a new, portable GC-MS system is described, which is totally self-contained with carrier gas supply and battery power source. Sample introduction is performed using SPME with a low thermal mass GC injector for rapid desorption. Chromatographic separation is performed using a low thermal mass GC, and the mass analyzer consists of a miniature toroidal ion trap mass spectrometer (TMS). Embedded software performs data analysis during which TMS spectra are matched with on-board library spectra for positive identification of target compounds.

2.2 Experimental

2.2.1 GC-TMS instrumentation

The portable GC-TMS system (Guardion-7, Torion Technologies, American Fork, UT, USA) consists of a low thermal mass injector, a low thermal mass GC and a miniature toroidal ion trap mass analyzer. The entire system is a stand alone instrument that can be used in the field without additional electrical power, gas supply, or equipment for data analysis and identification. The system is housed in a 47 x 36 x 18 cm (18.5 x 14 x 7 in.) Pelican case (Torrance, CA) and

weighs about 13 kg (28 lb), including batteries (Figure 2.1A). The portable GC-TMS can be fully operated without an external computer system. A 6 in. liquid crystal display (LCD) allows real-time monitoring of the chromatogram and mass spectra. A graphical user interface (GUI) is used to navigate via three buttons between different options and windows that are displayed on the LCD. The GC-TMS system uses spectral deconvolution software (Ion Signature Technologies, N. Smithfield, RI, USA) to enhance compound separation and identification.[56] The peak deconvolution algorithm improves the identification of poorly resolved GC peaks and obscure trace components. After completion of a run, accumulated data are deconvolved, and compounds that are detected and identified are displayed in tabular format on the LCD screen. Further data analysis can also be performed using a laptop via Ethernet connection or after downloading data from a flash memory card.

A 90 cm^3 disposable helium (He) cartridge provides the carrier gas to the GC-TMS system (Figure 2.1B). Cartridges are pressurized to 2500 psig, providing enough helium for about 100 analyses at a constant 25 psig column head pressure. The design of the GC-TMS instrument allows for easy access and replacement of the helium cartridges and batteries.

The peak power requirement of the GC-TMS is 80 W when all heaters (injection port, column and transfer line) are utilized during the chromatographic analysis. This power is supplied by two non-rechargeable 24 V, 7.5 Ah lithium/sulfur dioxide ($LiSO_2$) BA 5590 military-approved batteries, which allows roughly 50 consecutive analyses before the batteries must be replaced. The system could be modified for lithium ion rechargeable batteries (BB 2590) by changing the instrument power supply design. An AC-to-DC 24 V power converter can be used when 110 V AC is available.

A

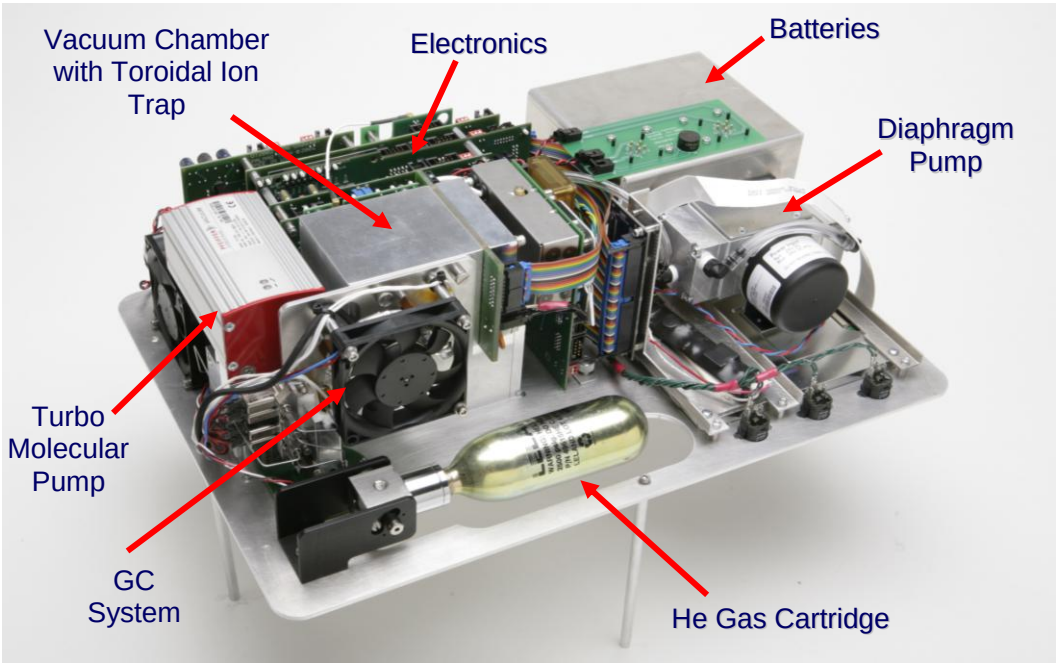

B

Figure 2.1. Photographs of the Guardion-7 GC-TMS showing (A) dimensions and (B) internal components.

The GC-TMS start-up time from power-on to ready state for injection is about 3 min, and the total sample analysis turnaround time is 5 min, including time for column cool-down.

2.2.2 Mass analyzer

The miniature toroidal radio frequency ion trap mass analyzer has been previously described by Lammert et al.[27] Figures 2.2A and 2.2B show photographs of the toroidal ion trap and Figure 2.2C shows a cross-sectional drawing of the TMS, which includes the electron-gun assembly, trapping region and the detector assembly. The toroidal trapping region has a radius (r_o) of 2 mm and provides a storage capacity similar to a conventional cylindrical ion trap of r_o=10 mm. A nominal RF trapping frequency of 3 MHz is used with a trapping amplitude of about 800 V_{p-p}. During mass analysis, an ejection frequency sweep is applied to the filament end-cap to perform resonance ejection. This type of mass analysis provides better mass resolution than the traditional linear amplitude RF scan. Furthermore, simpler electronics are needed, in that the RF generator needs only a fixed-amplitude power supply. During the scanning period, the ejection frequency is scanned from ca. 1.4 MHz to approximately 100 KHz with about 5 V_{p-p} amplitude over the course of 60 ms (7500 Th/s) (see timing diagram, Figure 2.3). The electron gun produces a gated electron beam (-70 eV) for ionization of analyte molecules. Ions are detected with a custom, continuous dynode electron multiplier detector (DeTech, Palmer, MA) with an approximate gain of 10^6 at 1300-1500 V. The electron multiplier voltage is automatically set by monitoring the noise level during the first few seconds of each run. Ionization timing control is used to regulate the number of ions that are trapped, preventing overloading and ensuring optimal mass resolution. Ionization timing (Figure 2.3) is automatically controlled to values between 0.03-60 ms. The number of ions in the trap is monitored for each 60-ms scan and kept below a specified level by automatically adjusting the ionization time. Since ionization

timing control is used, the sampling rate of the system varies from 8 to 16 scans/s, depending on the sample concentration. Work is in progress to increase the scanning rate to allow for faster separations and shorter analysis times.

2.2.3 Vacuum system

The GC-TMS pumping system consists of a miniature dual-stage diaphragm roughing pump and a miniature turbo-molecular pump (Figure 2.1B). The roughing pump is a two-stage diaphragm pump (Model PU1781-N84.0-8.05, KNF Neuberger, Trenton, NJ) and the turbo-molecular drag pump has a pumping capacity of 11 L/s, a rotation speed of 90,000 rpm, and can achieve pressures below $5x10^{-4}$ Torr (Model TPD 011, Pfeiffer Vacuum, Nashua, NH). The assembled vacuum system can achieve pressures below $1x10^{-3}$ Torr in 2 min with a 0.5 cm^3/min of helium flow through the GC column.

2.2.4 Low thermal mass GC

The low thermal mass GC column assembly is fabricated by RVM Scientific (Santa Barbara, CA) from a 5 m x 0.1 mm i.d. x 0.4 μm d_f MTX-5 column (Restek, Bellefonte, PA). Various columns can be used depending on user applications. The column is bundled with a resistive heating wire and thermocouples for temperature control. A small box fan is used for column cool-down (Figure 2.1B). This GC assembly is mounted on a fixture and connected to the low thermal mass injector and to the TMS through a transfer line. Under typical temperature programming conditions, the initial temperature (40°C) is held for 10 s before it ramps to a final temperature of 250°C at a ramp rate of 120°C/min. The low thermal mass injector and transfer line are kept at 270°C. Helium is used as the mobile phase with a flow rate of 0.4 mL/min at 100°C.

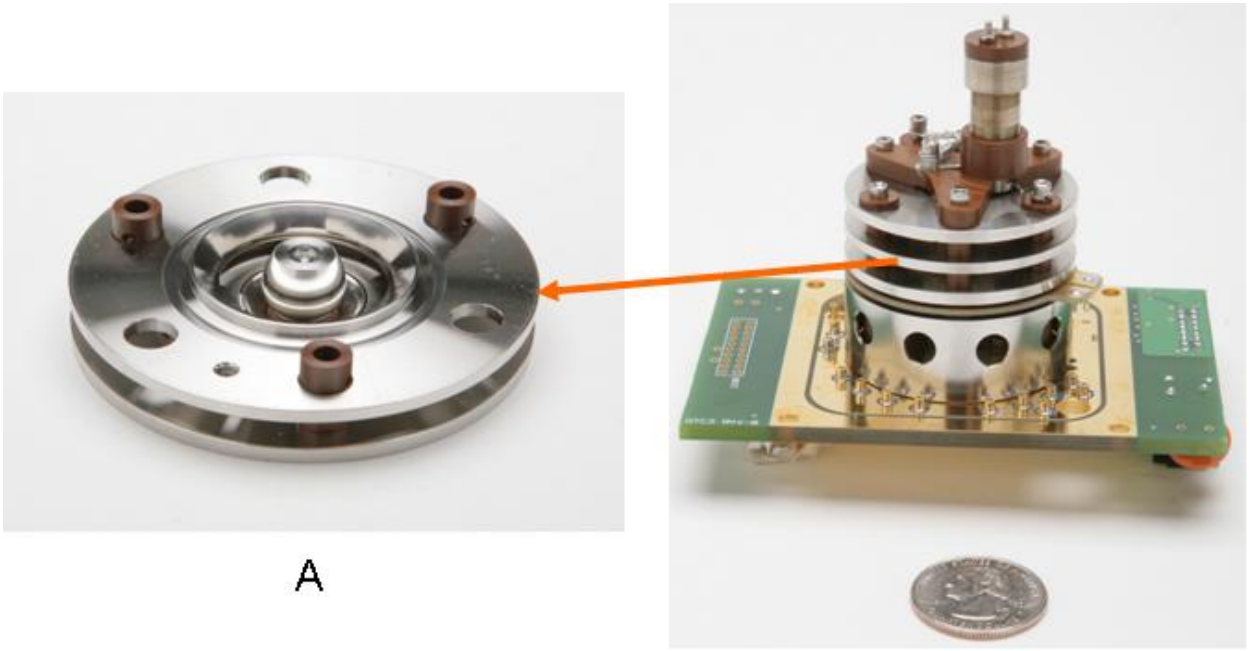

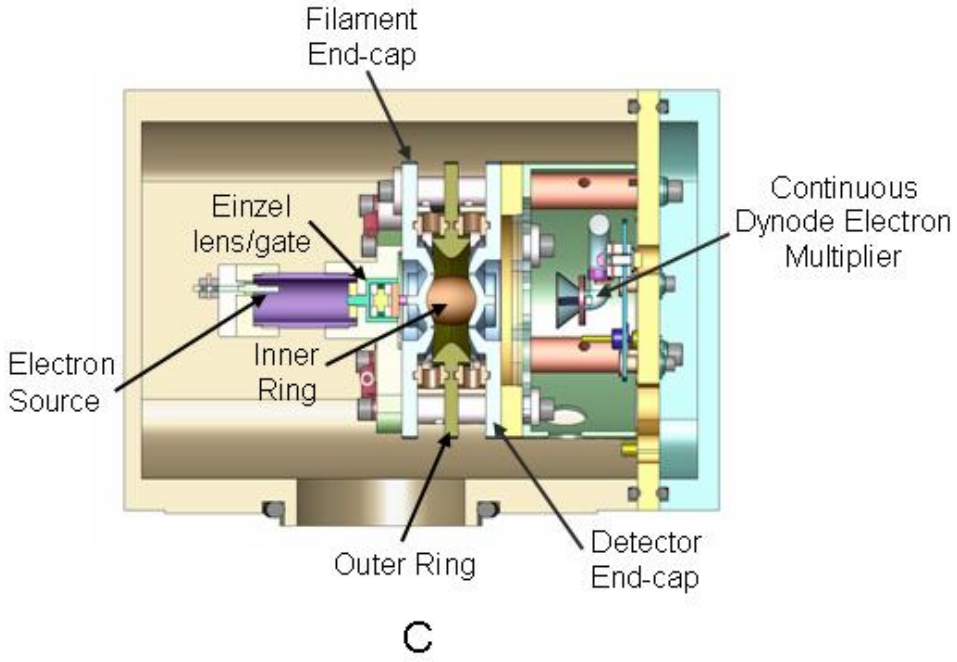

Figure 2.2. Miniature toroidal ion trap mass spectrometer. (A) Photograph of ion trap electrodes with top end-cap removed to show the ion storage region. (B) Photograph of ion trap stack and detector board assembly. (C) Cross-section diagram of toroidal ion trap mass analyzer showing major components. The end of the GC column (not shown) is placed between the filament end-cap and outer ring of the toroidal ion trap assembly.

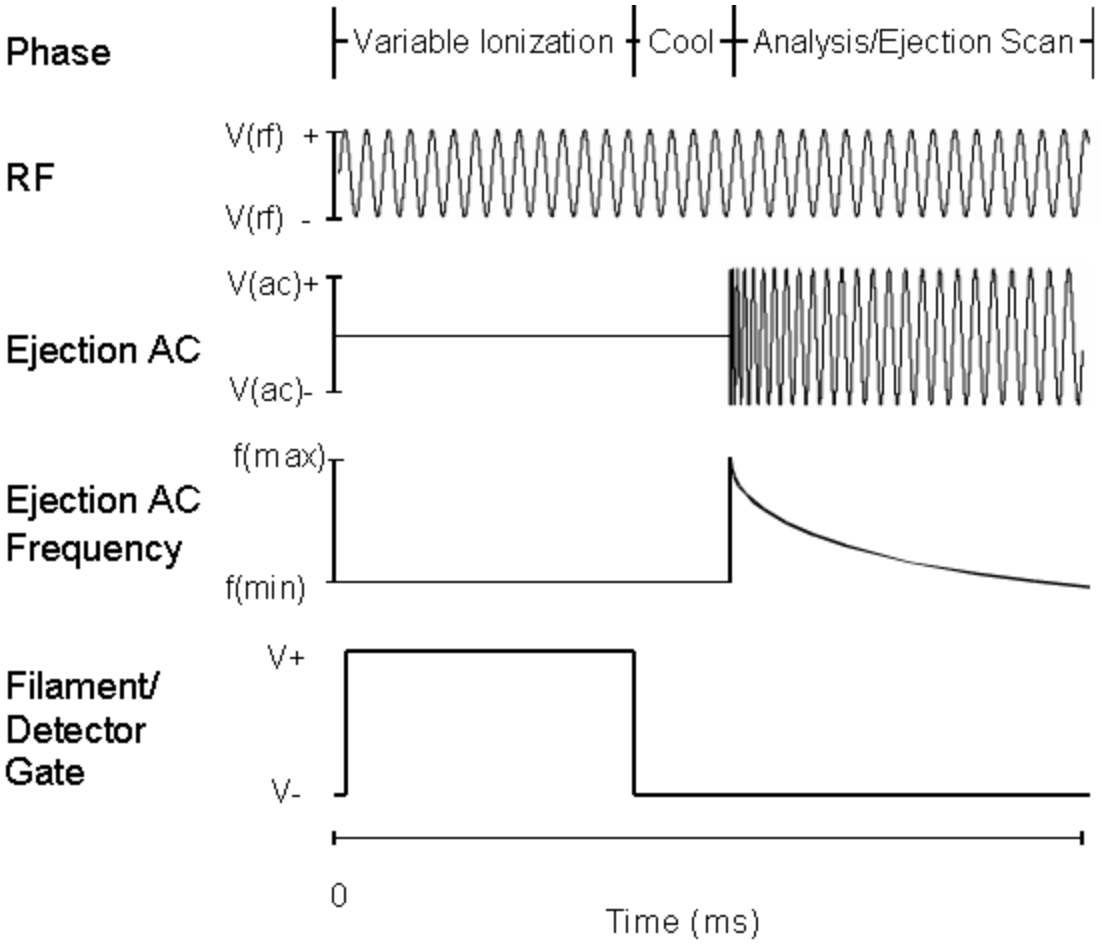

Figure 2.3. Timing diagram for the toroidal ion trap. The ejection frequency decreases with time according to 1/f to linearize the m/z scale; the filament gate is variable from 60.0 to 0.03 ms to control ionization; and the maximum ionization time is indicated.

2.2.5 SPME and SPME holder

SPME is an excellent solvent-free extraction method that combines extraction and concentration into a single step for the analysis of gases and liquid samples.[57] These features make SPME a convenient sampling method for on-site analysis. Because the GC-TMS system is designed for use in the field, a new SPME holder was developed to be easily operated with one hand while wearing bulky personal protective equipment. Figure 2.4 shows photographs of the

new SPME holder. The push button trigger (similar to the mechanism common to ball point pens) on top of the syringe enables the SPME fiber (65 µm PDMS-DVB, Supelco, Bellefonte, PA) to be extended from or withdrawn into a protective metal needle after sampling and while being inserted into the injection port of the GC-TMS. The SPME holder has a weight of 34.7 g (1.22 oz) and a length of 18.5 cm (7.2 in.) when the fiber is retracted. The active sample collection surface of the SPME fiber is 1-2 cm long and is coated with a 7-100 µm polymer film. Previous studies have indicated that polydimethylsiloxane-divinylbenzene (PDMS-DVB) is the preferred commercially available SPME coating for CWAs and TICs.[46-55] The GC temperature program and data acquisition automatically start when the SPME holder contacts the injection port. The SPME holder contains a miniature electronic board with a microchip that has the potential for receiving and storing sample related metadata.

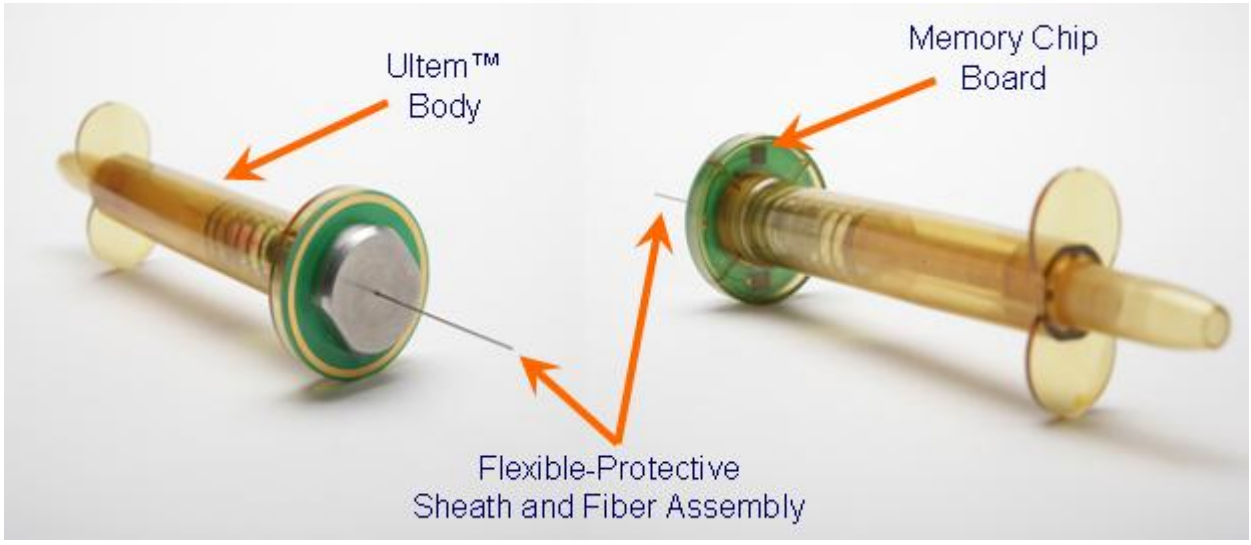

Figure 2.4. Photograph of SPME fiber holder syringe with memory chip for metadata storage.

2.2.6 Low thermal mass injector

The resistively heated split/splitless injector was specifically designed for SPME with a low volume in order to minimize band broadening during injection.[58-60] The custom-made injector was constructed from 0.31 mm i.d. stainless steel tubing wrapped with Nichrome 80 heating wire (Pelican Wire, Naples, FL). No liner was utilized in the design since SPME allows sampling of dirty matrices with minimal contamination of the injection system. However, possible adsorption of analytes was reduced by Sulfinert treatment (Restek) of the injector. If the injector does become contaminated, the injector assembly can be removed and cleaned. Because of its low thermal mass, the injector can be heated from room temperature to 270^{o}C in less than 3 min using less than 9 W of power and consuming only 6 W to maintain operating temperature. The use of Merlin Microseal septa (Restek) allows up to 2500 injections before replacement of a septum. For this work, splitless injections were performed by opening the split valve between 0.5 and 7 s after injection. The split ratio is nominally 20:1 when the split valve is open. The injector is also equipped with a septum purge that is typically operated at 1.0 mL/min continuous flow rate.

2.2.7 Data analysis

Quantitative deconvolution software (Ion Signature) is used for target compound identification. This software is embedded in the operating system of the GC-TMS. It uses both retention times and key mass spectral data to identify compounds. The data collected by the GC-TMS system are processed in near real time and matched against characteristic retention times and ion abundances for target analytes that are preloaded into the internal compound library. Identified compounds are listed on the LCD screen, along with hazard classification and match confidence level shortly after completing the analytical run.

2.2.8 Chemicals and standards

All chemicals used were commercially available. Diethylphthalate (99.5%), n-butylbenzene (99+%), and 2-chloroacetophenone (98%) were obtained from Sigma-Aldrich (Milwaukee, WI). Benzene (HPLC grade) was obtained from Spectrum Chemicals and Laboratory Equipment (Gardena, CA). Toluene (HPLC grade) and methyl salicylate (99%) were purchased from Fisher Scientific (Fairlawn, NJ), and naphthalene (Baker Analyzed Grade) was obtained from JT Baker (Phillipsburg, NJ). The 624 EPA volatile halocarbon mix (2000 μg/mL in methanol) was obtained from Restek. Disposable 90 cm^3 helium cartridges were custom packaged by Leland (South Plainfield, NJ).

2.2.9 Sampling methodology

Sample solutions were placed in 15-20 mL vials with septum caps. The SPME needle was pushed through the septum in the vial cap and the SPME fiber was exposed to either the solution or head space. The exposure period was 30 s and 5 min for liquid and head space sampling, respectively. The SPME exposure time was chosen to simulate realistic field sampling protocols. The sample was desorbed from the SPME fiber for about 8 s at 270°C after insertion of the syringe needle into the injection port of the GC-TMS.

2.3 Results and Discussion

2.3.1 Mass calibration

Routine mass calibration is performed automatically by the GC-TMS by introducing a standard mixture of compounds with known GC retention order and fragment peak abundances. Any compound can be used for mass calibration as long as retention time and selected m/z

values and abundances are provided. During mass analysis, an ejection frequency is applied so that masses are scanned from 35 to 535 m/z. To calibrate the mass scale for the acquired data, a scan index is used. The scan index is obtained by dividing the electron multiplier signal during the mass analysis scan (60 ms) into 4000 discrete indices (15 μs each). The signal for each 15-μs scan is summed and stored in the appropriate index. The automated mass calibration algorithm software looks for mass fragment peaks at the retention time specified and assign a scan index to the mass. A linear plot of the m/z versus scan index is then used as the mass calibration for the instrument.[61] A seven-component mixture consisting of benzene, toluene, n-butylbenzene, naphthalene, 2-chloroacetophenone, diethylphthalate, and decafluorotriphenylphosphene in water (10 ppm each) was used in this work for calibration. After sampling for 30 s, compounds were thermally desorbed into the GC-TMS injector. The ions selected for automatic calibration were m/z 78 from benzene, m/z 65 and 91 from toluene, m/z 105 from 2-chloroacetophenone, m/z 128 from naphthalene, m/z 134 from n-butylbenzene, and m/z 149, 177, and 222 from diethylphthalate, and m/z 275 and 442 from decafluorotriphenylphosphine. A linear least squares curve fit provided an R^2 value of 0.99994 for a mass range of 65 to 442 m/z. Automatic mass calibration is simple to perform and allows the GC-TMS instrument to be rapidly and frequently calibrated to ensure mass accuracy during field measurements.

2.3.2 Mass spectral resolution

Toluene, dibromochloromethane, and diethylphthalate were used to determine the mass spectral resolution of the TMS. Samples of these compounds were prepared at the same concentration and sampled using the same procedure as previously described for automatic mass calibration. The mass spectral resolution of the GC-TMS instrument at full-width half-maximum (FWHM) was 0.42, 0.68, and 0.80 Dalton for toluene (m/z = 91), dibromochloromethane (m/z =

127), and diethylphthalate (m/z = 222), respectively. Spectra for toluene and dibromochloromethane are shown in Figure 2.5. The fragment ions and isotope ratios in these spectra are in close agreement with theoretical (isotope ratios) and library reference values. Better than unit mass resolution was obtained for the m/z range from <100 to >200, which is comparable to the resolution achieved by most bench-top MS systems.

2.3.3 Detection limits

GC-TMS detection limits were determined from both direct liquid injection and SPME headspace sampling. Direct liquid injections of chemical agent simulants (di-n-butylsulfide and methyl salicylate) were performed to determine the minimum quantity of compound introduced into the GC column that could be detected. Ethanol solutions with concentrations from 1.6 to 1600 ppm were prepared. Direct liquid injections of 0.1 μL were performed using a 0.5 μL SGE syringe (Austin, TX). Detection limits corresponding to a total ion signal intensity that was 3σ above the background uncertainty from blank replicates were found to be 200 and 300 pg for methyl salicylate and di-n-butylsulfide, respectively. A linear response was observed for concentrations ranging from 0.2 to 160 ng with an R^2 value of 0.995 for di-n-butylsulfide.

Headspace sampling was performed to determine the method detection limits. A four compound mixture (benzene, toluene, n-butylbenzene, and naphthalene) was used, and aqueous solutions ranging in concentration from 0.1 to 100 ppb were prepared. A 15-mL aliquot of each solution was placed in 20 mL vials with septum caps. Headspace SPME sampling was performed for 5 min and then desorbed in the GC injector port. The method detection limits were 0.1 ppb for n-butylbenzene and naphthalene, 1 ppb for toluene, and 10 ppb for benzene.

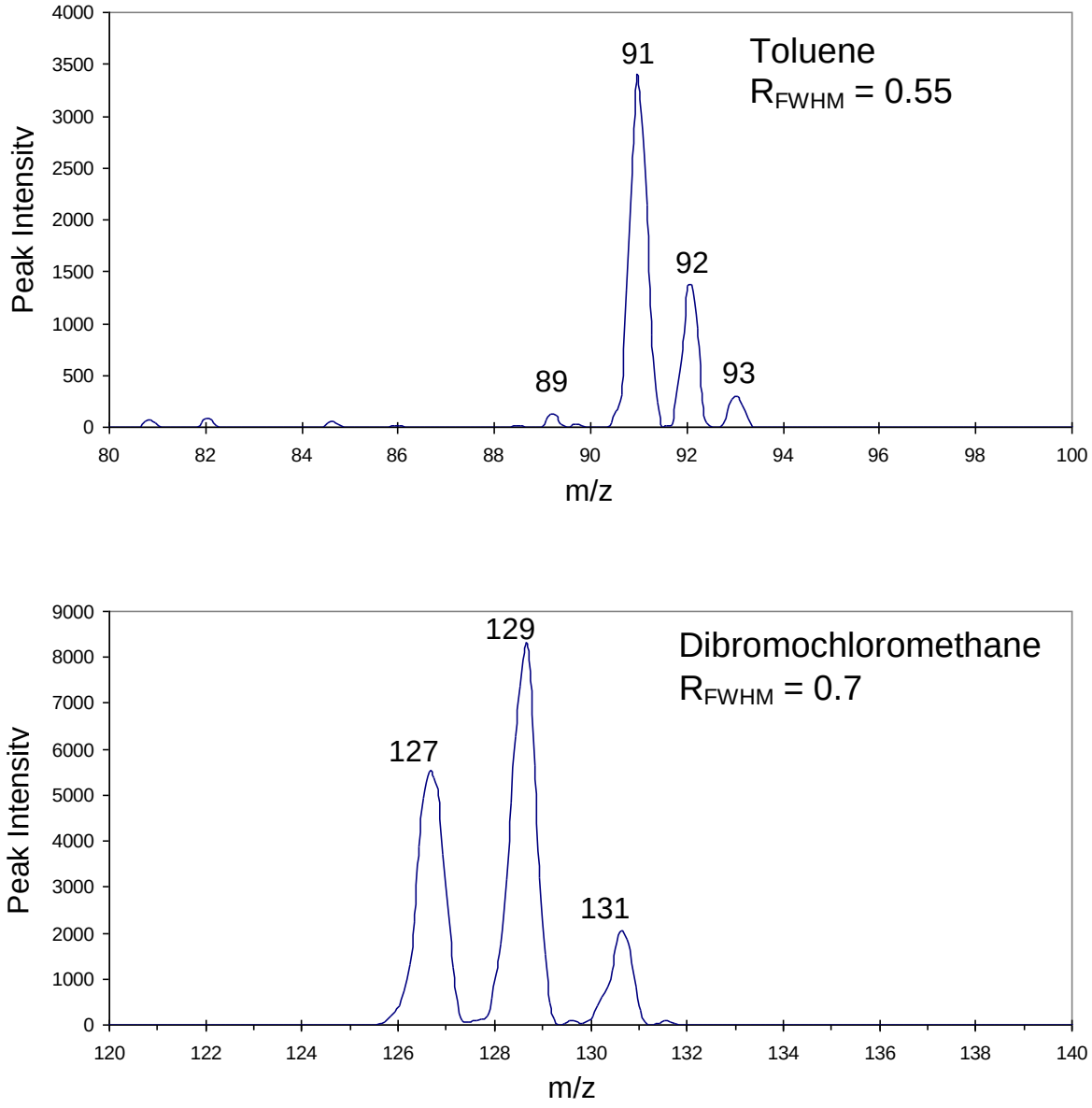

Figure 2.5. Mass spectra showing resolution of toluene and dibromochloromethane ions.

2.3.4 Analysis of chemical warfare agents

CWAs are substances that are intended for military purposes to be lethal, seriously injure, or incapacitate target individuals because of their physiological effects. Spectra were obtained using the GC-TMS for research development test and evaluation standards (50 µg/mL each in isopropanol) of the nerve agents sarin (GB), soman (GD), cyclosarin (GF), and VX, as well as the blister agent mustard (HD). Figure 2.6 shows mass spectra for HD, GB and VX. The ion fragments in these spectra are in close agreement with theoretical and library reference values. These analyses demonstrate the capability of the portable GC-TMS instrument for the detection of CWAs.

2.3.5 Analysis of EPA Method 624 volatile halocarbon compounds

EPA Method 624 is employed for the chemical analysis and determination of volatile organic compounds in municipal and industrial waste water.[60] A standard mixture of the EPA Method 624 volatile halocarbon compounds was diluted to 20 ppm in water, and SPME sampling was performed as previously described. Separation of the mixture was achieved in less than 65 s (Figure 2.7). Compounds that were not completely resolved chromatographically were resolved and identified using the deconvolution software described in the experimental section. Examples of spectra for tetrachloroethene and bromoform are given in Figure 2.9. This separation shows the ability of the portable GC-TMS system to rapidly separate and identify organic compounds in complex mixtures.

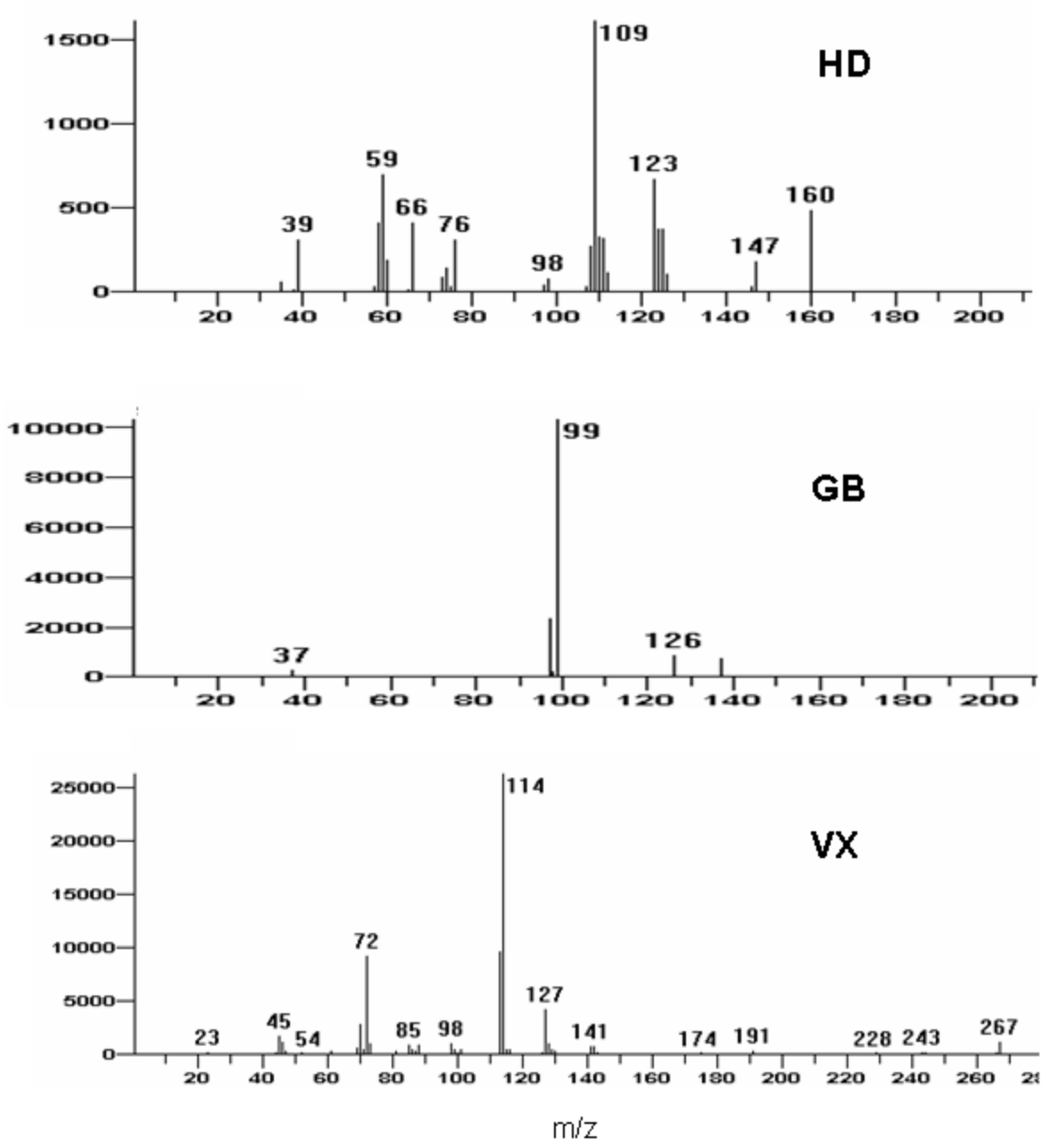

Figure 2.6. Mass spectra of HD blister agent and GB and VX nerve agents.

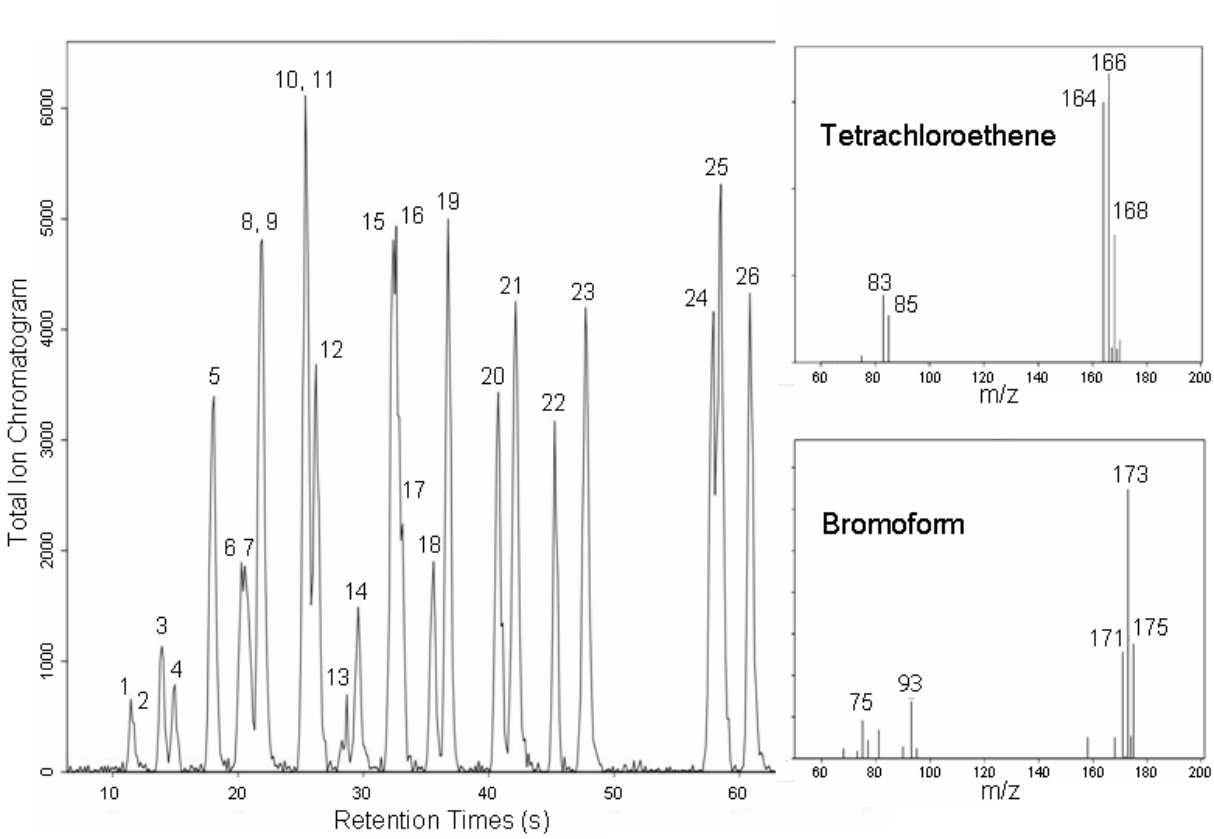

Figure 2.7. Total ion chromatogram of a 26 component EPA Method 624 volatile halocarbon compound mixture (20 ppm in water) with mass spectral inserts for tetrachloroethene (peak 19) and bromoform (peak 22). GC temperature program: 40 C^{o} for 10 s, then 120 C^{o}/min to 250 C^{o} and hold for 10 s. Peak identifications: (1) 1,1-dichloroethane, (2) methylene chloride, (3) trans-1,2-dichloroethene, (4) 1,1-dichloroethane, (5) chloroform, (6) 1,2-dichloroethane, (7) 1,1,1-trichloroethene, (8) benzene, (9) carbon tetrachloride, (10) 1,2-dichloropropane, (11) trichloroethylene, (12) bromodichloromethane, (13) 2-chloroethylvinyl ether, (14) cis-1,3-dichloropropene, (15) trans-1,3-dichloropropene, (16) toluene, (17) 1,1,2-trichloroethene, (18) dibromochloromethane, (19) tetrachloroethene, (20) chlorobenzene, (21) ethyl benzene, (22) bromoform, (23) 1,1,2,2-tetrachloroethane, (24) 1,3-dichlorobenzene, (25) 1,4-dichlorobenzene, (26) 1,2-dichlorobenzene.

2.4 Conclusions

The field portable GC-TMS system described has an effective m/z range of 50-442 with mass resolution at FWHM of 0.55 at m/z 91 and 0.80 at m/z 222. The system weighs < 13 kg (28 lbs), including batteries and helium carrier gas cartridge, and is totally self-contained within

dimensions of 47 x 36 x 18 cm (18.5 x 14 x 7 in.). System start-up takes about 3 min and sample analysis with library matching typically takes about 5 min, including time for column cool-down. Peak power consumption during sample analysis is about 80 W. Battery power and helium supply cartridges allow 50 and 100 consecutive analyses, respectively. An on-board library of target analytes is used to provide detection and identification of chemical compounds based on their characteristic retention times and mass spectra. The GC-TMS can detect 200 pg of methyl salicylate on-column. n-Butylbenzene and naphthalene can be detected at a concentration of 100 ppt in water from SPME analysis of the headspace. The GC-TMS system has been designed to easily make measurements in a variety of complex and harsh environments.

2.5 Acknowledgement

The authors gratefully acknowledge financial support from the Department of Defense, Defense Threat Reduction Agency, Contract No. DTRA01-03-C-0047).

2.6 References

1. Herbert H. Hill, J.; Martin, S. J., Conventional Analytical Methods for Chemical Warfare Agents. *Pure Appl. Chem.* **2002,** *74*, 2281-2291.
2. Iceman, G. A.; Stone, J. A., Ion Mobility Spectrometers in National Defense. *Anal. Chem.* **2004,** *76*, 391A-397A.
3. Seto, Y.; Kanamori-Kataoka, M.; Tsuge, K.; Ohsawa, I.; Matsushita, K.; Sekiguchi, H.; Itoi, T.; Iura, K.; Sano, Y.; Yamashiro, S., Sensing Technology for Chemical-Warfare Agents and Its Evaluation Using Authentic Agents. *Sens. Actuators B.* **2005,** *108*, 193-197.
4. Steiner, W. E.; Klopsch, S. J.; English, W. A.; Clowers, B. H.; Hill, H. H., Detection of a Chemical Warfare Agent Simulant in Various Aerosol Matrixes by Ion Mobility Time-of Flight Mass Spectrometry. *Anal. Chem.* **2005,** *77*, 4792-4799.
5. Smith, W. D., Analytical Chemistry at the Forefront of Homeland Defense. *Anal. Chem.* **2002,** *74*, 462A-466A.

6. Arnold, N. S.; Dworzanski, J. P.; Sheya, S. A.; McCleannen, W. H.; Meuzelaar, H. L. C., Design Considerations in Field-Portable GC-Based Hyphenated Instrumentation. *Field. Anal. Chem. Tech.* **2000,** *4*, 219-238.
7. Makas, A. L.; Troshkov, M. L., Field Gas Chromatography-Mass Spectrometry for Fast Analysis. *J. Chromatogr. B* **2004,** *800*, 55-61.
8. Eckenrode, B. A., Environmental and Forensic Applications of Field-Portable GC-MS: An Overview. *J. Am. Soc. Mass Spectrom.* **2001,** *12*, 683-693.
9. Smith, P. A.; Lepage, C. R. J.; Koch, D.; Wyatt, H. D. M.; Hook, G. L.; Betsinger, G.; Erickson, R. P.; Eckenrode, B. A., Detection of Gas-Phase Chemical Warfare Agents Using Field-Portable Gas Chromatography-Mass Spectrometry Systems: Instrument and Sampling Strategy Considerations. *Trends Anal. Chem.* **2004,** *23*, 296-306.
10. Mustacich, R.; Everson, J.; Richards, J., Fast GC: Thinking Outside the Box. *Am. Lab.* **2003,** *27*, 38-41.
11. Sloan, K. M.; Mustacich, R. V.; Eckenrode, B. A., Development and Evaluation of a Low Thermal Mass Fast Chromatograph for Rapid Forensic GC-MS Analyses. *Field. Anal. Chem. Tech.* **2001,** *5*, 288-301.
12. Lambertus, G.; Sensenig, K.; Potkay, J.; Agah, M.; Scheuering, S.; Dorman, K. W. F.; Sacks, R., Design, Fabrication, and Evaluation of Microfabricated Columns for Gas Chromatography. *Anal. Chem.* **2004,** *76*, 2629-2637.
13. Zampolli, S.; Elmi, I.; Sturmann, J.; Nicoletti, S.; Dori, L.; Cardinali, G. C., Selectivity Enhancement of Metal Oxide Gas Sensors Using a Micromachined Gas Chromatographic Column. *Sens. Actuators B* **2005,** *105*, 400-406.
14. Overton, E. B.; Carney, K. R.; Roques, N.; Dharmasena, H. P., Fast GC Instrumentation and Analysis for Field Applications. *Field Anal. Chem. Tech.* **2001,** *5*, 97-105.
15. Syage, J. A.; Hanning-Lee, M. A.; Hanold, K. A., A Man Portable, Photoionization Time-of-Flight Mass Spectrometer. *Field. Anal. Chem. Tech.* **2000,** *4*, 204-215.
16. Syage, J. A.; Nies, B. J.; Evans, M. D.; Hanold, K. A., Field-Portable, High-Speed GC/TOFMS. *J. Am. Soc. Mass Spectrom.* **2001,** *12*, 648-655.
17. Diaz, J. A.; Daley, P.; Miles, R.; Rohrs, H.; Polla, D., Integration Test of a Miniature ExB Mass Spectrometer with a Gas Chromatograph for Development of a Low-Cost, Portable, Chemical-Detection System. *Trends Anal. Chem.* **2004,** *23*, 314-321.
18. Microsaic Systems. www.microsaic.com
19. Diaz, J. A.; Giese, C. F.; Gentry, W. R., Portable Double-Focusing Mass-Spectrometer System for Field Gas Monitoring. *Field. Anal. Chem. Tech.* **2001,** *5*, 155-167.
20. Rimkus, W. V.; Davis, D. V.; Gallaher, K., Transportable Miniature FTMS for Analysis of Corrosives and Chemical Warfare Agents. In *4th Workshop on Harsh-Environment MS* St. Petersburg Beach, Florida, 2003.
21. Patterson, G. E.; Guymon, A. J.; Riter, L. S.; Everly, M.; Griep-Raming, J.; Laughlin, B. C.; Ouyang, Z.; Cooks, R. G., Miniature Cylindrical Ion Traps Mass Spectrometer. *Anal. Chem.* **2002,** *74*, 6145-6153.
22. Blain, M. G.; Riter, L. S.; Cruz, D.; Austin, D. E.; Wu, G.; Plass, W. R.; Cooks, R. G., Towards the Hand-Held Mass Spectrometer: Design Considerations, Simulation, and Fabrication of Micrometer-Scaled Cylindrical Ion Traps. *Int. J. Mass Spectrom.* **2004,** *236*, 91-104.

23. Riter, L. S.; Peng, Y.; Noll, R. J.; Patterson, G. E.; Aggerholm, T.; Cooks, R. G., Analytical Performance of a Miniature Cylindrical Ion Trap Mass Spectrometer. *Anal. Chem.* **2002,** *74*, 6154-6162.
24. Gao, L.; Song, Q.; Patterson, G. E.; Cooks, R. G.; Ouyang, Z., Handheld Rectilinear Ion Trap Mass Spectrometer. *Anal. Chem.* **2006,** *78*, 5994-6002.
25. Ouyang, Z.; Wu, G.; Song, Y.; Li, H.; Plass, W. R.; Cooks, R. G., Rectilinear Ion Trap: Concepts, Calculations, and Analytical Performance of a New Mass Analyzer. *Anal. Chem.* **2004,** *76*, 4595-4605.
26. Fico, M.; Yu, M.; Ouyang, Z.; Cooks, R. G.; Chappell, W. J., Miniaturization and Geometry Optimization of a Polymer-Based Rectilinear Ion Trap. *Anal. Chem.* **2007,** *79*, 8076-8082.
27. Lammert, S. A.; Rockwood, A. A.; Wang, M.; Lee, M.; Lee, E. D.; Tolley, S. E.; Oliphant, J. R.; Jones, J. L.; Waite, R. W., Miniature Toroidal Radio Frequency Ion Trap Mass Analyzer. *J. Am. Soc. Mass Spectrom.* **2006,** *17*, 916-922.
28. Austin, D. E.; Wang, M.; Tolley, S. E.; Maas, J. D.; Hawkins, A. R.; Rockwood, A. L.; Tolley, H. D.; Lee, E. D.; Lee, M. L., Halo Ion Trap Mass Spectrometer. *Anal. Chem.* **2007,** *79*, 2927-2932.
29. Keil, A.; Hernandez-Soto, H.; Noll, R. J.; Fico, M.; Gao, L; Ouyang, Z.; Cooks, R. G. Monitoring of Toxic Compounds in Air Using a Handheld Rectilinear Ion Trap Mass Spectrometer. *Anal Chem.* **2008**, 80, 734-741.
30. Meuzelaar, H. L. C.; Dworzanski, J. P.; Arnold, N. S.; McCleannen, W. H. Advances in Field-Portable Mobile GC/MS Instrumentation. *Field Anal. Chem. Tech*. **2000**, 4, 3-13.
31. Torion Technologies, Guardion-7 Hand-portable GC-TMS System. http://www.torion.net/
32. Griffin Analytical. http://www.griffinanalytical.com/griffin400.html
33. Daltronics, B. Enhanced Environmental Mass Spectrometer (E^2M). http://www.bdal.de/cbrn-detection/chemical-detection/e2m.html
34. Eckenrode, B. A., The Application of an Integrated Multifunctional Field-Portable GC/MS System. *Field. Anal. Chem. Tech.* **1998,** *2*, 3-20.
35. Gao, L.; Harper, J.; Cooks, R. G.; Ouyang, Z., Mini 11 Handheld Mass Spectrometer and its Applications in Biomedical Areas. In *59th Annual Pittsburgh Conference on Analytical Chemistry and Applied Spectroscopy*, New Orleans, LA, March 1 - 6, **2008**.
36. Inficon HAPSITE Smart Identification System. http://www.inficonchemicalidentificationsystems.com/en/hapsitechemicalidentification.html
37. Smith, P. A.; Sng, M. T.; Eckenrode, B. A.; Leow, S. Y.; Koch, D.; Erickson, R. P.; Lepage, C. R. J.; Hook, G. L., Towards Smaller and Faster Gas Chromatography-Mass Spectrometry Systems for Field Chemical Detection. *J. Chromatogr. A* **2005,** *1067*, 285-294.
38. Bier, M. E.; Cooks, R. G., Membrane Interface for Selective Introduction of Volatile Compounds Directly into the Ionization Chamber of a Mass Spectrometer. *Anal. Chem.* **1987,** *59*, 597-601.
39. Lammert, S. A.; Plass, W. R.; Thompson, C. V.; Wise, M. B., Design, Optimization and Initial Performance of a Toroidal rf Ion Trap Mass Spectrometer. *Int. J. Mass Spectrom.* **2001,** *212*, 25-40.

40. MacDonald, S. J.; Wheeler, D., Fast Temperature Programming by Resistive Heating with Conventional GCs. *Am. Lab.* **1998,** *30*, 27-28, 37-38, 40.
41. Jain, V.; Phillips, J. B., Fast Temperature Programming on Fused-Silica Open Tubular Capillary Columns by Direct Resistive Heating. *J. Chromatogr. Sci.* **1995,** *33*, 55-59.
42. Stearns, S. D.; Cai, H.; Koehn, J. A.; Brisbin, M.; Cowles, C.; Bishop, C., Direct Resistively Heated Columns for Fast and Portable Gas Chromatography. In *59th Annual Pittsburgh Conference on Analytical Chemistry and Applied Spectroscopy*, New Orleans, LA, March 1 - 6, **2008**.
43. Zhang, Z.; Yang, M. J.; Pawliszyn, J., Solid Phase Microextraction. *Anal. Chem.* **1994,** *66*, 844A-853A.
44. Alpendurada, M. d. F., Solid-Phase Microextraction: a Promising Technique for Sample Preparation in Environmental Analysis. *J. Chromatogr. A* **2000,** *889*, 3-14.
45. Pawliszyn, J., *Application of Solid Phase Microextraction*. Royal Society of Chemistry: Letchworth, Hertfordshire, UK, 1999; p 655.
46. Smith, P. A.; Sheely, M. V.; Kluchinsky, T. A. J., Solid Phase Microextraction with Analysis by Gas Chromatgoraphy to Determine Short Term Hydrogen Cyanide Concentrations in a Field Setting. *J. Sep. Sci.* **2002,** *25*, 917-921.
47. Hook, G. L.; Kimm, G.; Betsinger, G.; Savage, P. B.; Swift, A.; Logan, T.; Smith, P. A., Solid Phase Microextraction Sampling and Gas Chromatography/Mass Spectrometry for Field Detection of the Chemical Warfare Agent O-Ethyl S-(2-diisopropylaminoethyl) methylphosphonothiolate (VX). *J. Sep. Sci.* **2003,** *26*, 1091-1096.
48. Harvey, S. D.; Nelson, D. A.; Wright, B. W.; Grate, J. W., Selective Stationary Phase for Solid-Phase Microextraction Analysis of Sarin (GB). *J. Chromatogr. A* **2002,** *954*, 217-225.
49. Schneider, J. F.; Boparai, A. S.; Reed, L. L., Screening for Sarin in Air and Water by Solid-Phase Microextraction-Gas Chromatography-Mass Spectrometry. *J. Chromatogr. Sci.* **2001,** *39*, 420-424.
50. Lakso, H.-A.; Ng, W. F., Determination of Chemical Warfare Agents in Natural Water Samples by Solid-Phase Microextraction. *Anal. Chem.* **1997,** *69*, 1866-1872.
51. Kimm, G. L.; Hook, G. L.; Smith, P. A., Application of Headspace Solid-Phase Microextraction and Gas Chromatography-Mass Spectrometry for Detection of the Chemical Warfare Agent Bis(2-chloroethyl) sulfide in Soil. *J. Chromatogr. A* **2002,** *971*, 185-191.
52. Hook, G. L.; Kimm, G. L.; Koch, D.; Savage, P. B.; Bangwei, D.; Smith, P. A., Detection of VX Contamination in Soil Through Solid-Phase Microextraction Sampling and Gas Chromatography/Mass Spectrometry of the VX Degradation Product Bis(diisopropylaminoethyl)disulfide. *J. Chromatogr. A* **2003,** *992*, 1-9.
53. Rearden, P.; Harrington, P. B., Rapid Screening of Precursor and Degradation Products of Chemical Warfare Agents in Soil by Solid-Phase Microextraction Ion Mobility Spectrometry (SPME-IMS). *Anal. Chim. Acta* **2005,** *545*, 13-20.
54. Szostek, B.; Aldstadt, J. H., Determination of Organoarsenicals in the Environment by Solid-Phase Microextraction-Gas Chromatography-Mass Spectrometry. *J. Chromatogr. A* **1998,** *807*, 253-263.
55. Wooten, J. V.; Ashley, D. L.; Calafat, A. M., Quantitation of 2-chlorovinylarsonous Acid in Human Urine by Automated Solid-Phase Microextraction-Gas Chromatography-Mass Spectrometry. *J. Chromatogr. B* **2002,** *772*, 147-153.

56. U.S., E. P. A. *Innovations in Site Characterization*; EPA-542-R-98-006; Office of Solid Waste and Emergency Response: Washington, DC., September, 1998; p 48.
57. Arthur, C. L.; Pawliszyn, J., Solid Phase Microextraction with Thermal Desorption Using Fused Silica Optical Fibers. *Anal. Chem.* **1990,** *62*, 2145-2148.
58. Gorecki, T.; Pawliszyn, J., Sample Introduction Approaches for Solid Phase Microextraction Rapid GC. *Anal. Chem.* **1995,** *67*, 3265-3274.
59. Gorecki, T.; Belkin, M.; Caruso, J.; Pawliszyn, J., Solid Phase Microextraction as Sample Introduction Technique for Radio Frequency Glow Discharge Mass Spectrometry. *Anal. Commun.* **1997,** *34*, 275-277.
60. Grob, K.; Biedermann, M., The Two Options for Sample Evaporation in Hot GC Injectors: Thermospray and Band Formation Optimization of Conditions and Injector Design *Anal. Chem.* **2002,** *74*, 10-16.
61. Oliphant, J.; Tolley, S. E.; Later, D.; Lee, E. D.; Lee, E. D.; Lee, M. L. Operation and Design Challenges for a Hand-Portable GC/TMS. In *Proceedings of the 56th Annual American Society for Mass Spectrometry Conference on Mass Spectrometry*, Denver, CO, June 1-5, 2008.
62. Agency, E. P. Methods for Organic Chemical Analysis of Municipal and Industrial Wastwater (Method 624-Purgeables). http://www.epa.gov/

3 System for Testing Near-Real-Time Chemical Permeation Rates Through Materials*

3.1 Introduction

Protecting first responders and military personnel in potentially hazardous environments includes ensuring that their individual protective equipment (IPE) (gloves, boots, suits, masks, etc.) will serve as a personal barrier against toxic chemicals. IPE currently in use has not been tested extensively to ensure they provide adequate protection against toxic industrial chemicals (TICs) that first responders will likely encounter. Consequently, there is a need to evaluate emergency responder protective clothing for chemical permeation and break-through. Permeation resistance testing measures the molecular transfer of analyte through a material. The results from permeation resistance testing can be used to provide a measure of the overall effectiveness of IPE and can help establish the period of time the IPE is effective during exposure to specific chemicals under specific conditions.

Permeation testing entails exposing one side of a sample of IPE (a swatch) to a chemical and measuring the amount of that challenge that permeates across the protective barrier with the aid of a collection medium (air, water, nitrogen, etc.). The breakthrough time and steady state permeation rate are values generally reported for permeation testing.

* Publication in progress:
Murray, J. A.; Porter, N. L.; Bailey, C. A.; Nemelka, K. D.; Waite, R. W.; Bowerbank, C. R.; Fauseet, A. L.; Moss, R. S.; Ercanbrack, W. D.; Bonsteel, R. A.; Lee, M. L. System for Testing Near-Real-Time Chemical Permeation Rates Through Materials. In Progress.

The breakthrough time is the time required for the chemical to permeate across the protective material. The steady state permeation rate is the constant chemical flux through the material after breakthrough. Ideally, a long breakthrough time and a low steady state permeation rate are desired for optimal protection.

To standardize permeation testing and data reporting, the American Society for Testing and Materials (ASTM) developed the F739 method in 1981 entitled "Test for resistance of protective clothing materials to permeation by hazardous liquids" [1] based on a publication by Henry and Schlatter.[2] In 1985, the ASTM committee updated the method to include both liquid and vapor challenges.[3] It was subsequently revised in 1991, 1996, 1999 and 2007.[4-7] The method provides guidance on the design of the test cell in which the swatch is placed and describes the procedure and documentation for the reporting of results. While the ASTM method outlines the procedure, there are some aspects of the testing that are up to the discretion of the testing laboratory, such as the details of the test cell, mode of operation and analytical measurement technique.

The ASTM method describes a standard test cell apparatus which consists of two chambers separated by the test protective material. The ASTM method allows for alternative test cell designs as long as their performances are documented.[7] Although the recommended ASTM test cell is the "standard," it does have drawbacks. The test cell is bulky, fragile, and awkward to handle. Temperature control of the system requires placement of the test cell in an oven or water bath. A large amount of challenge chemical is also required to cover the entire swatch barrier. There are reports in the literature that describe alternative test cells to address some of the deficiencies with the standard ASTM test cell.[8-11] While test cells have been designed to be easier to handle, Verwolf et al. determined that temperature control, challenge method(s), and

flow path(s) were the minimum characteristics that should be investigated when designing a test cell for permeation testing.[11]

The ASTM method allows the user to perform measurements in either the closed-loop or open-loop mode. In the closed-loop mode, the permeate is received by a collection medium (liquid or gas) that is recycled through the system, whereas in the open-loop configuration, fresh collection medium is continuously purged through the test cell fixture. The advantage of the closed-loop mode is that the permeate is constantly accumulated or concentrated in a set volume of collection medium. Usually, higher sensitivity is achieved using this mode. However, there is the potential for saturating the collection medium, which can effect the permeation of challenge through the protective barrier and lead to inaccurate steady-state permeation measurements. The open-loop configuration reduces the chance of collection medium saturation, since new medium is continuously added to the system. However, the method detection limit is not as low as with the closed-loop configuration. Ultimately, the mode that is selected depends on the chemicals tested, the desired detection limit, and the analytical technique used for quantitative measurement.

The analytical techniques that can be used in permeation testing are wide-ranging. Popular techniques are infrared (IR) spectroscopy,[12] and gas[13-17] and liquid chromatography[18] For near-real-time analysis, direct reading detectors are also popular, such as the flame ionization detector (FID)[19-20] and photoionization detector (PID).[12, 21-22] Other detectors such as electroconductivity flow cell[13] and hydrogen flame emission spectroscopy[23] have been reported. Gas chromatography-mass spectrometry (GC-MS) has also been used in permeation testing, especially for studying the permeation of complex mixtures through protective clothing.[24-26] Not only is MS useful for complex samples, but it can also be used to indentify degradation products.

Regardless of the analytical technique used, it must be sensitive enough to detect low level breakthrough times, and be robust enough to handle large amounts of breakthrough analyte.

Since permeation testing is an on-going effort, it is important to develop automated systems that can test multiple samples simultaneously with little user involvement. A simple approach to incorporate the analytical measurement technique into an automated system containing multiple test cells is to have a dedicated detector for each sample stream.[22] While this approach minimizes carryover that could exist in a switching valve and universal transfer line, it could also be both cost and space prohibitive. The other approach is to use a single detector to monitor multiple sample streams with the use of one or more switching valves. Several automated systems that follow this approach have been reported in the literature.[10, 12-14, 21, 23, 27] While the use of a single detector minimizes the overall footprint of the automated permeation system, carryover from different sample streams can occur. Carryover can be reduced by purging and heating the common lines and valves. Walters et al. decreased carryover by alternatively loading and purging two sample loops that were installed in each of the sample streams.[14] This allowed more time to purge individual sample loops to prevent cross contamination. When using a single detector for monitoring multiple sample streams, the cycle time (i.e., time it takes to sample all sample steams) should also be considered. Longer cycle times reduce the number of data points collected for a single sample stream, which can prevent the determination of accurate breakthrough times. With the quantity of raw data generated by automated permeation systems, it is also important that data collection and analysis be automated. Furthermore, near-real-time analysis of the permeation process will allow the user to know when to end the test (i.e., when steady-state-permeation has been reached).

A

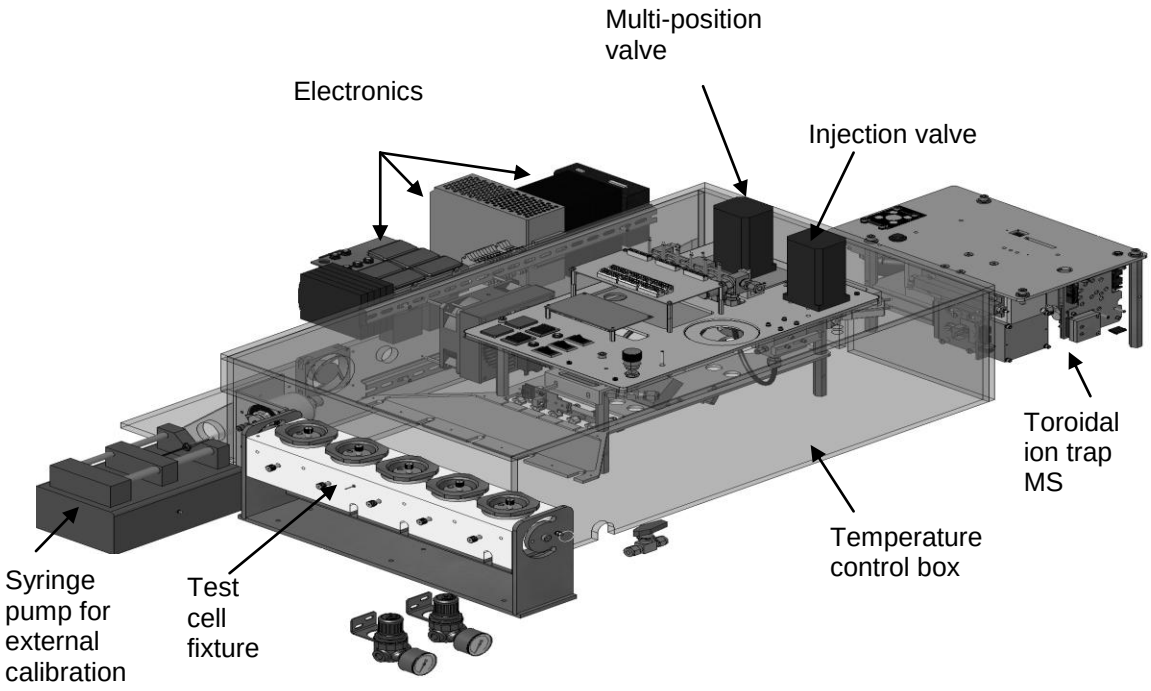

B

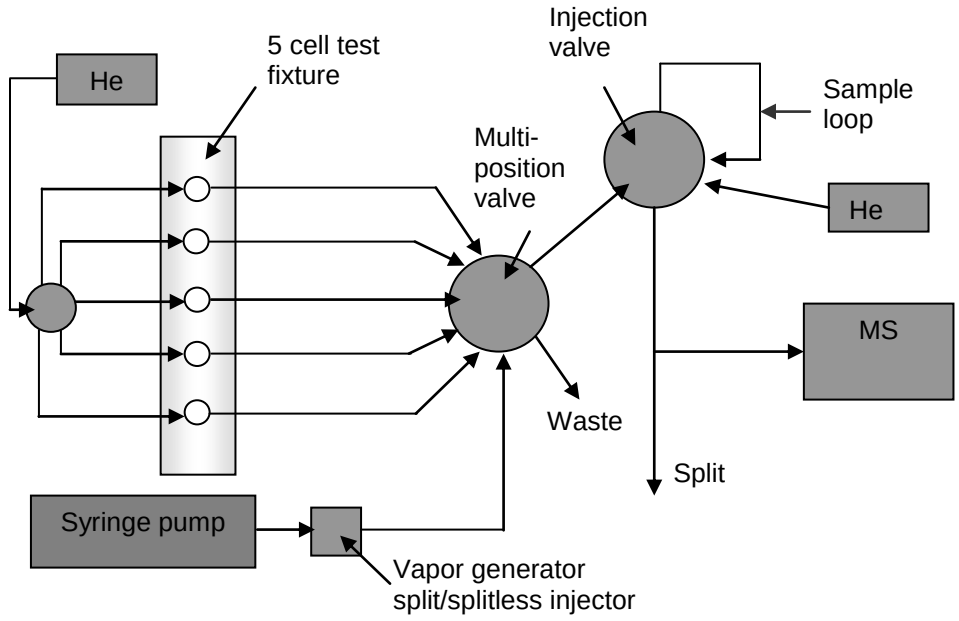

Figure 3.1. Schematic (A) permeation system with individually labeled components and (B) block diagram of the system.

The objective of this work was to develop an ASTM compliant prototype automated swatch chemical permeation testing system with near real-time detection to be used for evaluating protective clothing resistance to TICs. While the prototype described here has proven to be reliable, further developments are anticipated to advance the technology of permeation testing.

3.2 Experimental Section

3.2.1 Near-real-time permeation test system

The swatch chemical permeation system is a fully automated system with a small toroidal ion trap MS as a detector. The system contains a swatch cell fixture which can hold up to 5 swatch samples. The device contains a calibration system to correlate detector response to permeation rate. Transfer lines and valves are located in a temperature controlled manifold to maintain constant elevated temperature throughout the testing period. The system was designed to be placed in a hood and has overall dimensions of 109 x 61 x 33 cm. The system is fully automated with little user operation needed. Figures 3.1A and 3.1B show schematic drawing and block diagram of the system, respectively.

3.2.2 Swatch test cell fixture

A schematic of the swatch test cell fixture is shown in Figure 3.2. The cell block was constructed from bar stock aluminum to ensure good temperature stability and was gold plated to minimize chemical adsorption. The block is heated with a strip heater that is mounted on the bottom of the block, and the temperature is monitored using four resistive thermal devices (RTDs) at four separate locations. One RTD is used in a steady state relay to supply temperature

feedback control for the cell block. Within the cell block are five cells in which the sample swatches are placed. A swatch sample is loaded into the cell chamber and sealed between two polytetrafluoroethylene (PTFE) gaskets by tightening the compression ring. The gasket is keyed to prevent twisting of the swatch during loading. Figure 3.2 shows a schematic of how the swatch is loaded in the test cell fixture. The cell fixture holds swatches with diameter of 5.08 cm. The area of the swatch that is exposed to the challenge (defined by the PTFE gaskets) is 7.0 cm^2. A challenge is loaded onto one side of the swatch material by introducing it through the cell cap, which serves as a reservoir. The challenge is introduced into all test cells simultaneously by dispensing the challenge through a manifold. The swatch cell fixture allows both liquid and vapor challenges. For a liquid challenge, the test cell fixture is oriented upright, so that after the liquid challenge is introduced, it is in direct contact with the swatch. In the vapor mode, the test cell fixture is inverted and the liquid sample remains in the cap reservoir after introduction. In this mode, only the vapor of the liquid is in direct contact with the swatch. The swatch is swept with helium on the side opposite to where sample is introduced to collect and transfer any permeate to the detector for analysis.

3.2.3 Switching valves and temperature controlled transfer line manifold

The purge gas flows from all five test cells are directed into a multi-position valve (VICI, Houston, TX) that allows the selection of one sample stream at a time for analysis. All other sample streams are directed to waste through a common outlet. The selected stream is fed into a two-position injection valve (VICI) where it is fed through a 250 µL sample loop. When the injection valve is switched, a fresh supply of helium sweeps the sample from the sample loop and introduces part of the flow into the MS for detection (see Figure 3.1B for a block diagram). Sample stream lines and valves are located inside a temperature controlled enclosure with

dimensions of 74 x 43 x 20 cm. The temperature controlled enclosure is heated using a temperature control unit (Watlow, Winnona, MN) and fan heater (McMaster-Carr, Princeton, NJ).

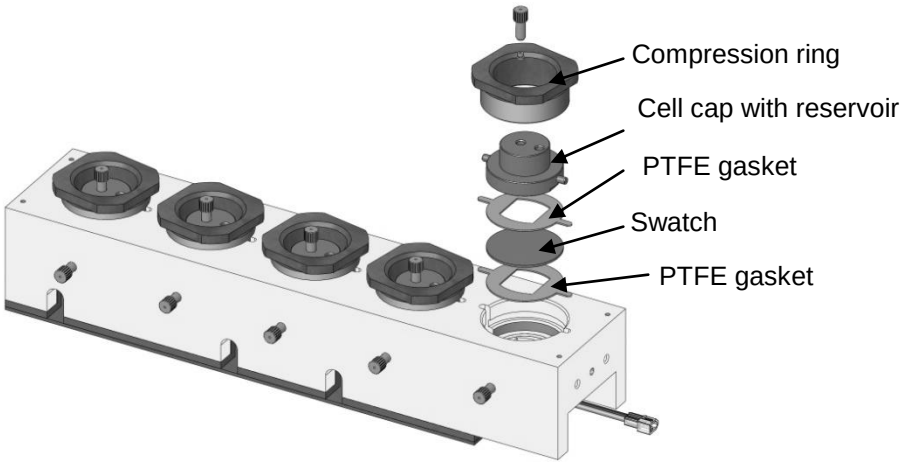

Figure 3.2. Schematic of test cell fixture which demonstrates the loading of the swatch.

3.2.4 Toroidal ion trap mass spectrometer

The detection system is a miniaturized toroidal ion trap MS from Torion Technologies (American Fork, UT), which has been described elsewhere.[28] MS was chosen for detection to allow for positive identification of the challenge and to determine if decomposition or artifact formation occurs during the permeation process. The miniaturized MS was also chosen due to its small footprint. Modifications to the MS were made to adapt it to the swatch system. The GC was removed from the system and the effluent from the swatch cells were fed directly into the

mass analyzer. The MS was computer controlled, and the average response was plotted in real time.

3.2.5 Calibration system

The system contains a calibration system for quantitation of analyte that permeates through the swatch. It contains a vapor dissemination system consisting of a split/splitless injector from an Agilent GC (Agilent Technologies, Santa Clara, CA). The analyte is introduced into the injector at a continuous speed with the use of a syringe pump (Harvard Apparatus, Hollison, MA). The concentration delivered can be adjusted by the speed of the syringe pump and the flow of helium introduced into the injector. The calibration system was typically calibrated from 0.05-500 $\mu g/cm^2$/min using the vapor generator device. The time for equilibration after changing concentrations was fast (usually less than 1 min). The flow rate from the injector was adjusted to be equal to the flow rate in the permeation cell (14 mL/min), and this line was plumbed to the sixth position in the multi-position valve. Typical calibration curves consisted of 11 points that were within ±15% tolerance. Calibration check samples at 10 $\mu g/cm^2$/min were analyzed before and after each permeation test.

3.2.6 System software

The system software allows the permeation system to be fully automated. The software controls the switching of the multi-position and injection valves, heaters, start and stop timing of the MS, and data collection. The cycle time is user defined; for this work, the multi-position valve was turned to one sample line for 20 s before switching to the next sample line. Of those 20 s, the MS was on for 10 s and the other 10 s was used for sample loop equilibration and downloading data. This allowed for the acquisition of one data point every 100 s (1.67 min). The

results are displayed in real time as a function of signal intensity with respect to time. This allows the user to visualize the permeation curve in real time and to stop the test when steady-state permeation is achieved. The software also logs the temperature of the test cell fixture and temperature control enclosure.

3.2.7 Materials

HPLC grade reagents were used for the permeation test challenge chemicals. The swatch material used for the liquid acetone experiments was neoprene as obtained from the ASTM Permeation Subcommittee. All other experiments were conducted using neoprene material supplied from another manufacturer. Swatches were cut from the same lot of material (5.08 cm in diameter by 0.406 mm thick). The exposed area of each swatch was 7.0 cm^2 (defined by the dimensions of the gaskets).

3.2.8 Test procedure

After system calibration, the swatch materials were loaded into the test cell fixture. The temperature of the cell block was maintained at 32±1°C. The swatches were equilibrated inside the test cell fixture at this temperature for 30 min before testing. The cell block was positioned upright for liquid challenges and inverted for vapor challenges. Helium flow was purged (14 ± 1.5 mL/min) on the opposite side of the swatch from test compound application. The clean helium supply introduced into the MS was set at 0.5 mL/min. A challenge volume of 1.5 mL was loaded on 4 out of the 5 swatches simultaneously using the dispensing system already described. The swatch that was not challenged was used as a negative control. The test began when the challenge was introduced into each cell and ended when steady state permeation was reached or when 60 min had elapsed, whichever was shorter.

3.3 Results and Discussion

3.3.1 Calibration

The use of a GC injector for volatilization and mixing of an analyte with a gas stream proved to be a fast and reliable method to produce a continuous vapor with known concentration. The use of a syringe pump to adjust the vapor concentration is common practice,[29] however, this approach often requires a large mixing chamber for even evaporation and mixing in order to produce a constant concentration. Unfortunately a large expansion volume increases the time for concentration stabilization. Using a GC injector for both vaporization and mixing of the liquid analyte in the gas stream provides a constant gas standard that stabilizes within 1 min after introducing or changing the concentration of the analyte. Rapid stabilization time allows construction of calibration curves over a large concentration range in a relatively short time. Figure 3.3 shows a portion of the raw data (6 concentrations) used to construct a calibration curve for ethyl acetate. It is clear from Figure 3.3 that the signal stabilized rapidly after each concentration change. Furthermore, the signal remained stable for each concentration, such that only a few min (4 min at higher concentrations) of collecting data are needed to provide an average with relative standard deviation less than 10%. The concentration of the vapor standard can be changed by changing the syringe pump speed or gas flow rate entering the injector, or a combination of both, allowing for calibration over a wide range of concentration.

The ASTM F 739 method requires that the analytical technique have a sensitivity of at least 0.1 $\mu g/cm^2$/min for open-loop testing.[7] In addition to this requirement, the analytical technique must also be able to handle high concentration levels. For most TICs investigated in this study, the required quantitation range was 0.05-500 $\mu g/cm^2$/min. Although the advanced auto

ionization features of the MS detector permitted continuous collection of data over the entire concentration range, obtaining a single calibration curve that fit the entire concentration range was not possible. Therefore, low and high concentration calibration curves were constructed for each TIC. The MS signal response to changing concentration was quadratic, not linear. For both low and high calibration curves, a quadratic equation was fit to the data, and R^2 values of 0.998 and higher were obtained for all calibration curves. While the MS provided quantitative results, it also required periodic maintenance due to the large analyte concentrations to which it was exposed.

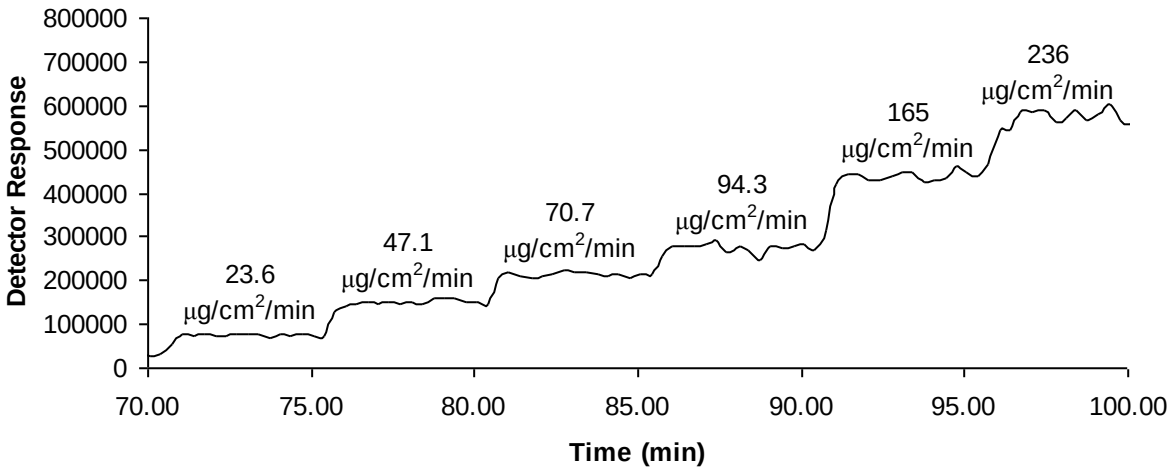

Figure 3.3. Partial ethyl acetate calibration showing stepwise response and fast equilibration time with each concentration change.

3.3.2 Test cell fixture

The test cell fixture was designed according to the following criteria: (1) test multiple swatch samples, (2) maintain constant temperature during testing, (3) test both liquid and vapor

challenges, and (4) sweep adequately the sampling side of the swatch. All 5 test cells were bored from a single block of aluminum bar stock to establish a uniform temperature. This design ensured that all 5 test cells were at the same temperature. It is critical that the temperature of the test cell be controlled due to the temperature dependence of the permeation process. The ASTM F 739-99 method requires the test cell to be within ±1.0°C of the test temperature.[6] The design of the test cell fixture easily meets this requirement. In addition to controlling the test cell fixture, the helium (collection gas) is conditioned to the test cell temperature prior to being introduced into the test cells. This is performed by coiling the helium inlet tubing within the cell block. It has been reported that if the collection medium is not conditioned to the test temperature, unintentional temperature gradients can occur which can effect breakthrough times and steady state permeation rates.[15]

The test cell fixture was designed to accommodate both liquid and vapor challenges. Applying a liquid challenge to the swatch is straightforward, only requiring that the swatch be covered and remain covered by the liquid challenge throughout the test. Delivering a constant vapor challenge can be more difficult. A saturated vapor challenge was applied to the swatch by inverting the test cell fixture and introducing the liquid analyte into the test cell cap. The distance between the liquid and the swatch was kept to a minimum to reduce the time for equilibrium between the molecules in the gas and liquid phases.

Proper collection of the permeate is required in order to acquire accurate steady state permeation rates. It was reported in the literature that different flow rates and different test cells resulted in different steady-state-permeation rates.[10, 15, 19] Anna et al. attributed this discrepancy to poor mixing, and demonstrated that high flow rates were needed to obtain accurate steady-state permeation rates.[15] As a result, the 1999 ASTM method recommends a flow rate of 50-150

mL/min to provide adequate mixing.[6] The 2007 version suggests that at least 5 volume changes per min be used, but also states that higher flow rates may be required if the solubility of the permeate in the collection medium is low.[7] The sweep volume and test cell shape can also affect the collection efficiency. Verwolf et al. determined that decreasing the sweep volume of the test cell increases the velocity of the collection medium, which decreases the permeate concentration on the desorption side of the swatch.[11] In the current test cell, the volume on the desorption side in each test cell is 1.1 mL. At a He flow rate of 14 mL/min, there was 12.7 volume changes per min, much larger than the ASTM minimum recommendation. The shape of the test cell was designed to distribute the sweep gas across the entire area of the swatch to improve collection efficiency. In this work, no calculations were performed to confirm adequate mixing.

3.3.3 Permeation curves

Up to 5 swatch samples can be tested simultaneously in the permeation system. Figure 3.4A shows 4 permeation curves that were obtained from a single test for liquid acetone through standard ASTM neoprene material. Swatch 3 in Figure 3.4A was a blank. The permeation profiles were very similar for all 4 samples, demonstrating that all test cells were uniform and behaved similarly. The average breakthrough time for the 4 samples in Figure 3.4A was 8.7 ± 0.4 min and the steady-state permeation rate was 80 ± 2 μg/cm^2/min. The data collection speed for each sample stream was 1 data point every 100 s (1.67 min). This cycle time is relatively fast and allows up to 36 data points per sample stream for a 60 min test. The permeation profile shown in Figure 3.4A is similar to what the analyst sees in real-time. Once a data point is obtained, it is plotted automatically by the software, enabling the analyst to monitor the permeation process throughout the test period. An example of a mass spectrum obtained from 1 data point of acetone permeation is shown in Figure 3.4B. The mass spectrum shows a good signal for the molecular

ion of acetone (m/z 58), however, a dimer ion peak is also present as m/z 116. We found that dimers of some TICs were formed in the ion trap at high concentrations. As a result, the molecular ion peak and the dimer peak were chosen for selected ion quantitation.

A

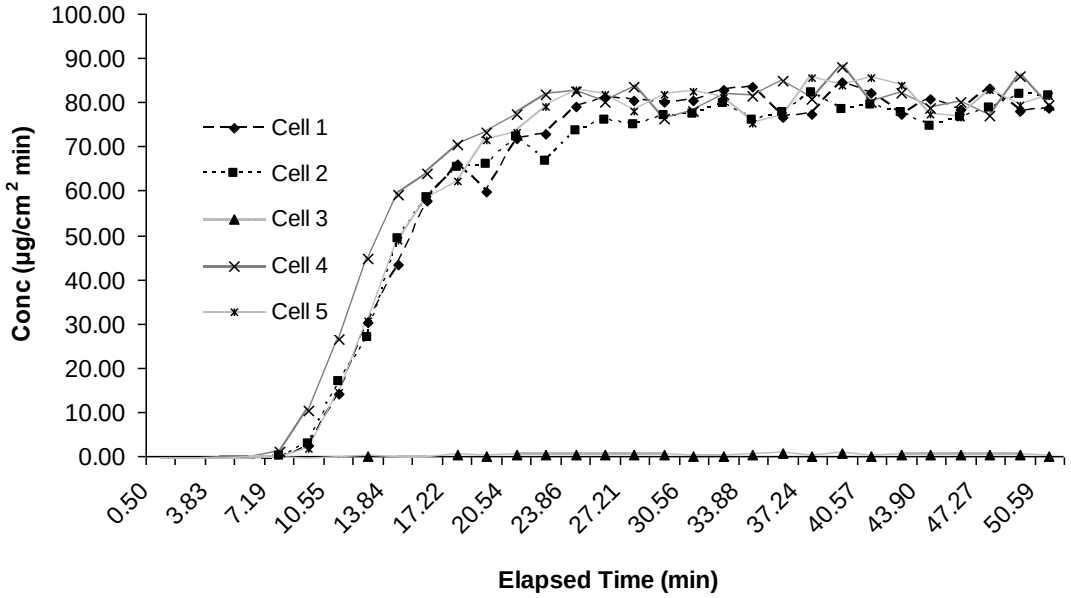

B

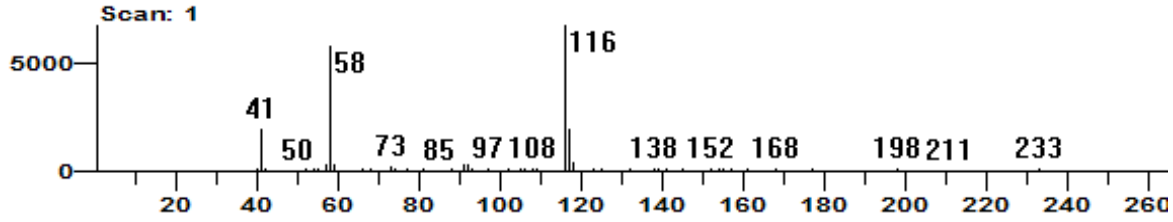

Figure 3.4. (A) Permeation curves for liquid acetone challenge on neoprene swatch samples for a test consisting of 4 parallel samples and cell 3 containing no challenge (blank). (B) Mass spectrum of acetone obtained after breakthrough (averaged 10 s analysis).

The ASTM committee performed an interlaboratory study of the method in 2005 and reported the results in the F739-07 method.[7] Data from the permeation of liquid acetone through ASTM neoprene material at a test temperature of 27 ± 2°C were obtained by several laboratories. The published standardized breakthrough time from the study was 8.7 ± 2.4 minutes and the steady-state permeation rate was 81.2 ± 60 μg/cm^2/min. The average breakthrough time and steady-state permeation rate obtained using the permeation system described in this work was 8.0 ± 0.6 min and 84 ± 8 μg/cm^2/min, respectively. However, the test temperature was 32°C instead of 27°C, and should not be directly compared to the results from the ASTM round robin study. The increased temperature would explain the earlier breakthrough time and the slightly higher steady-state permeation rate compared to the average reported in the round robin study. The temperature effect was observed in one set of experiments during which the test cell fixture was not heated and permeation occurred at room temperature (~22°C). This resulted in a 3 min delay in the breakthrough time and a slightly lower steady-state permeation rate. With this information, it was estimated that the breakthrough time at 27°C would occur approximately at 9.5 min, which is still within the standard deviation of the round robin study.

For the liquid acetone experiments, 12 replicates were performed using 3 separate test fixtures. All data were pooled together and an analysis of variance (ANOVA) was performed. There was no statistically detectable difference among the 3 different swatch test fixtures. The student T test was applied to the pooled data, which indicated no statistical difference in the data when using 4 replicates or more. Figure 3.5 shows both the 90 and 95% student T quantiles. Thus, a sample size of 4 replicates should be adequate to test the permeation of a TIC through a particular protective material using the new permeation system.

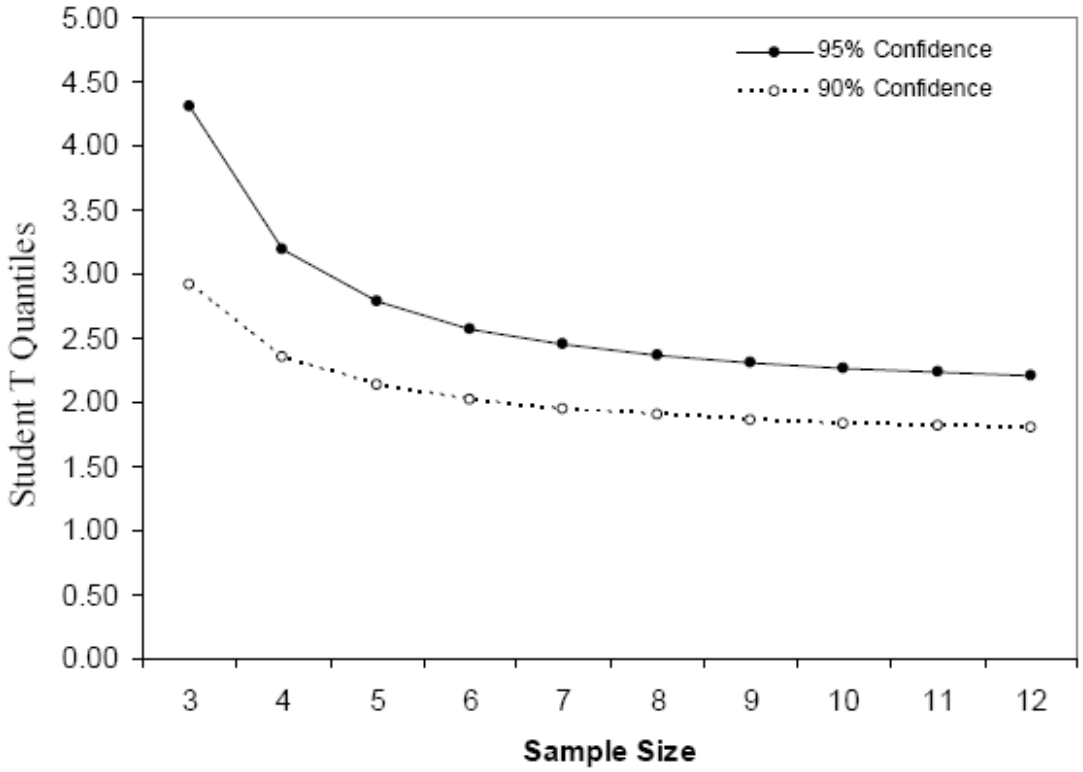

Figure 3.5. Student T quantiles versus sample size for pooled liquid acetone experiments.

In addition to acetone, 6 other TICs were tested with neoprene material. Both liquid and vapor challenges were performed for each TIC. The average breakthrough time and steady-state permeation rate for 12 replicate runs for each TIC are listed in Tables 3.1 and 3.2 for the liquid and vapor challenges, respectively. For each TIC, 4 challenged samples and 1 blank were tested 3 times for a total of 12 permeation curves and 3 blanks. The vapor challenge of dimethylformamide did not reach the steady state permeation rate within 60 min; as a result, no data for the steady state permeation rate is listed in Table 3.2 for this TIC. It should be noted that a different neoprene material was used for the acetone vapor test compared to the acetone liquid test, which could explain the high steady state permeation rate for acetone vapor.

Table 3.1. Statistical data for permeation testing of toxic industrial chemicals (TICs) through neoprene applied as liquids.

TIC	Mean breakthrough time (min)	Relative standard deviation (%)	Mean steady state permeation rate (μg/cm^2/min)	Relative standard deviation (%)
Acetone	8	8	84	10
Dichloromethane	3	18	44	15
Diethylamine	4	12	182	4
Dimethylformamide	15	8	2	19
Dimethylsulfate	NB[a]	NB	BDL[b]	BDL
Ethyl acetate	5	21	436	6
Formaldehyde[c]	19	14	ND[d]	ND

[a]No measureable breakthrough.
[b]Below detection limit (permeation was below the detection limit).
[c]35-37% aqueous solution.
[d]No data (TIC did not reach a steady state permeation rate).

Table 3.2. Statistical data for permeation testing of toxic industrial chemicals (TICs) through neoprene applied as vapors.

TIC	Mean breakthrough time (min)	Relative standard deviation (%)	Mean steady-state permeation rate (μg/cm^2/min)	Relative standard deviation (%)
Acetone	7	9	389	33
Dichloromethane	5	11	53	13
Diethylamine	6	8	92	18
Dimethylformamide	51	3	ND[a]	ND
Dimethylsulfate	NB[b]	NB	0.20	3
Ethylacetate	6	8	324	11
Formaldehyde[c]	20	11	ND	ND

[a]No data (TIC did not reach a steady state permeation rate).
[b]No measureable breakthrough.
[c]35-37% aqueous solution.

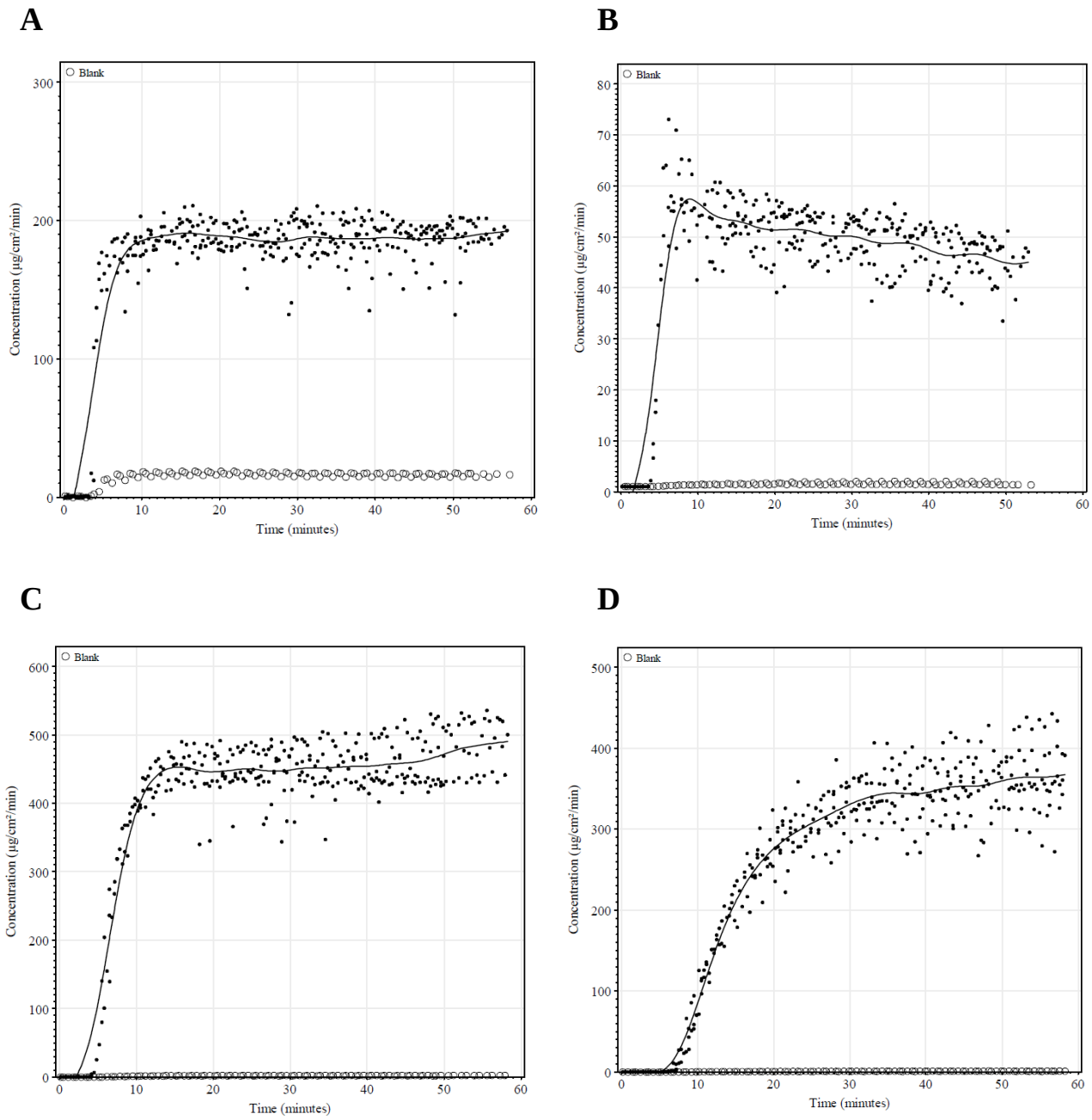

Figure 3.6. Permeation curves for (A) liquid diethylamine, (B) vapor diethylamine, (C) liquid ethyl acetate, and (D) vapor ethyl acetate through neoprene swatches. The filled circles represent individual data points consisting of 12 replicates (3 tests of 4 samples, simultaneously) and the non-filled circles represent blanks. The solid line represents the mean of the 12 challenges.

Figure 3.6 shows permeation data obtained for both liquid and vapor challenges of diethylamine and ethyl acetate. The data shown in Figure 3.6 indicate that there is no carryover between liquid and vapor challenges of ethyl acetate. However, for liquid and vapor challenges of diethylamine, there is considerable carryover when switching between sample streams as indicated by an increase in the blank signal. There was also carryover observed for liquid dimethylformamide (permeation plot not shown). This was most likely due to insufficient purge of the common line downstream from the multi-position valve. Some of the TIC was not swept out of the common sample line so that when the stream selector was actuated to the next cell, residual TIC was carried into the detector. This was apparent in the blank, but likely also occurred in every cell, which would have skewed the steady-state permeation rates. The 250 μL sample loop was flushed with clean He at a flow rate of 14 mL/min before sampling the next sample stream. This allowed for the volume of the sample loop to be swept approximately 9 times before sampling the next sample. This is obviously insufficient for the more persistent TICs. Future systems should have a much higher sweeping flow rate (~160 mL/min) to help alleviate the crossover problem. In addition the interior of all sample lines and valves should be treated to prevent adsorption. The transfer line should also be heated to a higher temperature to prevent condensation, and the length of the transfer line should be reduced.

The standard deviations for the steady state permeation rates for some of the TICs listed in Tables 3.1 and 3.2 are high. For example, the relative standard deviations for liquid challenge of dimethyl formamide and vapor challenge of acetone are 19 and 33%, respectively. While slight dissimilarities among different swatch samples can increase the standard deviations, there is likely another cause for the variations observed. In some samples, after steady-state permeation was reached, the signal fluctuated significantly. This fluctuation can be the result of

auto ionization errors, instability of the electron multiplier, overloading the ion trap and drift in the MS signal. Because of the detection requirement of 0.1 μg/cm^2/min, the amount of sample injected into the MS was often quite large once steady-state permeation was achieved for some TICs. High analyte concentrations produce averse affects on the ion trap, such as trap overloading, detector instability, and trap fouling, which decreases resolution. While MS detection allowed for confirmation of the identity of the permeate, quantitation with the MS proved to be challenging due to the large concentration range required for permeation testing

3.4 Conclusions

An automated permeation test system for evaluating emergency responder protective clothing against TICs was developed and evaluated. The capability of testing up to 5 swatch samples simultaneously improves sample throughput. Since the system only requires 4 replicates, all replicate testing for a particular material can be performed at the same time. The system also has the flexibility to test with both liquid and vapor challenges by changing the orientation of the test cell fixture. Calibration using a vapor generator constructed from a split/spitless injector and syringe pump proved to be a rapid and convenient method for calibrating over a large concentration range, which decreased the overall permeation test time. Furthermore, the entire system was automated, such that operators were not required to run the device after testing began. The shortcomings of the system include insufficient purge of the common lines and detector instability at high concentrations. These shortcomings can be addressed through minor changes in the system.

3.5 Acknowledgments

The Science and Technology Directorate of the US Department of Homeland Security sponsored the production of this material under an Interagency Agreement with the National Institute of Standards and Technology. We thank Mathew Klee from Agilent Technologies for providing the GC injector system.

3.6 References

1. ASTM, Test for Resistance of Protective Clothing Materials to Permeation by Hazardous Liquid Chemicals. In *F 739-81*, 1916 Race Street, Philadelphia, PA 19130, 1981.
2. Henry, N. W.; Schlatter, C. N., The Development of a Standard Method for Evaluating Chemical Protective Clothing to Permeation by Hazardous Liquids. *Am. Ind. Hyg. Assoc. J.* **1981,** *42*, 202-207.
3. ASTM, Standard Test Method F 739-85: Resistance of Protective Clothing Materials to Permeation by Liquids or Gases. Philadelphia, 1985.
4. ASTM, Standard Test Method for Resistance of Protective Clothing Materials to Permeation by Liquids or Gases under Conditions of Continuous Contact In *F 739-91*, ASTM: Philadelphia, 1991.
5. ASTM, Standard Test Method for Resistance of Protective Clothing Materials to Permeation by Liquids or Gases under Conditions of Continuous Contact. In *F 739-96*, ASTM: Philadelphia, 1996.
6. ASTM, Resistance of Protective Clothing to Permeation by Liquids and Gases. Materials, ASTM. Philadelphia, 1999.
7. ASTM, Standard Test Method for Permeation of Liquids and Gases through Protective Clothing Materials under Conditions of Continuous Contact. Philadelphia, 2007.
8. Berardinelli, S. P.; Mickelsen, R. L.; Roder, M. M., Chemical Protective Clothing - a Comparison of Chemical Permeation Test Cells and Direct-Reading Instruments. *Am. Ind. Hyg. Assoc. J* **1983,** *44*, 886-889.
9. Mellstrom, G. A.; Landersjo, L.; Roman, A. S., Permeation of Neoprene Protective Gloves by Acetone - Comparison of 3 Different Permeation Cells in an Open-Loop System. *Am. Ind. Hyg. Assoc. J* **1989,** *50*, 554-559.
10. Bromwich, D., The Validation of a Permeation Cell for Testing Chemical Protective Clothing. *Am. Ind. Hyg. Assoc. J.* **1998,** *59*, 842-851.
11. Verwolf, A.; Farwell, S. O.; Cai, Z. T.; Smith, P., Performance-Based Design of Permeation Test Cells for Reliable Evaluation of Chemical Protective Materials. *Polym. Test.* **2009,** *28*, 437-445.
12. Berardinelli, S. P.; Moyer, E. S., Chemical Protective Clothing Breakthrough Time - Comparison of Several Test Systems. *Am. Ind. Hyg. Assoc. J.* **1988,** *49*, 89-94.

13. Conoley, M.; Prokopetz, A. T.; Walters, D. B. *Permeation of Chemical Protective Clothing. 2. Cumulative Permeation Test Results for the National Toxicology Program*; Radian Corp.,Austin,TX,USA.: 1990; p 36 pp.
14. Walters, D. B.; Prokopetz, A. T.; Conoley, M.; Garcia, D. B.; Keith, L. H. *Permeation of Chemical Protective Clothing. 1. Design and Operation of an Automated Glove Permeation Testing System*; Radian Corp.,Austin,TX,USA.: 1990; p 22 pp.
15. Anna, D. H.; Zellers, E. T.; Sulewski, R., Astm F739 Method for Testing the Permeation Resistance of Protective Clothing Materials: Critical Analysis with Proposed Changes in Procedure and Test Cell Design. *Am. Ind. Hyg. Assoc. J.* **1998,** *59*, 547-556.
16. Chao, K. P.; Lee, P. H.; Wu, M. J., Organic Solvents Permeation through Protective Nitrile Gloves. *J. Hazard. Mater.* **2003,** *99*, 191-201.
17. Lee, H. S.; Lin, Y. W., Permeation of Hair Dye Ingredients, P-Phenylenediamine and Aminophenol Isomers, through Protective Gloves. *Ann. Occup. Hyg.* **2009,** *53*, 289-296.
18. Lind, M. L.; Johnsson, S.; Meding, B.; Boman, A., Permeability of Hair Dye Compounds P-Phenylenediamine, Toluene-2,5-Diaminesulfate and Resorcinol through Protective Gloves in Hairdressing. *Ann. Occup. Hyg.* **2007,** *51*, 479-485.
19. Mellstroem, G. A.; Landersjoe, L.; Boman, A. S., Permeation Testing of Protective Gloves by Using Two Different Permeation Cells in an Open-Loop System (Neoprene-Toluene). *Am. Ind. Hyg. Assoc. J.* **1991,** *52*, 309-314.
20. Nelson, G. O.; Priante, S. J.; Strong, M.; Anderson, D.; Fallon-Carine, J., Permeation of Substituted Silanes and Siloxanes through Selected Gloves and Protective Clothing. *AIHAJ* **2000,** *61*, 709-714.
21. Stull, J. O.; Herring, B., Selection and Testing of a Glove Combination for Use with the United-States-Coast-Guard Chemical Response Suit. *Am. Ind. Hyg. Assoc. J.* **1990,** *51*, 378-383.
22. Chin, J. Y.; Batterman, S. A., Permeation of Gasoline, Diesel, Bioethanol (E85), and Biodiesel (B20) Fuels through Six Glove Materials. *J. Occup. Environ. Hyg.* **2010,** *7*, 417-428.
23. Urmson, J.; Maurits, W. J.; Flinn, G., Automated Permeation Testing Systems Using Hydrogen Flame Emission-Spectroscopy. *Am. Lab.* **1987,** *19*, 68.
24. Lin, Y. W.; Hee, S. S. Q., Glove Permeation Tests Using Novel Microchemical Techniques for 2,4-Dichlorophenoxyacetic Acid (2,4-D) Derivatives. *Arch. Environ. Contam. Toxicol.* **1999,** *36*, 485-489.
25. Phalen, R. N.; Hee, S. S. Q., Permeation of Captan through Disposable Nitrile Glove. *J. Hazard. Mater.* **2003,** *100*, 95-107.
26. Hee, S. S. Q.; Zainal, H., Permeation of Herbicidal Dichlobenil from a Casoron Formulation through Nitrile Gloves. *Arch. Environ. Contam. Toxicol.* **2010,** *58*, 249-254.
27. Farwell, S. O.; Verwolf, A.; Cai, Z.; Smith, P.; Roy, W., Design and Performance of an Integrated Analytical Swatch Testing System. *Instrum Sci. Technol.* **2008,** *36*, 577-597.
28. Contreras, J. A.; Murray, J. A.; Tolley, S. E.; Oliphant, J. L.; Tolley, H. D.; Lammert, S. A.; Lee, E. D.; Later, D. W.; Lee, M. L., Hand-Portable Gas Chromatograph-Toroidal Ion Trap Mass Spectrometer (GC-TMS) for Detection of Hazardous Compounds. *J. Am. Soc. Mass Spectrom.* **2008,** *19*, 1425-1434.
29. Nelson, G. O., *Gas Mixutres: Preparation and Control*. Lewis Publishers: Boca Raton, 1992; p 109-137.

4 Trapping at High Flows Using Multi-Capillary Open Tubular Traps

4.1 Introduction

Traditional air sampling in the field for trace organic compound analysis consists of passing a large volume of air through a solid sorbent.[1] Disadvantages of solid sorbent traps are the production of artifacts from the sorbent, non-instantaneous desorption rates, and a pressure drop due to the packing material. To overcome these limitations, fused silica open tubular columns coated with thick polymer films have been used to trap analytes.[2-8] Advantages of open tubular traps include fast desorption, low flow resistance and good transfer of analyte between the trap and the analytical column. A review of previous work using open tubular traps was discussed in Chapter 1 (Section 1.2.3).

In this chapter, several approaches to improve the retention in open tubular traps are described, including the use of porous coatings to increase the surface area, thick films, long trap lengths, and bundled capillary traps. A multi-capillary (bundled capillary) trap was constructed to demonstrate the ability to sample at high flow rates. The analytes trapped in this system were re-focused on a second smaller trap. The results demonstrate how such a sampling strategy can provide fast sampling of trace analytes in the field.

4.2 Experimental

4.2.1 Preparation of sol-gel coated capillary traps

Two types of sol-gel coated capillary traps were prepared: PDMS and cyano-PDMS. The procedure for preparation of the sol-gel coated capillaries was adapted from the procedures reported by Chong et al.[9] and Kulkarni et al.[10] Fused silica capillary tubing with 320 and 530 μm id. (Polymicro Technologies, Phoenix, AZ) was hydrothermal treated according to a procedure reported by Shende et al.[11] Briefly, the tubing was pretreated by rinsing with 5 mL of methylene chloride, methanol and deionized water in this order. After rinsing, the capillary was purged with nitrogen gas for 5 min. Both ends of the capillary were sealed with a flame and placed in an oven at 340°C for 2 h. Then the ends were cut and nitrogen was purged through the column while it was heated from 40°C to 250°C at a temperature program ramp of 5°C/min. The column was held at the maximum temperature for 2 h. To prepare the PDMS sol-gel trap, 190 μL hydroxyl-terminated PDMS, 30 μL of poly(methylhydrosiloxane), 300 μL of methyltrimethoxysilane and 200 μL of 95% trifluoroacetic acid (5% water) (all from Sigma-Aldrich, St. Louis, MO) were vortexed in a centrifuge tube and centrifuged at 13,000 rpm for 5 min. The sol-gel solution was then introduced into the pretreated fused silica capillary column using pressure. The end of the capillary was then plugged with a septum and the sol-gel reactive species was allowed to react in the column for 1-3 h. The excess sol-gel solution was then purged out with nitrogen gas, which was left flowing for 2 h. The capillary was then conditioned in a GC oven starting at a temperature of 25°C and ramping up at a rate of 0.2°C/min to 150°C, then from 150°C to 300°C at a temperature ramp of 1°C/min, and finally holding at 300°C for 2 h. The cyano-PDMS sol-gel coated capillary trap was prepared in the same manner, except 95 μL of hydroxyl-terminated

PDMS and 95 µL of 3-cyanopropyltriethoxysilane (Gelest, Morrisville, PA) were used; all other chemicals and procedures were as described above for the PDMS procedure.

4.2.2 Preparation of polymer-coated capillary traps

A 5-µm thick open tubular trap was prepared to compare with the sol-gel traps. A solution of SE-54 was prepared by mixing 0.230 g of SE-54 stationary phase gum (Supelco, Bellefonte, PA) with 2.26 g of pentane. Dicumyl peroxide (Sigma-Aldrich) was added as a crosslinker and 35 µL of a 9% (wt/wt) solution of dicumyl peroxide in toluene was added. The stationary phase solution was loaded into a 320 µm i.d. fused silica capillary (Polymicro Technologies) with a syringe pump (Harvard Apparatus, Holliston, MA), taking care that no bubbles entered the fused silica. One end was sealed with vacuum grease (Dow Corning, Midland, MI) making certain that no air bubbles were introduced. The other end was connected to a vacuum pump. The column was placed in a temperature bath at 30°C and left overnight for the solvent to evaporate. The film thickness of the trap was calculated to be 5.4 µm. The trap was conditioned in an oven with helium flow starting at 40°C and applying a temperature ramp of 5°C/min up to 250°C. The trap remained at the upper temperature for 2 h.

To prepare thick PDMS traps (40-80 µm), a procedure was used similar to that described by Blomberg and Roeraade,[12] which is an adaptation of the dynamic coating method. Sylgard 184 Silicone elastomer (Dow Corning, Midland, MI) was used as the polymer coating. The elastomer contains a reagent that, when heated, cross-links the polymer and allows the film to be fixed to the walls of the capillary. The elastomer was placed in a 500 µL gas tight syringe (Hamilton, Reno, NV) and degassed. For the coating procedure, a liquid brake was used as described by Van Dalen.[13] One end of a 530 µm i.d. fused silica capillary (Polymicro Technologies) was connected to the gas tight syringe through a luer adapter union (VICI,

Houston, TX) and the other end was connected to a nitrogen gas supply. A syringe pump was used to fill the fused silica tubing with the PDMS. To move the stationary phase through the capillary at a constant rate, leaving a thick film on the walls, a pressure of 50 psig of nitrogen gas was applied to one end while the syringe pump was used in the withdraw mode to remove solution from the other end. The speed of the meniscus was determined by the speed of the syringe pump, and a withdraw speed of 5 μL/min was used to deposit a 40 μm thick film. In order to immediately cross-link the polymer, an oven was built using an aluminum block (5 cm x 10 cm) with a slit through the block (0.5 cm x 0.8 cm) that was heated with two 200 W, 120 V cartridge heaters (McMaster-Carr, Princeton, NJ). The temperature was controlled using a temperature controlled unit (Watlow, Winnona, MN). The column was moved through the oven by a spring loaded roller driven by a stepper motor (Hurst Manufacturing, Princeton, ID). The spring loaded roller was obtained from an old glass drawing machine (Hupe and Busch, Grotzingen, Germany). During the coating procedure, as the meniscus moved down, the fused silica was moved directly into the oven that was set at 150°C. Figure 4.1 shows a schematic of the procedure.

4.2.3 Commercially available coated capillary traps

A 30 m x 0.53 mm Carboxen 1006 PLOT capillary column (Supelco, Bellefonte, PA) was cut into lengths of 10-20 cm. Before using each section as a trap, it was conditioned from 30°C to 250°C at a temperature program rate of 24°C/min and held at the maximum temperature for 2 h.

Metal PDMS coated traps were cut from a 60 m x 0.53 mm i.d. x 7 μm d_f RXT-1 column (Restek, Bellefonte, PA). Prior to use, the traps were conditioned from 30°C-250°C at a temperature program rate of 24°C/min and held at the maximum temperature for 2 h.

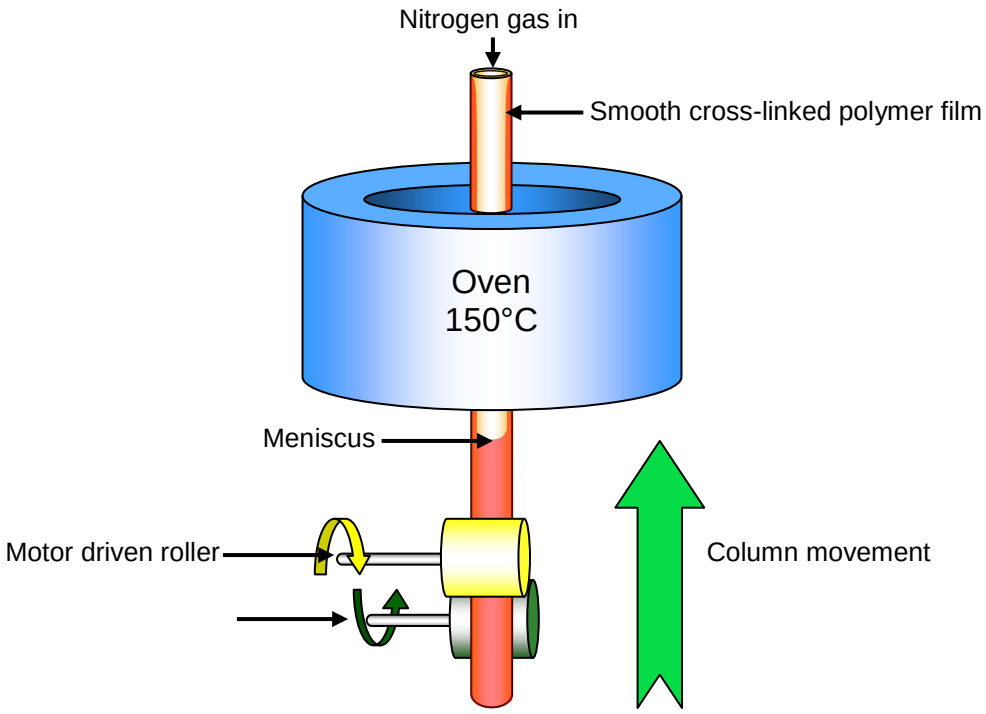

Figure 4.1. Schematic of the immediate cross-linking dynamic method for coating thick film open tubular traps. As the solution is being coated by the dynamic method with the use of a liquid brake, the fused silica is physically moved through an oven where the elastomer solution is cross-linked. For the 40 μm trap, the syringe pump was set to withdraw the solution at a rate of 5 μL/min.

4.2.4 Determination of breakthrough times by frontal chromatography

To determine breakthrough times for a capillary trap by frontal chromatography, a continuous vapor sample was introduced into the capillary, and the signal was monitored with an FID. A split/splitless injector removed from a Hewlett Packard 5890 GC was used to generate a constant vapor standard. The analyte was introduced into the heated injector at a constant speed using a syringe pump (Harvard Apparatus, Hollison, MA) where the analyte was vaporized. The concentration delivered could be adjusted by the speed of the syringe pump and the flow of carrier gas (nitrogen) introduced into the injector. The injector was mounted on the side of an

Agilent 6890 GC. The flow from the injector was fed into a 2-position, 6-port valve (VICI, Houston, TX) that was utilized as a 4-way valve. The desorption gas supply, one end of the capillary trap, and a waste reservoir were also connected to the 6-port valve. The sample flow was either fed through the trap or to the waste. When the sample was directed to the waste, a clean nitrogen supply (the desorption gas) was fed through the trap. The other end of the trap was connected to a tee where a portion of the flow was directed into the FID of the GC system to measure the output of the trap. The flow through the FID was maintained between 4-50 mL/min. The flow of the split was controlled by a needle valve (Swagelok, Solon, OH). Figure 4.2 shows a schematic of the system.

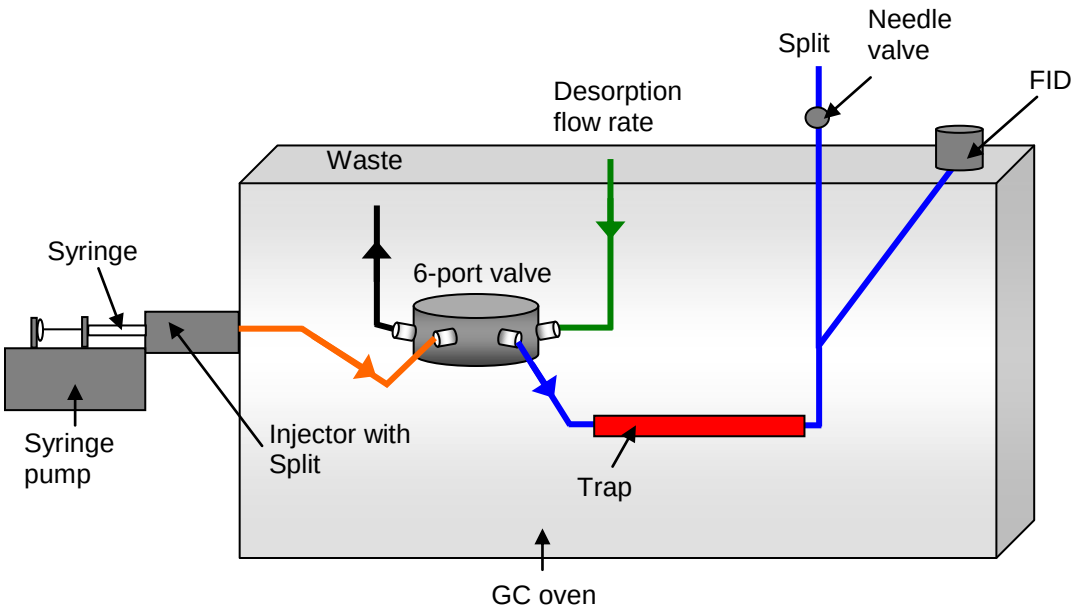

Figure 4.2. Schematic of the system assembled to determine breakthrough times by frontal chromatography. A constant vapor standard was introduced using a split/splitless injector.

4.2.5 Characterization of open tubular traps by elution chromatography

Characterization of the absorption based capillary traps was carried out using elution chromatography, in which a sample plug was used to determine breakthrough times from retention times and peak widths. The capillary was connected directly to the injector of an Agilent 6890 GC. The other end was connected to the detector. Pressure was applied to the injector and through the column to obtain the desired flow rate. At flow rates exceeding the maximum flow rate of the FID (50 mL/min), the effluent from the trap was split. The oven was set at the desired temperatures for the experiments (30-70°C). Injections of 1 µL solutions of analyte at concentrations around 1000 µg/mL were made using an Agilent 7683 series autosampler (Agilent, Santa Clara, CA). Retention times and peak widths were used to calculate the breakthrough times.

4.2.6 Preparation of multi-capillary bundle

Sealing multiple open tubular traps together to form a multi-capillary bundle consisted of gluing a bundle of capillaries with high temperature epoxy in small pieces of ¼" copper or stainless steel tubing in which Swagelok fittings could be attached. First the open tubular traps were cut to the desired length (10-20 cm for the Carboxen trap and 1 m for the 7 µm thick PDMS trap) and fed through the 2 short (~3 cm in length) pieces of ¼" o.d. tubing. The number of traps was determined by the number of single traps that fit through both ¼" sections of tubing. Once the number of capillaries was determined, the short pieces were removed. High temperature heat conductive epoxy (H70E) obtained from Epoxy Technology (Billerica, MA) was placed around each individual capillary approximately 0.5 cm from one end. Once epoxy was coated around each of the capillaries, one of the ¼" o.d. tubes was placed over the end of the bundle, so that the capillary ends were inside the tube. When the capillaries were inside the ¼" tube, epoxy was

placed around the tube to create the seal. After drying on its own for a day or two, the epoxy was fully cured in an oven at a temperature of 150°C for 5 min, under an inert gas. The procedure was repeated for the other end of the capillary. The epoxy used produced minimal off-gassing at high temperatures. Figure 4.3 shows a trap consisting of 33 individual capillaries with lengths of 10 cm prepared in the manner just described.

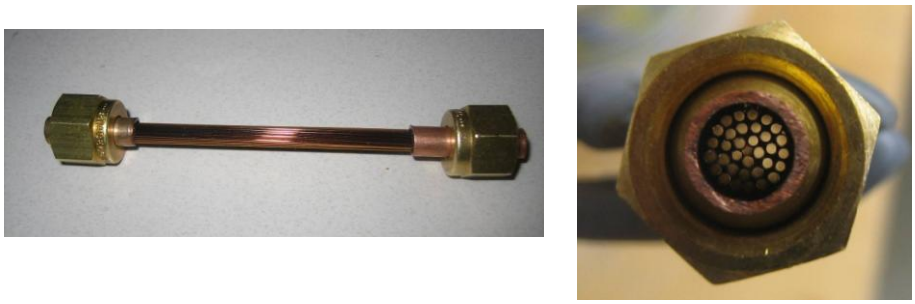

Figure 4.3. Multi-capillary trap consisting of 33 capillaries bundled together.

4.2.7 Secondary traps

Two traps were investigated for use as a secondary trap to refocus analytes from the multi-capillary bundle. The first was a commercially available trap designed to be used in the Miniature Continuous Air Monitoring System (MINICAMS) made by CMS Field Products (Pelham, AL) which is a portable GC for continuous air monitoring applications. The MINICAMS trap consisted of 60/80 mesh Tenax adsorbent material packed inside a glass tube (3 mm x 100 mm). The packing material itself was approximately 1.5 cm in length and contained approximately 20 mg of adsorbent material.

The second trap investigated was a microtrap that was prepared using 60/80 mesh Tenax-TA (Scientific Instrument Services, Ringoes, NJ). The Tenax material was packed inside a 530 μm i.d. fused silica capillary tube. To pack the adsorbent, the fused silica was dabbed into the adsorbent, and the small amount of adsorbent that was forced inside the capillary was pushed further inside by a smaller wire. This process was repeated until approximately 1 cm in length of packing material was reached (~0.7 mg of Tenax). Pesticide grade glass wool (Supelco, Bellefonte, PA) was also placed at both ends of the packing material. To ensure that the packing material remained in place inside the fused silica capillary, 320 μm i.d. fused silica capillary was glued inside the 530 μm i.d. capillary with the same high temperature epoxy used for the open tubular traps. The trap was then conditioned at 250°C under nitrogen for 2-3 h. Figure 4.4 shows a photograph of the microtrap that was prepared.

Figure 4.4. Photograph of Tenax microtrap packed in 530 μm i.d. fused silica tubing.

4.2.8 2-Trap system

A system was constructed that allowed sampling at high flow rates through a multi-capillary trap, after which the trapped analytes were then desorbed at lower flows and focused into a second trap. Then they were desorbed at even lower flows to be compatible with flow rates of a GC-MS system. A schematic of the system is shown in Figure 4.5.

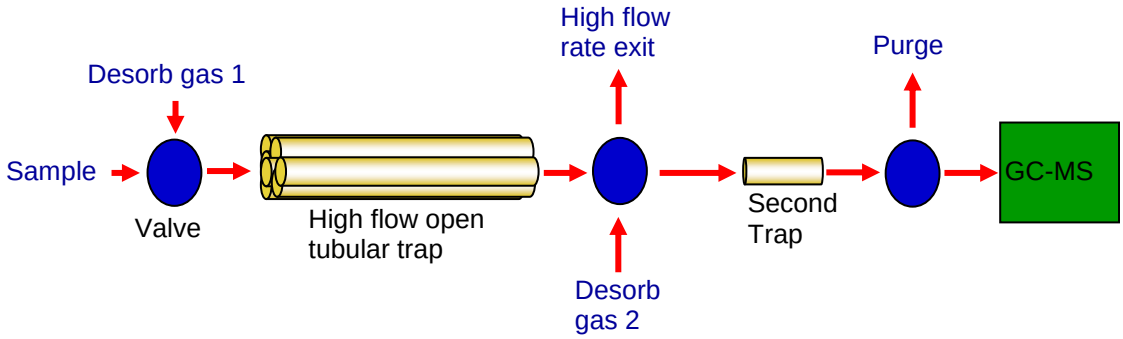

Figure 4.5. Schematic of a high flow rate air sampling system. The high flow multi-capillary open tubular trap allows for trapping at high flow rates and contains a purge for the high flow rate exit. A desorb gas is then introduced into the high flow rate trap, and the analytes are desorbed and focused in the second trap. The flow rate is then decreased once more, and the second trap is desorbed and fed into a GC-MS system for analysis (FID for this work).

The system described above required the introduction of 3 separate flow rates and 2 purges. This was accomplished with two 6-port valves (2-position). The valves and most of the transfer lines were housed in the GC oven to maintain high temperature. Figure 4.6 shows a schematic of the plumbing of the system. The vapor standard generated by the vapor dissemination system described above (consisting of a split/splitless GC injector) was fed through 0.3 m of 320 μm i.d. fused silica into a 1/8" Swagelok tee, where it was mixed with diluent gas. The diluent gas was controlled by a separate regulator, which controlled the total flow of the sample.

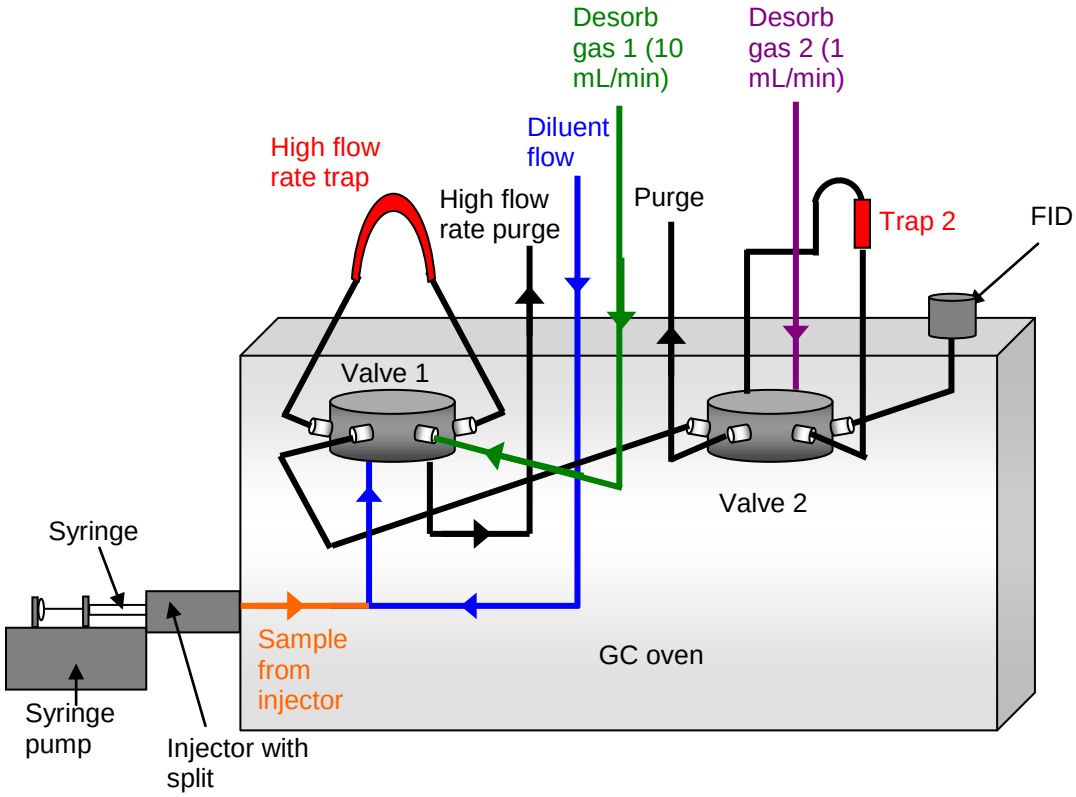

Figure 4.6. Schematic of the 2-trap system consisting of two 6-port valves, a high flow rate sample, and 2 desorption flows. The GC oven was kept at 250°C to keep the valves and transfer lines hot.

The sample stream was then fed into a high temperature, 2-position, 6-port valve with 1/8" fittings and 0.067" ports (VICI, Houston, TX) via approximately 0.3 m of 1/8" stainless steel tubing with 1/16" i.d. The first trap of the 2-trap system (high flow rate trap) was placed outside the oven and was connected to two of the ports of the valve through 1/8" o.d. stainless steel tubing. The trap was connected to the 1/8" tubing by Swagelok reducing unions (1/4" to 1/8"). Another source of nitrogen was required to desorb from the first trap and, hence, a desorbing gas of approximately 10 mL/min was also fed into the 6-port valve using the 1/8" o.d. stainless steel tubing. This desorption gas was controlled with its own dedicated regulator. One of the ports on the first 6-port valve was used for a high flow rate purge, which was directed from the oven with

1/8” o.d. stainless steel tubing, so that the flow could be measured using a rotameter. The last port was used to direct the effluent from the first valve (from the 10 mL/min desorption gas) to the second valve. The plumbing of the first valve allowed the high sample flow to be directed through the first trap during the sampling period and out the high flow rate purge, while the desorption gas 1 was directed to the second valve. During the desorption period, the valve was switched so that the high flow rate sample was directed to the high flow rate purge, while the desorption gas was directed through the trap and into the second valve. The switching schematic of the first valve can be seen in Figures 4.7A and 4.7B.

The second valve in the setup was a high temperature, 2-position 6-port valve with 1/16” fittings and 0.030” ports (VICI). The sample from the first valve was plumbed into one of the ports on the second valve. A 1/8” to 1/16” Swagelok reducing union was used to connect the 1/8” o.d. tubing from the first valve to the 1/16” o.d. tubing from the second valve. The second trap was placed outside the GC oven, and a transfer line consisting of 1/16” o.d. stainless steel tubing with 0.03” i.d. was used to connect one end of the second trap to valve 2. A transfer line consisting of 1/16” o.d. x 0.01” was used to connect the other end of the second trap to the valve. A line for the desorption flow was also plumbed to the second valve using 1/16” o.d. x 0.03” i.d. stainless steel tubing. The purge flow was directed from the valve to outside the oven with 1/16” o.d. tubing, as well, to monitor the flow rate. The flow from the last port was directed to the FID using a 3 cm section of 1/16” o.d. stainless steel tubing that was connected to a 320 μm i.d. fused silica capillary with a union and graphite ferrule (VICI). The flow schematics for sampling and desorption from valve 2 are shown in Figures 4.7C and 4.7D, respectively. The flow from the first trap was directed into the second trap during sampling, while the second desorption flow was directed to the FID. When it was time to desorb, the valve was manually switched to the

desorption position, where the second desorption flow (~ 1 mL/min) was fed through the second trap and out to the FID, while the flow from the first trap was vented to waste.

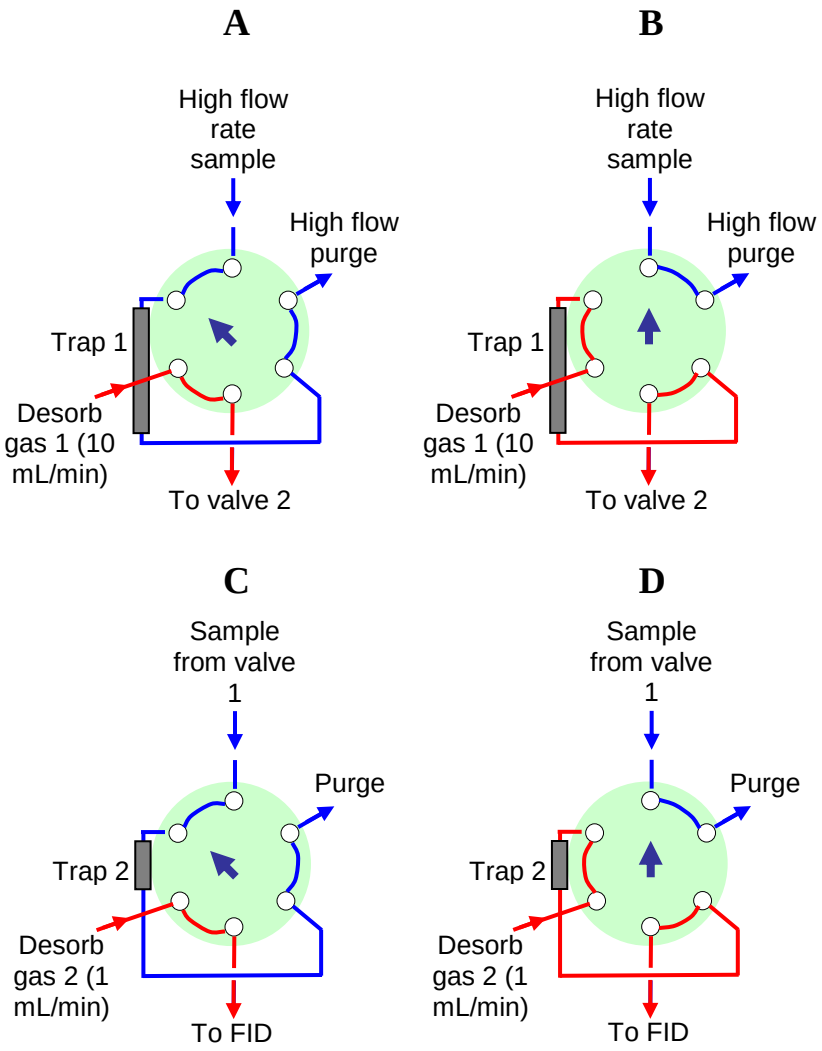

Figure 4.7. Switching schematics of the 2-position, 6-port valves in the 2-trap setup. (A) Valve 1 flow schematic during the sampling period, where the high flow rate sample was directed through the first trap, and the desorption gas was directed to valve 2. (B) Valve 1 flow schematic during desorption of the first trap for the desorption flow was directed through the first trap and into valve 2, while the high sample flow was directed out the high flow purge vent. (C) Valve 2 flow schematic during the focusing period, where the analytes that were desorbed from trap 1 (Valve 1) were fed into valve 2 as the slower desorption gas was fed into the FID. (D) Valve 2 flow schematic during desorption of the second trap, where the second desorption flow purged the second trap into the detector for analysis, while the effluent from valve 1 was directed to the purge vent.

The multi-capillary trap was desorbed using heat tape controlled by a variable autotransformer. The second trap (either micro or MINICAMS) was desorbed using double glass silicone insulated resistively heated wire (Nichrome 80, 5 Ω/ft) from Driver-Harris (Harrison, NJ) that was also controlled using a variable autotransformer.

4.3 Results and Discussion

4.3.1 Trap characterization methods

One of the most conventional methods to characterize traps is by determining the breakthrough time or volume. The breakthrough time (or volume) is defined in the literature as the time (or volume) when 1-5% breakthrough is reached, and this is generally determined by breakthrough curves.[14] Breakthrough curves are obtained by introducing a continuous sample (i.e., frontal chromatography) into the trap and monitoring the output. It is the breakthrough time that determines the length of time that can be sampled with the trap (under exhaustive sampling techniques) for a set of given parameters. The breakthrough volume can also be reported, which describes the total volume of air that can be sampled before breakthrough. In this chapter, the breakthrough time is used to compare the retention capabilities of different traps, and is defined as the time when the signal is 1% of the maximum amount.

The breakthrough time for sorbents that follow a linear isotherm (i.e., breakthrough time does not depend on sample concentration) can also be obtained through elution chromatography, since the trap can be treated essentially as a short chromatographic column. Figure 4.8 shows the relationship between frontal and elution chromatography.[14-16] Hence, the breakthrough time can be determined from elution chromatography by Equation 4.1

$$t_B = t_R - \frac{w}{2} \tag{4.1}$$

Where t_B is the breakthrough time, t_R is the retention time in elution chromatography and w is the width at baseline (in time).

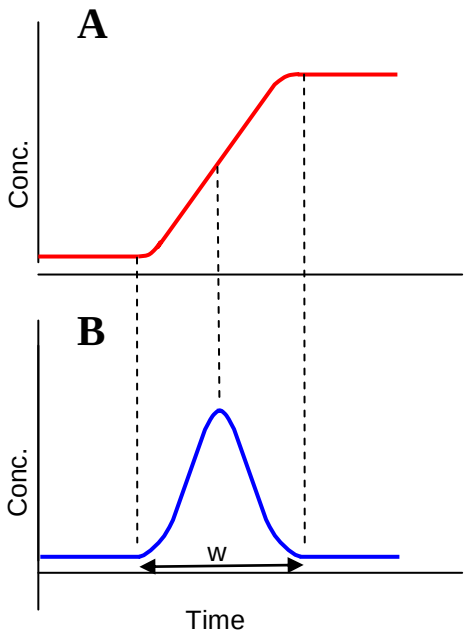

Figure 4.8. Concentration profile at trap outlet for (A) frontal chromatography and (B) elution chromatography.

Elution chromatography was used to determine t_B values for traps with linear isotherms, such as the sol-gel traps and the PDMS traps. It was found that t_B for the Carboxen traps was concentration dependent; therefore, frontal chromatography was performed to obtain t_B values.

4.3.2 Sorbents in open tubular traps

The film thickness and/or surface area of the stationary phase of an open tubular trap can be increased to increase retention. Three different types of stationary phases were investigated for use as open tubular traps: PLOT (increased surface area), sol-gel PDMS (increased surface area), and thick film PDMS. Figure 4.9 shows the breakthrough curves for these coatings in capillaries with the same internal diameter and length for a continuous sample of undecane at a concentration of 25 mg/m^3 and a flow rate of 50 mL/min.

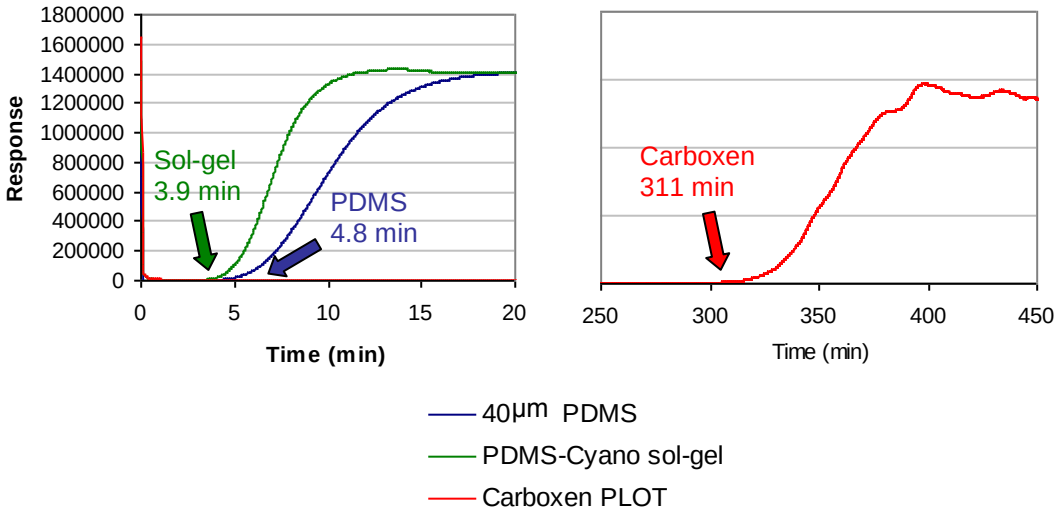

Figure 4.9. Breakthrough curves and breakthrough times of 25 mg/m^3 undecane at 50 mL/min on 20 cm x 0.530 mm i.d. traps. The film thickness for the sol-gel cyanopropyl PDMS trap was approximately 5 µm, the film thickness for the PDMS trap was 40 µm and that for the Carboxen PLOT trap was approximately 17 µm.

The sol-gel cyanopropyl-PDMS trap demonstrated the least retention compared to the other traps in Figure 4.9. However, this observation is not truly representative, since it had a very thin film of coating. Compared to traditional polymeric stationary phases with comparable film

thicknesses, the sol-gel trap provides much higher retention. Table 4.1 compares the t_B of toluene and octane on 1-m long traps coated with PDMS sol-gel, cyano-PDMS sol-gel, and 5-µm thick SE-54 (traditional polymer film for GC). For these experiments, the trap was coupled directly to the injector and detector of a GC system, and elution chromatography was performed. As can be seen from Table 4.1, retention is much greater for the sol-gel traps compared to the polymeric phase. One explanation is that the sol-gel coating is porous, providing a larger surface area for sorption. Sol-gel chemistry offers a method to chemically bond an organic-inorganic porous hybrid polymer to the inside wall of a fused silica capillary by extensive cross-linking. The sol-gel trap was prepared by filling a column with a solution containing an alkoxide-based precursor, a hydroxyl-terminated active polymer, a surface derivatizing reagent, and an acid catalyst. The hydrolysis of the precursor allows for polycondensation reactions with the sol-gel reactive species. This allows the formation of a three-dimensional porous polymer. Figure 4.10 shows a schematic of the reactions that take place to generate the sol-gel porous film.

Table 4.1. Dimensions, chromatographic parameters, and breakthrough times for toluene and octane for two sol-gel traps compared to an SE-54 trap.

Type of phase	i.d. (µm)	Length (m)	d_f (µm)	Temp (°C)	Flow (mL/min)	Lin vel (cm/s)	t_B toluene (min)	t_B octane (min)
Sol-gel PDMS	320	0.96	1.3	26	1.03	21	11.74	53.05
Sol-gel cyano-PDMS	320	1.01	3	26	1.03	21	15.81	60.15
Polymer SE-54	320	1	5	26	1.13	23	3.93	5.69

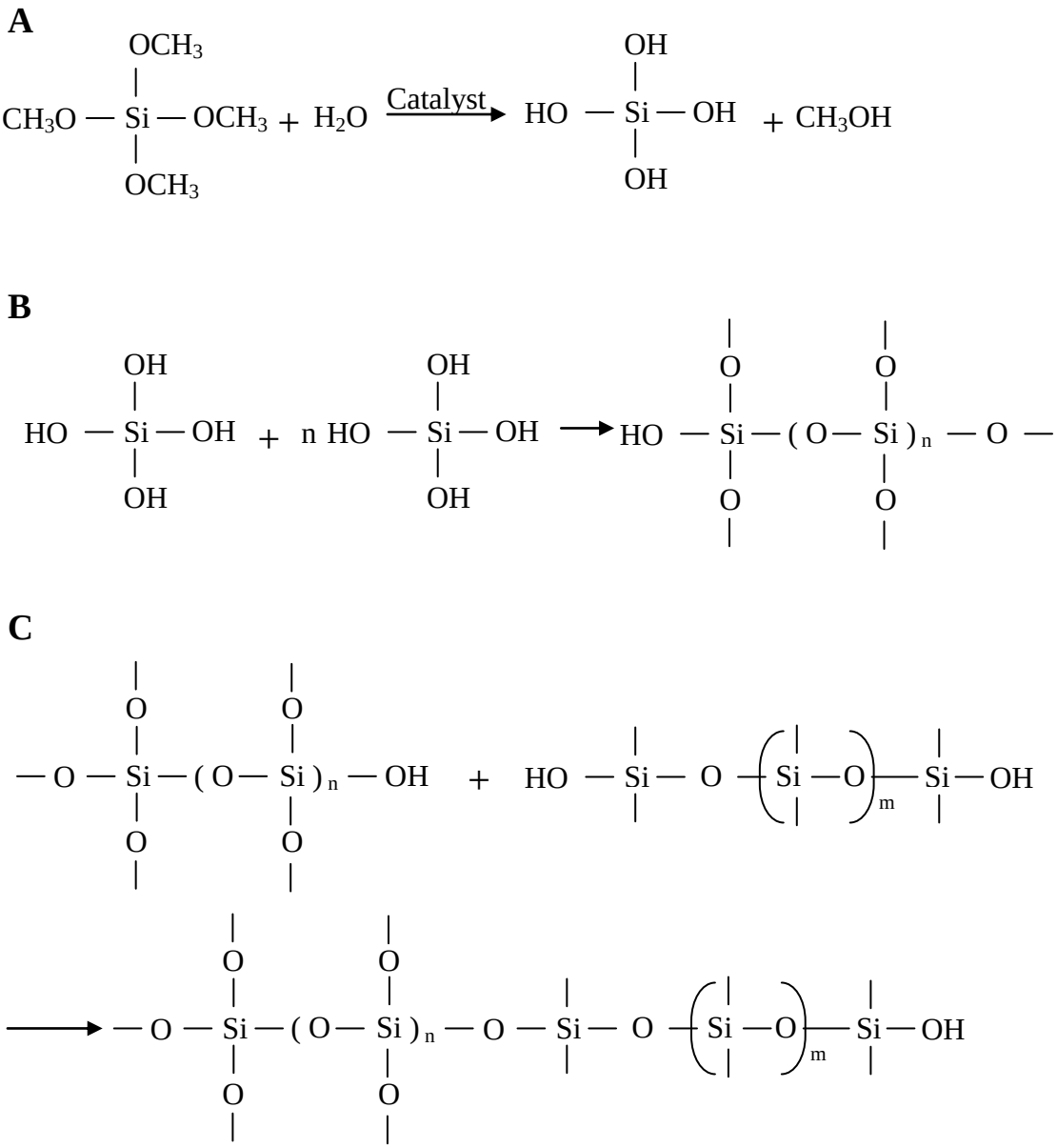

Figure 4.10. Schematic of the sol-gel reactions. (A) Hydrolysis of an alkoxide based precursor, (B) polycondensation of hydrolyzed products, and (C) condensation of hydroxyl-terminated sol-gel reactive species.

Additional functional groups can be added to the sol-gel network to change its sorption behavior. For example, 3-cyanopropyltriethoxysilane is added as an additional precursor to

incorporate a cyano group in the moiety to increase the polarity of the phase. This allows flexibility in preparing different coatings with different polarities. The silanol groups on the fused silica walls can also participate in the condensation reactions and, thus, the phase becomes chemically bound to the fused silica capillary. This enhances the stability of the phase and, as a result, allows it to withstand high temperatures.[9-10] From the literature, the porous nature of sol-gel coatings can be seen through scanning electron microscope (SEM) images.[9-10] SEM images were taken of the sol-gel traps prepared, however, the porosity of the sol-gel was not visible at the resolution of the image (Figure 4.11A).

A disadvantage of the sol-gel phase is that it has a tendency to crack during the drying process, especially for film thickness greater than 0.5-1 μm.[9] Shrinking and cracking during the drying process is a result of solvent evaporation from the pores. When trying to prepare thicker coatings, cracking of the phase resulted, an example of which is shown in the SEM image in Figure 4.11B. To prevent shrinking and cracking during the drying process, the sol-gel trap was conditioned at a slow temperature ramp of 0.2°C/min. This procedure decreased cracking, however, it was still evident for thicker phases. With the correct protocol, cracking can be avoided as demonstrated by Chong et al. who were able to prepare 10-μm thick PDMS sol-gel coatings on SPME fibers.

Despite my difficulties in preparing reproducible sol-gel traps, it has been shown in the literature that the preparation of sol-gel phases can be very reproducible. Kulkarni et al. showed that for 3 capillaries, the %RSD of peak area for several different chemical classes was typically less than 5%.[10]

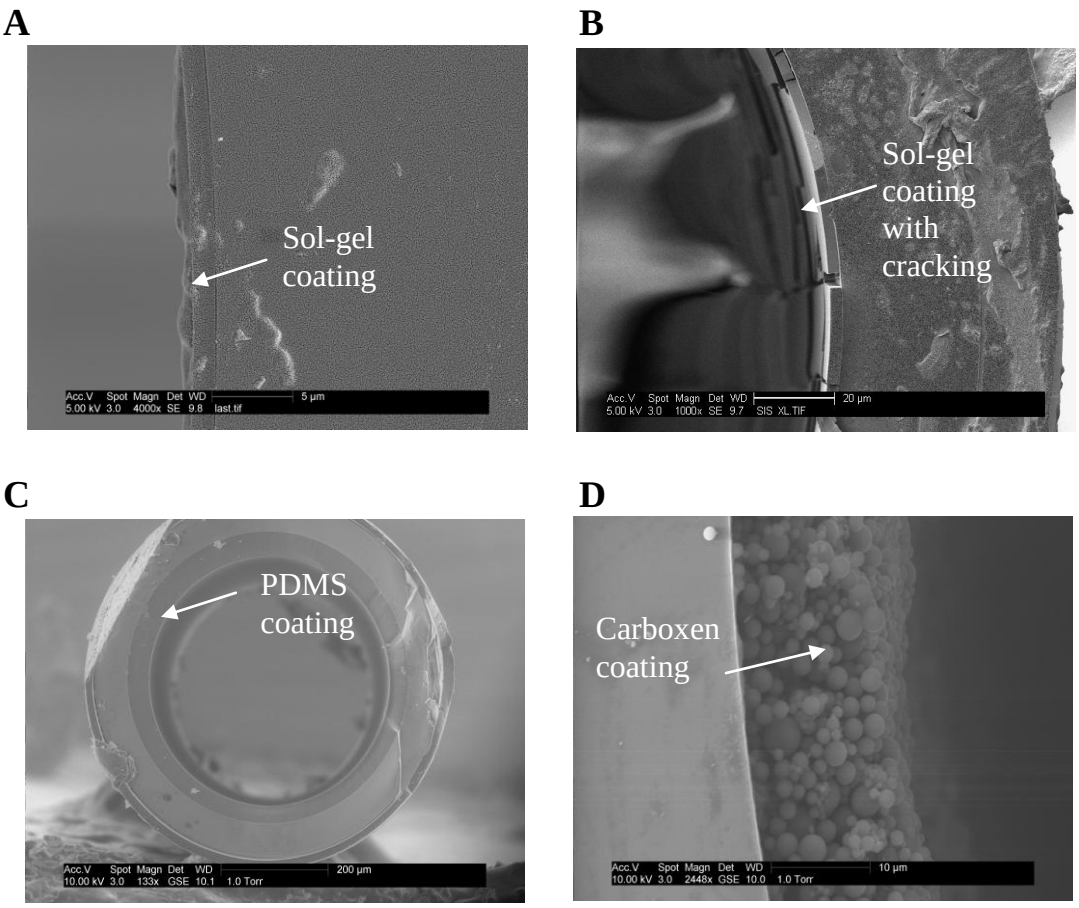

Figure 4.11. (A) SEM image of a sol-gel PDMS coating in a 320 µm fused silica capillary (film thickness was estimated to be 1.3 µm). (B) SEM image of a sol-gel cyano-PDMS coating in a 320 µm i.d. fused silica trap showing cracking (Film thickness was estimated to be 3.3 µm). (C) SEM image of a thick PDMS film in a 530 µm i.d. fused silica capillary (film thickness was estimated to be 30-45 µm). (D) SEM image of the surface of a Carboxen PLOT column (estimated thickness of Carboxen particles is 17 µm).

The retention characteristics of the trap were also increased by coating the trap with a thick film of PDMS. The retention of a 40 µm thick PDMS trap was slightly higher compared to a sol-gel cyano-PDMS trap (Figure 4.9). Preparation of a thick PDMS trap was not trivial. It was difficult to prepare a thick polymer coating using traditional methods (static and dynamic coating procedures) due to Raleigh instabilty.[17] This phenomenon causes ripples in the stationary phases,

and can also clog the column. The amplitude of the ripples are larger for thicker films and longer column preparations as noted by Equation 4.2 [17]

$$\ln \frac{b}{b_0} = \frac{\gamma d_f{}^3 t}{12 \eta a^4} \tag{4.2}$$

where b and b_0 are the amplitudes of the waves (i.e., ripples) at times t and 0, respectively, γ is the surface tension, d_f is the film thickness, t is the column preparation time, η is the viscosity of the coating solution, and a is the i.d. of the capillary being coated. If the stationary phase is immediately cross-linked, then the ripples will be minimized. Blomberg and Roeraade demonstrated that if the phase is immediately cross-linked during the coating process, thick films can be obtained.[12] An adaptation of their protocol was used to coat a 40 μm thick PDMS film. An SEM of this trap is shown in Figure 4.11C. The film was not completely centered in the fused silica (i.e., parts of the coating were thicker at certain locations). Blomberg and Roeraade also observed a similar effect and noted that it could have resulted from mechanical vibrations and temperature gradients.[12] Since this method is essentially the dynamic coating procedure, the film thickness can be estimated by using Equation 4.3 [18]

$$d_f = \frac{C r}{200} \sqrt{\frac{u \eta}{\gamma}} \tag{4.3}$$

where C is the concentration of the coating solution, r is the i.d. of the capillary, u is the velocity of the coating plug, η is the viscosity of the coating solution, and γ is the surface tension of the coating solution. Taking the viscosity and surface tension of the Sylgard 184 elastomer solution

from the literature,[12] the thickness of the trap in Figure 4.8 was calculated to be 28.5 μm. From the SEM image, the film thickness ranged from 30-45 μm. The coating speed was not uniform throughout the coating process; sometimes the speed would change as the column was fed into the oven. This may have caused slight fluctuations in the coating process. Furthermore, there were times when air bubbles were noticed inside the syringe, indicating a leak somewhere in the system. Overall, however, the method worked well to produce short traps with thick coatings.

There are several advantages of using PDMS as the coating for open tubular traps. First, PDMS is well characterized since it has been used as a stationary phase for separations in GC for many years. PDMS is an inert polymer, and analytes will not react with it, as may be the case for many adsorbents that are used in air sampling applications.[19] Desorption from PDMS is fast.[19] Furthermore, PDMS has a low affinity for water, which makes it a good phase for trapping in high humidity. Analytes are partitioned (absorbed) into the liquid PDMS phase, instead of being adsorbed. Since the analytes are dissolved in the phase, they are not often displaced by other analytes, which occurs more frequently for adsorption based sorbents. In addition, PDMS also has a linear isotherm and, hence, retention is not concentration dependent. This can be an advantage since breakthrough times can be determined easily for different sampling conditions, which is demonstrated later in this chapter with a 7 μm thick PDMS trap. The main disadvantage of PDMS is its low retention. However, as demonstrated above, thick films can be coated for trapping applications.

The Carboxen PLOT trap demonstrated the highest retention of the three traps in Figure 4.9. The high capacity of the Carboxen material is partially attributed to its high surface area available for adsorption. The PLOT coating consists of a thick (~17 μm) coating of Carboxen 1006 particles, as seen by the SEM image in Figure 4.11D. In addition to the thick layer of

Carboxen particles, the particles are also porous to increase retention. Carboxen 1006 particles have an even distribution of micro, meso, and macro pores with a total pore volume of 0.78 mL/g.[20]

Since the Carboxen PLOT trap has high capacity, effort was spent to characterize a 10 cm length trap for different analyte concentrations. A length of 10 cm was chosen because it is a good practical length to build a multi-capillary bundle. Breakthrough plots were obtained for a 10 cm length Carboxen single trap using benzene as a test analyte. Different concentrations were introduced into the trap. Figure 4.12 shows the relationship of t_B with respect to concentration. Triplicate measurements were obtained at each concentration. The error bars are also displayed in the figure.

Figure 4.12 shows the breakthrough dependency on concentration for the Carboxen PLOT trap, which indicates a non-linear adsorption isotherm. Harper experimentally obtained both breakthrough curves and adsorption isotherms for several different analytes on Chromosorb 106 adsorbent. The concentration dependency observed in his results is similar to that in Figure 4.12. All of the adsorption isotherms obtained in Harper's work were non-linear and concave to the concentration axis over the range of concentrations studied (up to 3000 mg/m^3).[21] Although adsorption isotherms were not obtained for the Carboxen PLOT trap, the non-linearity of the trap is evident from the data shown in Figure 4.12.

Since the relationship between t_B and analyte concentration is powered, a plot of log concentration vs. log breakthrough time gives a straight line. Data were also taken for similar concentrations at flows of 50 and 100 mL/min, and the log t_B vs. log concentration plots and error bars are shown in Figure 4.13 (3 replicates). The coefficients of the linear regression and standard deviations (SD) are given in Table 4.2.

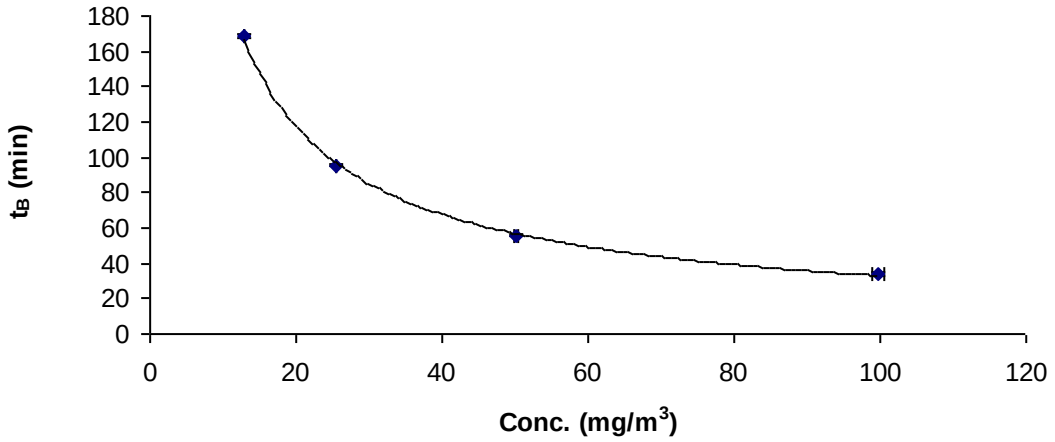

Figure 4.12. Average breakthrough time (3 replicates) versus concentration of benzene (12.8, 25.6, 50.1, and 99.7 mg/m^3) on a 10 cm Carboxen trap at a flow rate of 18.6 mL/min and a temperature of 40°C.

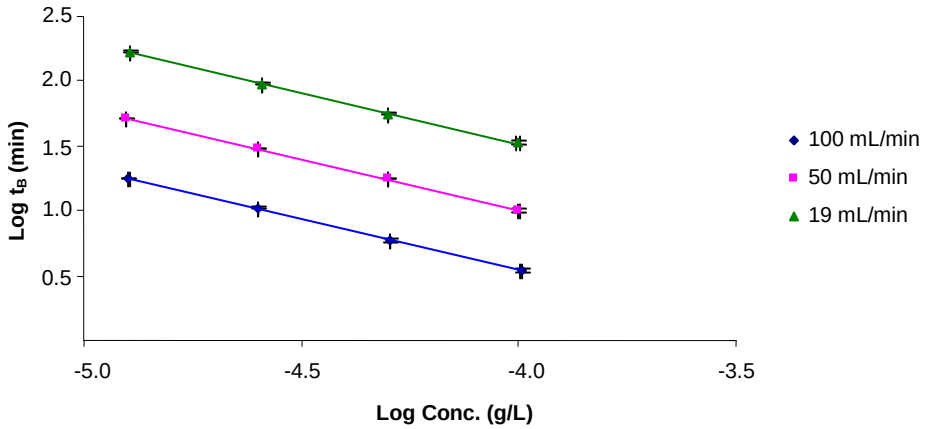

Figure 4.13. Plot of log t_B vs. log concentration for 3 different flows containing benzene in a 10 cm Carboxen PLOT trap at a temperature of 40°C. Points are an average of 3 measurements.

Table 4.2. Slope and y-intercepts for the linear regressions of the log t_B vs. log benzene concentration for flows of 100, 50, and 19 mL/min on a 10 cm Carboxen PLOT trap at 40°C (see Figure 4.13).

Flow (mL/min)	Slope	Slope SD	y-Intercept	y-intercept SD	R^2
100	-0.79	0.02	-2.61	0.06	0.9992
50	-0.79	0.01	-2.14	0.07	0.9993
19	-0.79	0.01	-1.64	0.06	0.9995

From Table 4.2 it can be seen that the slopes for all three flow rates are the same, however, the y-intercepts are different. There is a relationship between the flow rate and the y-intercept, which is shown in Figure 4.14.

To calculate the breakthrough time at another flow rate and concentration for the 10 cm Carboxen PLOT trap, a y-intercept can be extrapolated by the linear regression of Figure 4.14, and that intercept can then be applied to the linear regressions in Figure 4.13 and Table 4.2 to determine the new t_B. The breakthrough time was calculated for a concentration of 100 and 50 mg/m^3 at a flow rate of 75 mL/min and compared to experimental results with 3 replicates performed at each concentration (Table 4.3).

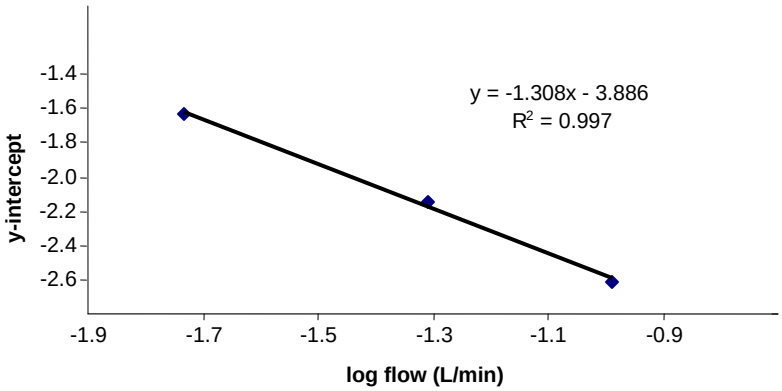

Figure 4.14. Relationship between the y-intercept (obtained from linear regressions of log benzene concentration vs. log t_B) and the flow rate for a 10 cm Carboxen trap at 40°C.

Although there appears to be relationships to predict the breakthrough times for conditions that were not tested, estimating breakthrough times for real conditions may be difficult for an adsorption based phase. The experiments performed here only involved trapping one analyte. Displacement of one analyte by another when sampling multiple analytes can occur and can quickly complicate models used to predict breakthrough times.

Table 4.3. Experimental and calculated breakthrough times for benzene on a 10 cm Carboxen trap at a flow rate of 75 mL/min at 40°C.

Conc. (mg/m^3)	Experimental t_B (min)	SD	Calculated t_B (min)	SD
100.7	5.7	0.1	5.4	0.3
50.4	9.3	0.1	9.4	0.3

Multiple sections of the Carboxen PLOT trap were tested to determine trap-to-trap reproducibility. Table 4.4 lists the average breakthrough times (n=3) of benzene at 40°C at 4 different concentrations on 3 different traps.

Table 4.4. Breakthrough times of benzene on 3 different 10 cm Carboxen traps at 4 different concentrations at a flow rate of 50 mL/min and at 40°C.

	Run-to-run reproducibility						Trap-to-trap reproducibility	
	Trap 1		Trap 2		Trap 3			
Conc. (mg/m^3).	mean t_B (min)	%RSD	mean t_B (min)	%RSD	mean t_B (min)	%RSD	mean t_B (min)	%RSD
12.5	51.4	1.0	45.9	2.0	41.2	1.5	46.2	11.1
25	30.3	1.6	26.5	1.8	24.7	2.5	27.2	10.5
50	17.9	0.7	15.7	3.5	14.1	1.6	15.9	12.1
100	9.98	3.3	9.3	3.6	8.6	1.5	9.3	7.2

As can be seen from Table 4.4, the run-to-run reproducibility was good, with % RSD less than 3.6%. The trap-to-trap reproducibility of all 3 traps was less than 12%. However, the difference in t_B at the 12.5 mg/m^3 concentration for traps 1 and 3 was approximately 16%. The traps were taken from different portions of a 15 m long Carboxen column. The reason that traps 1 and 3 had the largest variance is because these two traps were taken from different ends of the column, which would be expected to have the largest variance.

The obvious advantage of the Carboxen PLOT trap is its high retention as evident in Figure 4.9. However, Carboxen does have several disadvantages. It was shown in the literature that several types of Carboxen particles have high retention for water vapor at high humidty.[22]

Trapped water may displace other analytes. Because of the small pores in the Carboxen 1006 particles, desorption of heavy analytes can be slow; for this reason it is not recommended for semi-VOCs.[20]

Another method to increase retention is to increase the length of the trap. However, the dimensions become more of a concern if the trap is to be used in the field. Long traps can be cumbersome in the field unless they are coiled to smaller dimensions. Traps made from fused silica columns can be coiled, however, their coil radius is limited due to the fragile nature of fused silica, especially for larger i.d. columns. Metal columns can be coiled tighter than their fused silica counterparts and are more robust. Hence, the use of long metal open tubular traps can be feasible for field use.

A metal PDMS column with 530 μm i.d. x 7 μm film thickness was purchased for constructing a multi-capillary bundle for semi-volatile organic compounds. An individual 1-m long capillary was used for preliminary experiments. Elution chromatography was used to determine breakthrough times for different analytes at different flow rates and at different temperatures. Tables 4.5 lists the breakthrough times (3 replicates) for decane (C10), undecane (C11), dodecane (C12) tridecane (C13), tetradecane (C14), methyl salicylate (MES), dimethyl methylphosphonate (DMMP), triethyl phosphate (TEP), and diethyl phthalate (DEP) at flows of 10, 25, 50, 75, and 100 mL/min at temperatures ranging from 30-70°C. MES, DMMP, TEP and DEP were chosen as analytes because they are chemical agent simulants.

Despite the long length of the 7 μm PDMS trap, retention of the lighter analytes in Table 4.5 was low. For example, the breakthrough times for DMMP were less than 1 min for all conditions tested. This trap is not a realistic trap to be used for VOC. However, the trap retains heavier analytes well, especially DEP. .

Table 4.5. Breakthrough times (3 replicates) determined by elution chromatography for 1 m x 0.53 mm i.d. x 7 µm PDMS trap at different flow rates and temperatures. The analytes for the study were decane (C10), undecane (C11), dodecane (C12) tridecane (C13), tetradecane (C14), methyl salicylate (MES), dimethyl methylphosphonate (DMMP), triethyl phosphate (TEP), and diethyl phthalate (DEP).

30°C

Analyte	t_B (min) at 49.5 mL/min	SD	t_B (min) at 100.1 mL/min	SD
C10	1.174	0.004	0.61	0.02
C11	3.15	0.03	1.73	0.08
C12	8.1	0.1	4.56	0.07
C13	20.50	0.05	11.9	0.1
C14	54	1	30.5	0.4
MES	5.076	0.007	2.65	0.08
DMMP	0.276	0.006	0.178	0.01
TEP	3.02	0.02	2.0	0.2
DEP				

40°C

Analyte	t_B (min) at 10 mL/min	SD	t_B (min) at 25 mL/min	SD	t_B (min) at 49.1 mL/min	SD	t_B (min) at 74.5 mL/min	SD	t_B (min) at 99.8 mL/min	SD
C10	3.81	0.04	1.407	0.003	0.649	0.007	0.489	0.004	0.317	0.002
C11	9.4	0.1	3.5	0.3	1.64	0.03	1.27	0.03	0.83	0.01
C12	23.0	0.2	8.46	0.08	4.06	0.03	3.11	0.05	2.14	0.03
C13			20.6	0.1	9.71	0.01	7.6	0.1	5.42	0.06
C14			49.8	0.3	23.8	0.2	18.2	0.3	13.2	0.1
MES	14.8	0.1	5.57	0.05	2.662	0.008	1.97	0.01	1.35	0.03
DMMP	0.941	0.003	0.349	0.002	0.166	0.001	0.143	0.001	0.105	0.001
TEP	8.873	0.001	3.306	0.008	1.52	0.02	1.280	0.003	0.92	0.03
DEP					71.2	0.4			40	4

Table 4.5 (Cont.)

50°C Analyte	t_B (min) at 25 mL/min	SD	t_B (min) at 49.5 mL/min	SD	t_B (min) at 75 mL/min	SD	t_B (min) at 99.1 mL/min	SD
C10	0.806	0.002	0.369	0.003	0.282	0.003	0.196	0.004
C11	1.906	0.008	0.90	0.02	0.69	0.01	0.49	0.01
C12	4.41	0.01	2.092	0.006	1.65	0.01	1.19	0.06
C13	10.15	0.07	4.77	0.01	3.77	0.01	2.79	0.02
C14	23.2	0.1	10.88	0.07	8.79	0.02	6.50	0.06
MES	3.089	1E-03	1.41	0.01	1.082	0.005	0.755	0.004
DMMP	0.2175	0.0001	0.1056	0.0001	0.094	0.001	0.073	0.003
TEP	1.757	0.004	0.790	0.001	0.68	0.02	0.52	0.01
DEP	69.1	0.7	31.2	0.6	25	1	17.2	0.8

60°C Analyte	t_B (min) at 25 mL/min	SD	t_B (min) at 49.5 mL/min	SD	t_B (min) at 75.3 mL/min	SD	t_B (min) at 99.6 mL/min	SD
C10	0.481	0.002	0.225	0.007	0.170	0.003	0.1200	0.0005
C11	1.081	0.002	0.52	0.03	0.385	0.004	0.275	0.005
C12	2.384	0.008	1.16	0.02	0.90	0.02	0.65	0.03
C13	5.23	0.03	2.51	0.06	1.977	0.006	1.458	0.004
C14	11.4	0.1	5.50	0.08	4.30	0.03	3.22	0.02
MES	1.74	0.01	0.797	0.002	0.615	0.003	0.4274	0.0009
DMMP	0.143	0.002	0.074	0.001	0.063	0.003	0.0493	0.0001
TEP	0.980	0.003	0.442	0.002	0.371	0.005	0.263	0.002
DEP	32.56	0.02	14.4	0.2	11.1	0.1	7.6	0.1

Table 4.5 (Cont.)

70°C Analyte	t_B (min) at 25 mL/min	SD	t_B (min) at 49.5 mL/min	SD
C10	0.305	0.006	0.1376	0.0008
C11	0.65	0.01	0.300	0.001
C12	1.38	0.02	0.661	0.001
C13	2.89	0.04	1.364	0.002
C14	6.0	0.1	2.84	0.01
MES	1.05	0.02	0.474	0.002
DMMP	0.101	0.004	0.057	0.003
TEP	0.591	0.003	0.263	0.002
DEP	16.50	0.08	7.10	0.02

For a given flow rate, a plot of log t_B vs. 1/T is linear.[15] Furthermore, the breakthrough times at other temperatures can be predicted. Figure 4.15 shows such a plot for C12 at a flow rate of 49.5 mL/min (triplicate measurements). Error bars are also indicated in the figure. From the curve in Figure 4.15, the breakthrough time was estimated for other temperatures. The t_B values at 25, 20, and 10°C were 11.5, 16.7 and 36.7 min, respectively.

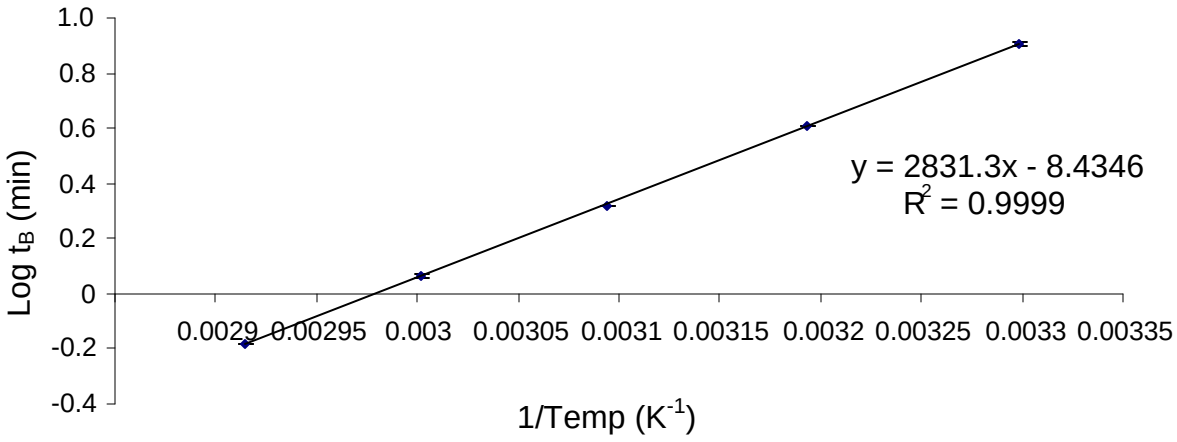

Figure 4.15. Plot of log t_B (min) vs. 1/T for decane (n=3) at a flow rate of 49.5 mL/min on a 1 m x 7 µm d_f PDMS trap.

4.3.3 Multi-capillary open tubular traps

Another approach to increase retention on open tubular traps is to bundle a number of traps in parallel. This increases the capacity of the entire trap and also increases the total flow that can be sampled. Increasing the sample flow allows sampling trace concentrations for shorter times, which decreases the time that emergency personnel spend in potentially hazardous environments.

The flow rates of individual capillaries were studied for a 40-capillary Carboxen trap with a length of 20 cm. During construction, before the second bundled end was sealed, the flow rate of each capillary was measured to determine the variability in flow rates for individual capillaries. The average flow and related statistics are listed in Table 4.6. As can be seen, the flow rates for the capillaries were very similar. With a flow rate of 150 mL/min through each capillary, a total flow rate of 6 L/min can be easily achieved.

Table 4.6. Average, standard deviation, minimum, maximum and median flow rates measured for a 20 cm 40capillary Carboxen trap.

Avg. flow rate (mL/min)	147.7
Standard deviation (mL/min)	6.6
Minimum flow rate (mL/min)	134.3
Maximum flow rate (mL/min)	162.4
Median flow rate (mL/min)	147.8

One advantage of the open tubular bundle is that it has lower pressure drop compared to packed traps. To demonstrate this, a 20 cm long, 40 capillary Carboxen trap was constructed and compared to a commercially available trap (MINICAMS). Figure 4.16 shows the breakthrough curves for both traps for the same benzene concentration. With the open tubular trap, 6 L/min was achieved through the trap. When the same pressure was used for the packed HayeSepe D MINICAMS trap, only 2 L/min was achieved.

The average breakthrough time for three replicates of the 40 capillary trap was 4.51 ± 0.03 min, and the breakthrough time for the packed HayeSep D trap was 0.44 ± 0.01 min. Although the experiment in Figure 4.16 was not directly comparable (different flow rates, packing material, amount of adsorbent material, etc.), it demonstrates that higher flow rates can be achieved through open tubular traps. If more packing material were used to increase the capacity of the packed trap, this would further increase the pressure drop through the trap.

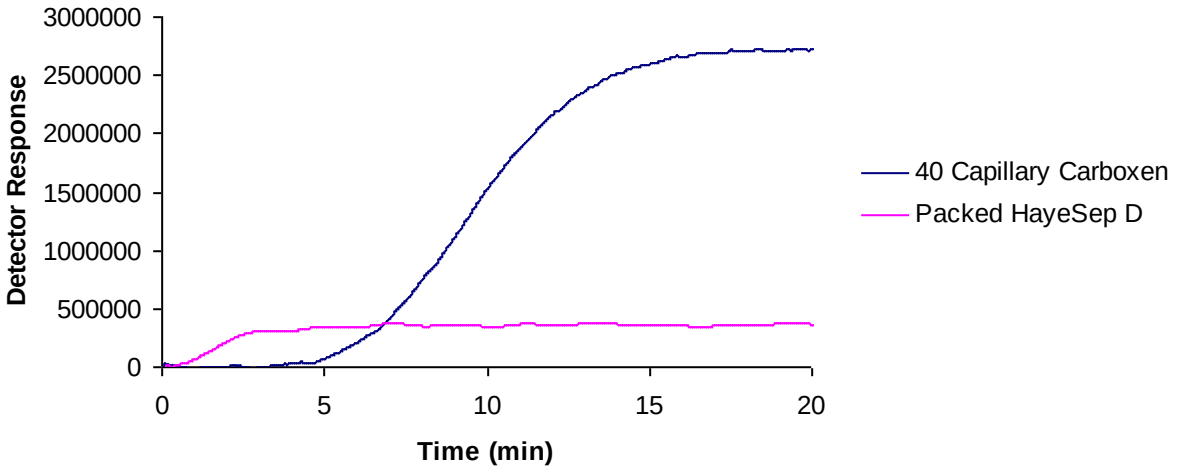

Figure 4.16. Breakthrough plots for a 40 capillary Carboxen trap at a flow rate of 6 L/min and a MINICAMS trap packed with HayeSep D at 2 L/min, benzene concentration of 100 mg/m^3, and temperature of 40°C.

4.3.4 Secondary traps

With high flow rate multi-capillary traps, it becomes necessary to focus the analytes in a smaller trap at lower flow rate before introducing the sample into the GC-MS system. The second trap can be a small packed trap, a single open tubular trap, or a gradient system as described in Chapter 5. Two traps were investigated in this work for use as the second trap: a microtrap and a larger packed trap. Breakthrough occurred almost immediately using the microtrap since it contained very little adsorbent. Despite breakthrough, the microtrap could be used for quantitation. The peak area desorbed from the microtrap increased with the amount introduced and desorbed from the first trap. Figure 4.17 shows the mass recovered from the second trap (detector response was calibrated) as a function of the amount (ng) that was introduced into the first trap. For these experiments, sample was loaded onto a primary trap and desorbed into the microtrap. The first trap consisted of 2 Tenax MINICAMS traps in series. Sample was loaded into the primary trap at a flow rate of 10 mL/min and desorbed at 250°C at a

flow rate of 10.52 mL/min into the microtrap. After allowing 1 min to desorb sample from the first trap, the microtrap was desorbed at a temperature of ~220°C and a flow rate of 1.18 mL/min.

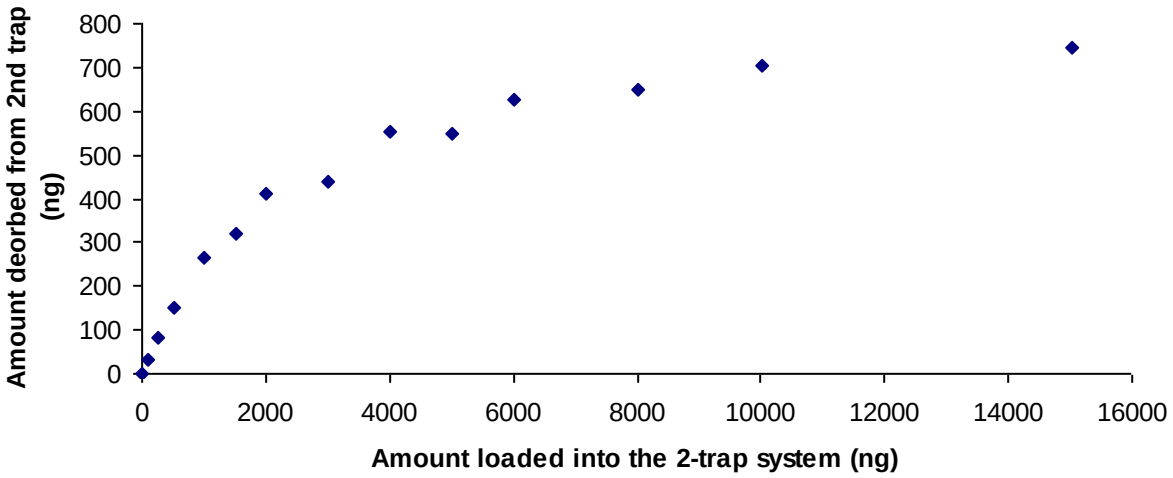

Figure 4.17. Plot of peak area desorbed from a microtrap with respect to the amount of benzene that was loaded onto the primary trap (1 replicate). The first trap consisted of 2 MINICAMS Tenax traps connected in series, which were desorbed simultaneously. The second trap was a Tenax microtrap that was 1 cm in length. The desorption flow from the first trap into the second trap was 10.16 mL/min. The microtrap was desorbed at a flow rate of 1.08 mL/min at a temperature of 220°C.

With this arrangement, the peak area increases until it reaches the capacity of the first trap (~18,000 ng). Since the first trap is then desorbed, the analyte that is introduced into the second trap is a plug, rather than a continuous sample at constant concentration. The larger the amount trapped in the first trap, the larger the plug that is introduced into the second trap. As more sample is introduced into the second trap, more of the analyte favors the stationary phase and, hence, more is retained in the second trap. Essentially, Figure 4.17 is an adsorption isotherm in which the x-axis is essentially the concentration in the mobile phase and the y-axis is the amount of analyte in the stationary phase. As the concentration in the mobile phase increases, this

increases the amount that is adsorbed into the stationary phase. Unfortunately, the capacity of the first trap was exceeded in the experiment represented by Figure 4.17, so the behavior of the microtrap at higher concentration was not determined. Despite this, the results indicate that a microtrap can be used for quantitation. An advantage of the microtrap is that it can be used to limit the amount that is introduced into the detection system. For example, although there were 15 μg loaded into the first trap, the maximum amount that was desorbed from the microtrap was only 744 ng. A microtrap could be optimized to allow no more than 1000-2000 ng to enter the MS, preventing overloading of the system when high concentrations are present.

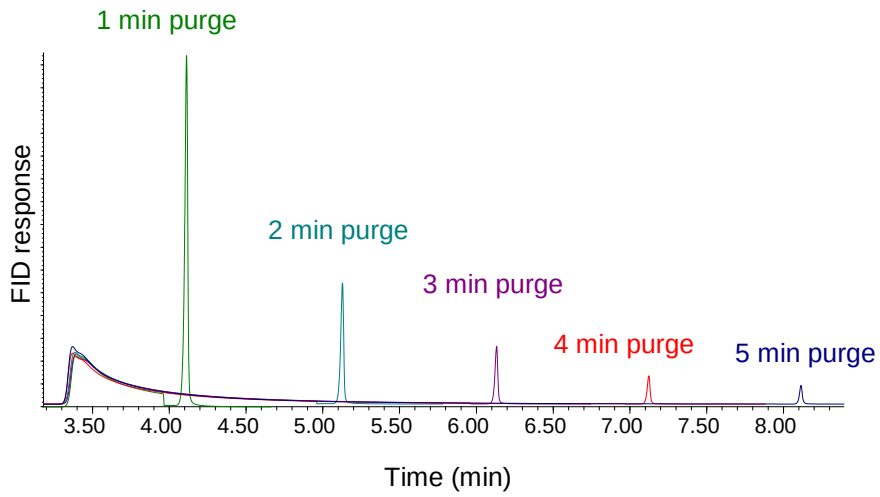

Figure 4.18. Overlayed chromatograms obtained using a microtrap as the second trap for different purge times from the first trap. A mass of 501 ng was introduced into the primary trap for all purge times. The flow rate for loading the sample into the first trap was 10 mL/min. The first trap was desorbed at 250°C at a flow rate of 10.52 mL/min onto trap 2. Trap 2 was desorbed at a flow rate of 1.18 mL/min at 250°C.

Since there is almost immediate breakthrough from the microtrap, the amount of analyte that is desorbed from the microtrap is dependent on the length of time the microtrap is allowed to purge during desorption. Figure 4.18 shows an overlay of several chromatograms for which the same amount of benzene was loaded onto the first trap, and the purge time of the second trap was

changed from 1-5 min. In these experiments, the second trap was plumbed directly to the FID to monitor the breakthrough. The breakthrough can be seen as the first wide peak in Figure 4.18. The area counts of these peaks are shown graphically in Figure 4.19 for 3 replicates at each purge length (error bars are also indicated in the figure). Hence, the amount of analyte that is trapped by the microtrap can also be controlled by the length of the purge time.

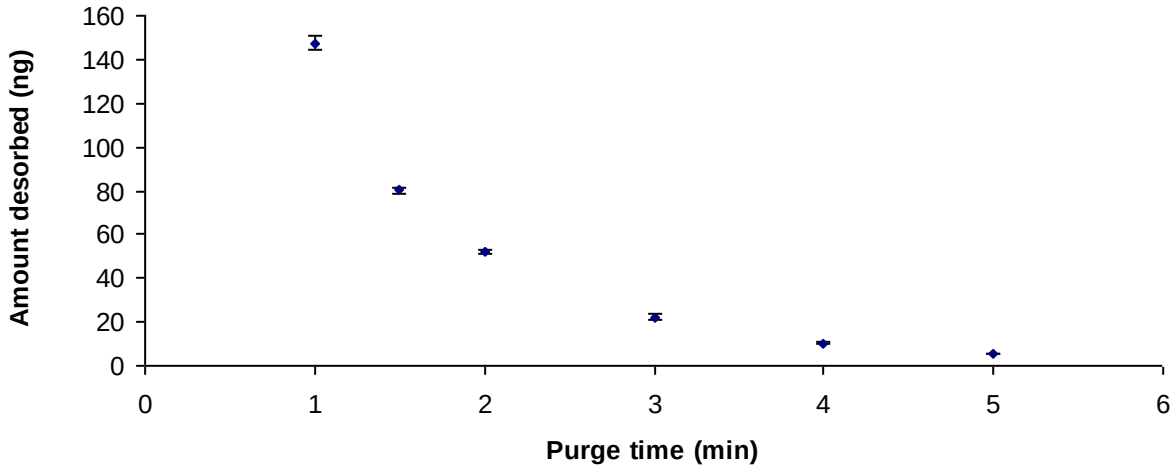

Figure 4.19. Amount (ng) desorbed from the second trap for different purge times (n=3). A mass of 501 ng was introduced into the primary trap for all purge times.

A commercially available trap was investigated for use as a secondary trap for exhaustive sampling. The trap was a Tenax (60/80 mesh) MINICAMS trap. The trap dimensions were 11 mm x 3 mm i.d., and it contained approximately 1.5 cm in length of packing material (20 mg). The capacity of this MINICAMS trap was investigated. Benzene was introduced into the first trap (8 cm long Carboxen trap) and desorbed into the second trap at flow rates of 5, 10, and 15 mL/min. The amount introduced into the 2-trap system was increased until there was an increase in signal before desorbing the secondary trap (the secondary trap was hooked directly to the FID

to allow for detection of breakthrough). Table 4.8 gives the amount of benzene introduced into the 2–trap system at breakthrough. The flow rate at which the first trap is desorbed and the flow rate at which the analytes are trapped in the second trap effect the amount that can be trapped exhaustively on the second trap. Higher amounts are achieved at lower flow rates, however, this also increases the time needed to desorb from the first trap. The flow rate should be considered when optimizing the system.

Table 4.8. Capacity of the MINICAMS Tenax trap for exhaustive secondary trapping for different flow rates.

Desorption flow rate from trap 1 (mL/min)	Amount introduced in the 2-trap system (ng)
5.0	20,240
9.83	5,008
15.0	1,002

4.3.5 High flow rate sampling and focusing

A high flow open tubular trap system was developed from the individual components discussed this far. The system consisted of 2 traps as shown in the schematic in Figure 4.5, where sample at a high flow rate was introduced into a multiple-capillary trap, and desorbed at a lower flow rate and focused in a second trap, and finally desorbed at even a lower flow rate of 1 mL/min for introduction into a GC-MS system. The multi-capillary bundle for these experiments consisted of 24 capillaries of 1 m x 0.53 mm i.d. x 7 μm PDMS. The second trap used was a MINICAMS Tenax trap. Since semi-volatile analytes were tested, all valves and transfer lines were heated to 250°C to prevent condensation. Figure 4.20 shows three replicates of a desorption peak and three replicates of blanks that were obtained using the 2-trap system. MES was introduced into the first trap at a flow rate of 1200 mL/min (50 mL/min through each individual

capillary), desorbed from the first trap at a flow rate of 11.53 mL/min and focused on the second trap. The second trap was then desorbed at a flow rate of 1.3 mL/min.

Desorption from the first trap was long (5 min), which can be reduced by heating the trap faster. Resistance heating wire that would be required to wrap the 1 m trap would be too high to effectively heat the trap rapidly. Because of this limitation, the trap was heated using heat tape, which can heat the trap to the desired temperature, however, it takes up to 3 min to reach the final desorption temperature. This can be overcome in the future by reducing the resistance of the heating wire by wrapping the trap with multiple sections of shorter lengths and connecting the sections in parallel.

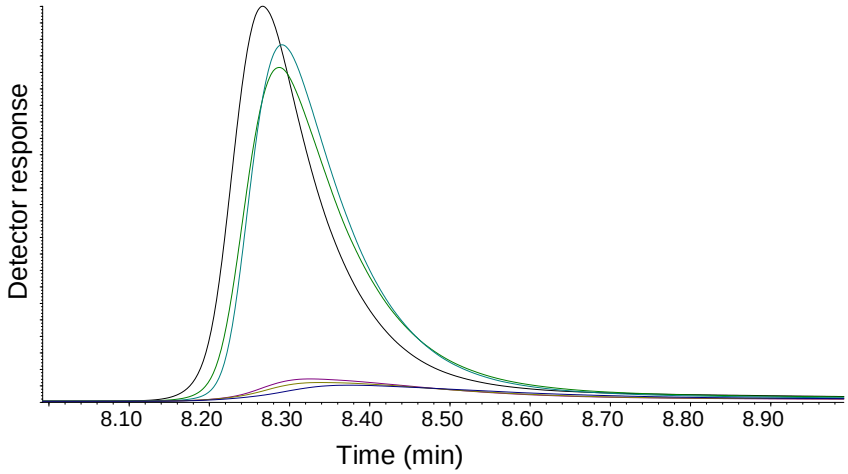

Figure 4.20 Desorption peaks of MES from the high flow open tubular trapping system. A constant concentration of 34 mg/m^3 of MES was introduced through a 24-capillary PDMS trap (1 m x 0.530 mm i.d. x 7 µm d_f) at a flow rate of 1200 mL/min. The MES was desorbed from the multi-capillary trap at a temperature of 200°C for 5 min and focused on a Tenax MINICAMS second trap at a flow of 11.53 mL/min. The second trap was desorbed at 250°C at a flow rate of 1.34 mL/min.

Rather high baselines were observed for the blank runs (Figure 4.20). This could be attributed to bleeding from the stationary phase from the first trap or off-gassing from the high temperature epoxy that was used to bind the capillaries together. Since trapped components from the first trap were focused on the second trap, any bleeding or off-gassing from the first trap would also be concentrated and focused. It is suspected that the stationary phase was damaged during the bundling process, and that the high baseline came from the stationary phase. The high temperature epoxy used had a low off-gas rating. It has been shown in the literature that when using a similar epoxy to glue HPLC particles to a solid support to create SPME coatings, that there was a low background from the epoxy at 250°C.[23]

The average peak width (FWHM) for the three replicates shown in Figure 4.20 was 0.161 min (9.66 s). Peak widths of 1-2 s are desired for introduction into a GC-MS system. The larger peak width can be attributed to dead volume after the second trap. Since the traps had to be placed outside the oven, a long transfer line was needed to connect the second trap to the valve, which was located inside the oven. Another transfer line was needed to connect the valve to the FID. The size of the second trap also had an influence on the width of the band. Smaller traps with less packing material would produce narrower peaks, however, the sample capacity would be compromised. A balance between the sample capacity and the peak width will have to be made when optimizing the system, if exhaustive sampling is desired (no sample loss). Using a microtrap as described above will result in the desired peak widths. The average peak width obtained for the microtrap in the experiments shown in Figure 4.17 was 1.48 s (8.2% RSD). The microtrap will also prevent overloading of the GC-MS system.

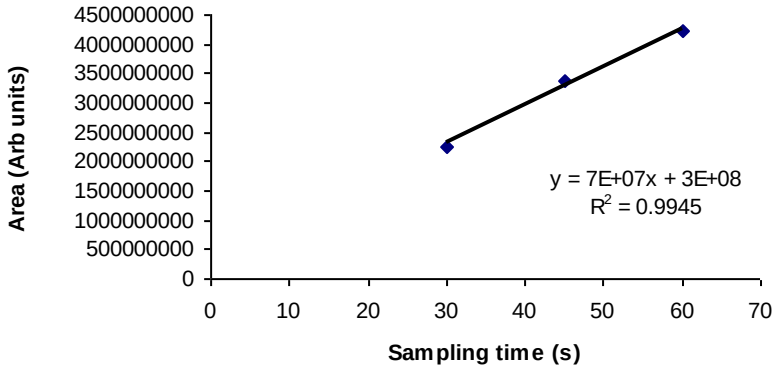

Figure 4.21. Peak area of the focused desorbed peak from the high flow rate trap as a function of sampling time. A constant concentration of 34 mg/m^3 of MES was introduced for 0.5, 1 and 1.5 min through a 24-capillary PDMS trap (1 m x 0.530 mm i.d. x 7 μm d_f) at a flow of 1200 mL/min. MES was desorbed from the multi-capillary trap at a temperature of 200°C for 5 min and focused on a Tenax MINICAMS trap at a flow rate of 11.53 mL/min. The second trap was desorbed at 250°C at a flow rate of 1.34 mL/min.

To further demonstrate the capability of the high flow rate open tubular trap system, peak areas obtained from three different sampling times were compared. The response was linear as shown in Figure 4.21. This demonstrates that analytes can be sampled at high flow rates using a multi-capillary open tubular trap. Total flows can be increased by increasing the number of capillaries in the bundle.

4.4 Conclusions

In this chapter, it was shown that retention on open tubular traps can be improved by increasing the film thickness, surface area, and length. Retention can also be increased by bundling multi-capillaries in parallel. Sol-gel coated open tubular traps showed promise for trapping since they displayed good compound retention considering the small film thickness. However, preparing reproducible traps proved problematic. Thick film PDMS traps also showed good retention capability for trapping, however, the preparation procedure must be perfected to

coat uniform films. The Carboxen PLOT traps demonstrated excellent retention, even for volatile analytes such as benzene. However, these traps exhibited concentration dependency, and detailed characterization is required in order to predict breakthrough times for different parameters. In addition, many Carboxen materials have high water retention at high humidity. Polymer films appear to be beneficial for open tubular traps since they are already well characterized. A commercially available capillary with a 7 μm film thickness was characterized for several different analytes at different flow rates, and temperatures.

Bundling multiple open tubular traps in parallel increases the sampling flow rate. This decreases the time needed for sampling trace analytes in the field. A prototype high flow multi-capillary open tubular trap system was constructed to demonstrate how multi-capillary trap systems can be used at high flow rates, followed by focusing on a secondary trap. Even higher flows could be easily utilized by incorporating a larger number of capillaries in the bundle. Narrow peaks can be realized using a microtrap as the second trap, as long as sample overload is prevented.

4.5 References

1. Camel, V.; Caude, M., Trace Enrichment Methods for the Determination of Organic Pollutants in Ambient Air. *J. Chromatogr. A* **1995,** *710*, 3-19.
2. Grob, K.; Habrich, A., Headspace Gas Analysis: The Role and the Design of Concentration Traps Specifically Suitable for Capillary Gas Chromatography. *J. Chromatogr.* **1985,** *321*, 45-58.
3. Burger, B. V.; Munro, Z., Headspace Gas Analysis. Quantitative Trapping and Thermal Desorption of Volatiles Using Fused-Silica Open Tubular Capillary Traps. *J. Chromatogr.* **1986,** *370*, 449-64.
4. Bicchi, C.; D'Amato, A.; David, F.; Sandra, P., Capturing of Volatiles Emitted by Living Plants by Means of Thick Film Open Tubular Traps. *J. High. Resolut. Chromatogr.* **1989,** *12*, 316-321.
5. Bicchi, C.; D'Amato, A.; David, F.; Sandra, P., Direct Capture of Volatiles Emitted by Living Plants. *Flavour Frag. J.* **1987,** *2*, 49-54.

6. Bicchi, C.; D'Amato, A.; David, F.; Sandra, P., Direct Capture of Volatiles Emitted by Living Plants. Part II. *Flavour Frag. J.* **1988,** *3*, 143-53.
7. Blomberg, S.; Roeraade, J., Preparative Capillary Gas Chromatography. II. Fraction Collection on Traps Coated with a Very Thick Film of Immobilized Stationary Phase. *J. Chromatogr.* **1987,** *394*, 443-53.
8. Gordin, A.; Amirav, A., Snifprobe: New Method and Device for Vapor and Gas Sampling. *J. Chromatogr. A* **2000,** *903*, 155-172.
9. Chong, S. L.; Wang, D.; Hayes, J. D.; Wilhite, B. W.; Malik, A., Sol-Gel Coating Technology for the Preparation of Solid-Phase Microextraction Fibers of Enhanced Thermal Stability. *Anal. Chem.* **1997,** *69*, 3889-3898.
10. Kulkarni, S.; Fang, L.; Alhooshani, K.; Malik, A., Sol-Gel Immobilized Cyano-Polydimethylsiloxane Coating for Capillary Microextraction of Aqueous Trace Analytes Ranging from Polycyclic Aromatic Hydrocarbons to Free Fatty Acids. *J. Chromatogr. A* **2006,** *1124*, 205-216.
11. Shende, C.; Kabir, A.; Townsend, E.; Malik, A., Sol-Gel Poly(Ethylene Glycol) Stationary Phase for High-Resolution Capillary Gas Chromatography. *Anal. Chem.* **2003,** *75*, 3518-3530.
12. Blomberg, S.; Roeraade, J., A Technique for Coating Capillary Columns with a Very Thick Film of Crosslinked Stationary Phase for Gas Chromatography. *HRC & CC* **1988,** *11*, 457-461.
13. Van Dalen, J. P. J., Method for Liquid Flow Control During Dynamic Coating of Open Tubular Columns in Gas Chromatography. *Chromatographia* **1972,** *5*, 354-6.
14. Bielicka-Daszkiewicz, K.; Voelkel, A., Theoretical and Experimental Methods of Determination of the Breakthrough Volume of SPE Sorbents. *Talanta* **2009,** *80*, 614-621.
15. Raymond, A.; Guiochon, G., Use of Graphitized Carbon Black as a Trapping Material for Organic Compounds in Light Gases before a Gas-Chromatographic Analysis. *J. Chromatogr. Sci.* **1975,** *13*, 173-177.
16. Roeraade, J.; Blomberg, S., New Methodologies in Trace Analysisi of Volatile Organic Compounds. *J. High Resolut. Chromatogr.* **1989,** *12*, 138-141.
17. Bartle, K. D.; Woolley, C. L.; Markides, K. E.; Lee, M. L.; Hansen, R. S., Rayleigh Instability of Stationary Phase Films in Capillary Column Chromatography. *HRC & CC* **1987,** *10*, 128-136.
18. Bartle, K. D., Film Thickness of Dynamically Coated Open-Tubular Glass Columns for Gas Chromatography. *Anal. Chem.* **1973,** *45*, 1831-6.
19. Grob, K.; Habich, A., Headspace Gas Analysis: The Role and the Design of Concentration Traps Specifically Suitable for Capillary Gas Chromatography. *J. Chromatogr.* **1985,** *321*, 45-58.
20. Shirey, R. E., SPME Fibers and Selection for Specific Applications. In *Solid Phase Microextraction: A Practical Guide*, Wercinski, S. S., Ed. Marcel Dekker: New York, 1999; pp 59-110.
21. Harper, M., Evaluation of Solid Sorbent Sampling Methods by Breakthrough Volume Studies. *Ann. Occup. Hyg.* **1993,** *37*, 65-88.
22. Gawlowski, J.; Gierczak, T.; Jezo, A.; Niedzielski, J., Adsorption of Water Vapour in the Solid Sorbents Used for the Sampling of Volatile Organic Compounds. *Analyst* **1999,** *124*, 1553-1558.

23. Liu, Y.; Shen, Y.; Lee, M. L., Porous Layer Solid Phase Microextraction Using Silica Bonded Phases. *Anal. Chem.* **1997,** *69,* 190-195.

5 Simultaneous Sampling, Focusing and Separation of a Continuous Sample of Semi-Volatile Organic Compounds in a Negative Temperature Gradient

5.1 Introduction

Typical air sampling analysis often requires the need to focus analytes before injection into an analytical instrument for analysis. Microdevices (microtraps, SPME, etc) and cold traps have been used to produce narrow bandwidths. There have also been reports of analyte focusing and separation on traps that are subjected to a negative temperature gradient. In a negative gradient system, the temperature of the trap varies along the length of the trap. The temperature of the inlet of the trap is at a higher temperature then the outlet. The front end of an analyte peak is at a lower temperature than the rear end of the peak, and as a result it moves slower then the rear end, which focuses the analytes. This focusing effect is important when sampling from a large volume of air. In addition to focusing, analytes can also be separated in a negative temperature gradient. Analytes with different volatilities will refocus at different temperatures. Thus, a trap with a negative temperature gradient has the unique ability to separate and focus analytes while sampling.

Kaiser first reported an apparatus for enrichment of a large sample, based on a packed trap with a negative temperature gradient, which was formed by introducing chilled nitrogen into one end of a sheath around the trap.[1-2] This end was colder than the end where it exited, creating the gradient. Drozd et al. described a method where splitless analysis from large volume gas samples can be focused with a negative temperature gradient on a 0.5 m open tubular trap before GC analysis.[3-4] The authors demonstrated that the technique can be used to focus large syringe

gas samples and also to focus analytes from solid sorbent tubes. More recently, Reglero et al. used a double thermal focusing effect for focusing analytes from headspace analysis.[5] In this study a negative temperature gradient was established opposite of the carrier gas where the front of the peak was decelerated by the temperature gradient. The analytes were then desorbed by applying heat in the direction of the carrier gas that allowed the rear of the peak to be accelerated, allowing for a double focusing effect.

In this chapter, an open tubular trap subjected to a negative temperature gradient is used to sample from a continuous sample stream, where the analytes are able to focus and separate. Two systems are used to generate the negative temperature gradient, and the gradient and method of generating the gradient are described. The gradient system was used to focus and separate analytes from a first trap. By using a negative temperature gradient, it is possible to separate the analytes while focusing and sampling, potentially eliminating the need for a separation step downstream, which would shorten the overall analysis.

5.2 Experimental Section

5.2.1 Construction of thermal gradient devices

Two devices were used to generate negative temperature gradients: one using nitrogen gas with a heat exchanger to cool a portion of the trap, and the second using resistively heated wire to generate the gradient. The first device consisted of a capillary trap inside a low thermal mass electroformed nickel sleeve with 0.024" (0.61 mm) o.d. and 0.017" (0.43 mm) i.d. that was obtained as a gift from VICI (Houston, TX). Current was directed through the nickel sleeve using a variable autotransformer, and the entire trap was heated to the same temperature (~120°C). The nickel sleeve was placed inside a heat exchanger tube, where nitrogen cooling gas

was introduced at the detector end of the tubing and purged toward the inlet end of the trap. This assembly created a negative temperature gradient along the length of the capillary trap from the inlet to the outlet. Figure 5.1 shows a schematic of the device. The construction of the low thermal mass heat exchanger was previously described by Contreras.[6] Briefly, the heat exchanger was constructed by wrapping polyimide tape that was 1/2" wide x 0.0025" thick (McMaster-Carr, Los Angeles, CA) with the nonadhesive side down around a ¼" o.d. tube that served as a template. A second layer of tape was placed over the first with adhesive side down. When approximately 1 m length of polyimide tape was wrapped, it was removed from the ¼" o.d. tubing. A small coiled wire was placed inside the polyimide heat exchanger in order to hold the Ni metal sleeve in the middle of the heat exchanger tubing. The ends of the polyimide tubing were placed in a Swagelok ¼" tee fitting. The tee allowed for the introduction and exit of nitrogen gas while allowing the Ni sleeve to be connected to the inlet and the detector through heated transfer lines. Since the heat exchanger was 1 m in length, it was coiled twice in order to make it easier to handle. To monitor the temperature, three small holes were drilled in the polyimide heat exchanger, and three type K thermocouples (0.005" i.d.) from Omega (Stamford, CT) were inserted through the holes next to the Ni sleeve at the front, middle, and end of the trap. When nitrogen gas was introduced, the temperature of the Ni sleeve closest to the end of the capillary trap cooled down. The nitrogen gas gradually warmed up as it moved through the heat exchanger. Higher flow rates of nitrogen gas could be used to decrease the temperature along the gradient. Liquid nitrogen could also be used to chill the nitrogen gas by placing the tubing carrying the nitrogen gas in a Dewar containing liquid nitrogen. To remove the trapped bands from the temperature gradient, the flow of nitrogen was stopped, and the entire Ni sleeve was allowed to warm up to the initial isotherm temperature. To desorb the bands faster, hot nitrogen

gas was introduced into the heat exchanger at the detector end (the cold nitrogen gas was turned off at the same time as the hot gas was turned on). To heat the nitrogen, a 10" x ¼" o.d. copper tube was packed with aluminum wool and the tube was heated using 1" wide heating tape obtained from Omega. The temperature of the heater was typically set at 350°C.

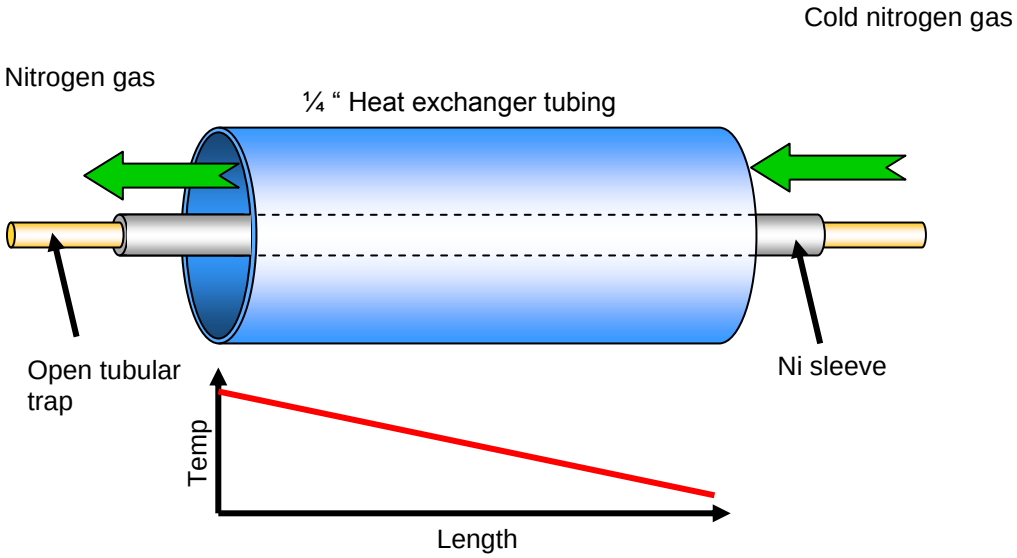

Figure 5.1. Schematic of the first device for generating a negative temperature gradient trap. The trap was heated by applying current along the Ni sleeve. The gradient was formed by introducing nitrogen gas through the heat exchanger tubing.

A second method for generating the negative temperature gradient consisted of inserting the capillary trap through a 1/16" o.d., 0.014" i.d. (0.36 mm) copper tube that was obtained from Special Shapes (Chicago, IL). The tubing was wrapped with double glass silicone insulated resistively heated wire (Nichrome 80, 5 Ω/ft) from Driver-Harris (Harrison, NJ) with gradually changing wrapping density. At the hotter portion of the gradient, the resistively heated wire was wrapped tightly. The spacing between adjacent wrappings was slowly increased along the copper tubing to produce a gradient when current was supplied to the resistively heated wire. Figure

5.2A shows a schematic of this device. To desorb the analytes, another resistively heated wire was wrapped around the copper tubing and the first resistively heated wire as shown in Figure 5.2B. Resistive heating was generally turned off before applying current to the resistively heated desorbing wire. Variable autotransformers were used to control the temperatures of the heated wires for gradient establishment and desorption.

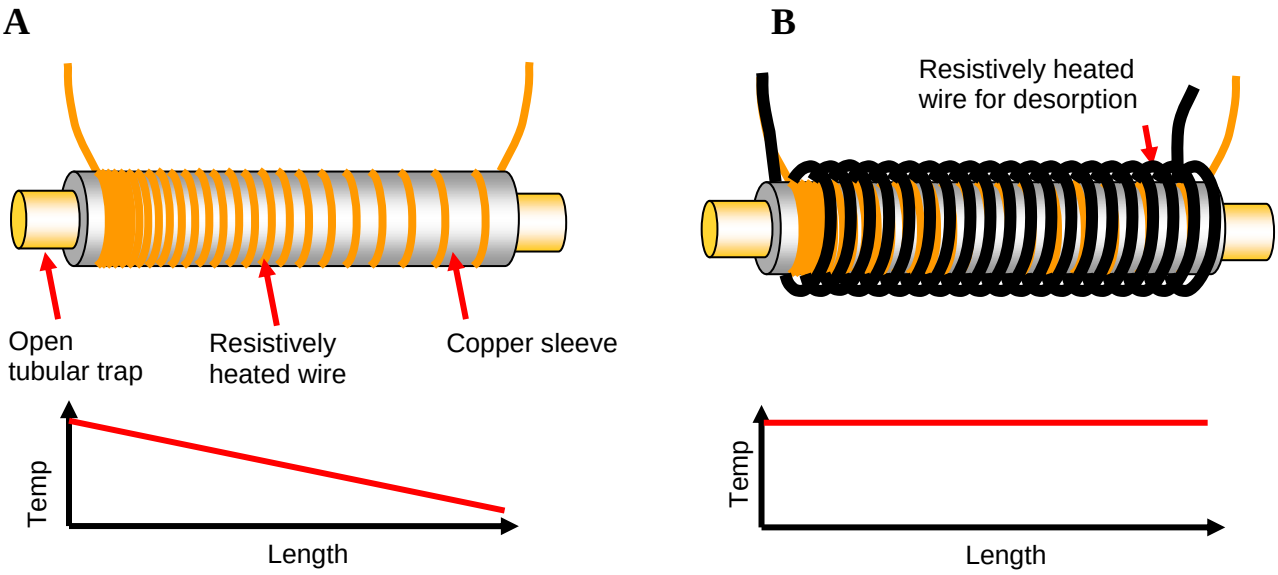

Figure 5.2. Schematics of the second device for generating a negative temperature gradient. (A) General approach for wrapping the heating wire around the copper sleeve, and (B) the uniform outer resistively heated wire used for desorption.

5.2.2 Preparation of sol-gel columns/traps

A sol-gel cyano-propyl polydimethylsiloxane (PDMS) column was prepared for evaluation of the two gradient systems described in this chapter. The procedure for preparation of the sol-gel columns are adapted from the procedures reported by Chong et al.[7] and Kulkarni et

al.[8] Fused silica capillary tubing with 250 μm id. (Polymicro Technologies, Phoenix, AZ) was pretreated by rinsing with 5 mL of methylene chloride, methanol and dionized water in this order. After rinsing, the capillary was purged with nitrogen gas for 5 min at room temperature. Both ends of the capillary were sealed with a flame and placed in an oven at 340°C for 2 h. Then the ends were cut and nitrogen was purged through the column while it was heated from 40°C to 250°C at a temperature program ramp of 5°C/min. The column was held at the maximum temperature for 2 h. After pretreatment of the capillary column, a sol-gel solution was prepared. First, 95 μL of hydroxyl-terminated PDMS (Sigma-Aldrich, St. Louis, MO), 95 μL of 3-cyanopropyltriethoxysilane (Gelest, Morrisville, PA), 30 μL of poly(methylhydrosiloxane) (Sigma-Aldrich), 300 μL of methyltrimethoxysilane (Sigma-Aldrich), and 200 μL of 95% trifluoroacetic acid (5% water) (Sigma-Aldrich) were vortexed in a centrifuge tube and centrifuged at 13,000 rpm for 5 min. The sol-gel solution was then introduced into the pretreated fused silica capillary column by pressure. The end of the capillary was then plugged with a septum and the sol-gel reactive species was allowed to react in the column for 3 h. The excess sol-gel solution was then purged out with nitrogen gas and left to purge for 2 additional hours. The column was then conditioned in a GC oven starting at a temperature of 25°C and ramping up at a rate of 0.2°C/min to 150°C, then from 150°C to 300°C at 1°C/min, and finally holding at 300°C for 2 h.

5.2.3 Sample introduction

To introduce a continuous sample into the trap to be separated and refocused in the negative temperature gradient, an injection port of a GC was used. Small amounts of three analytes (nitrobenzene, naphthalene, and 3-nitrotoluene) were placed in a Swagelok cap (1/4”), the cap was placed in a Swagelok tee, and helium was purged across the top of the sample. The

helium flow was controlled by a regulator. Sample that diffused into the helium stream was fed into a needle containing an on/off valve. The needle was placed directly inside the GC injection port. The thermal gradient trap was connected to the outlet of the GC injection port to receive the constant flow of headspace sample.

5.2.4 Analytical equipment

A 6890 Agilent GC with flame ionization detector was used. The injector port of the GC was used to introduce the sample. The detector was used to detect the analytes. The oven of the GC was not used as the nickel sleeve and resistively heated wires that were independently controlled were used to generate the gradient and desorb the analytes.

5.3 Results and Discussion

The focusing effect of a sample inside a negative temperature gradient was explored. A shallow gradient ranging from a high temperature of 86°C to a cold temperature of 47°C was generated by using the nickel sleeve and heat exchanger apparatus as shown in Figure 5.1. A continuous sample of a mixture of nitrobenzene, naphthalene, and 3-nitrotoluene was fed into the trap for 30 s. The sample was then allowed to focus for 4 different lengths of time, and the results are shown in Figure 5.3. It is clear even in this shallow temperature gradient that analytes become focused and continue to focus for the time they are in the gradient. The retention of the analyte is higher at the front of the peak and, hence, moves at a lower velocity than the rear of the peak, leading to a focused band. This behavior is different than what is experienced in trapping under isothermal conditions, where the longer the analyte is in the trap, the wider the band becomes due to longitudinal diffusion.

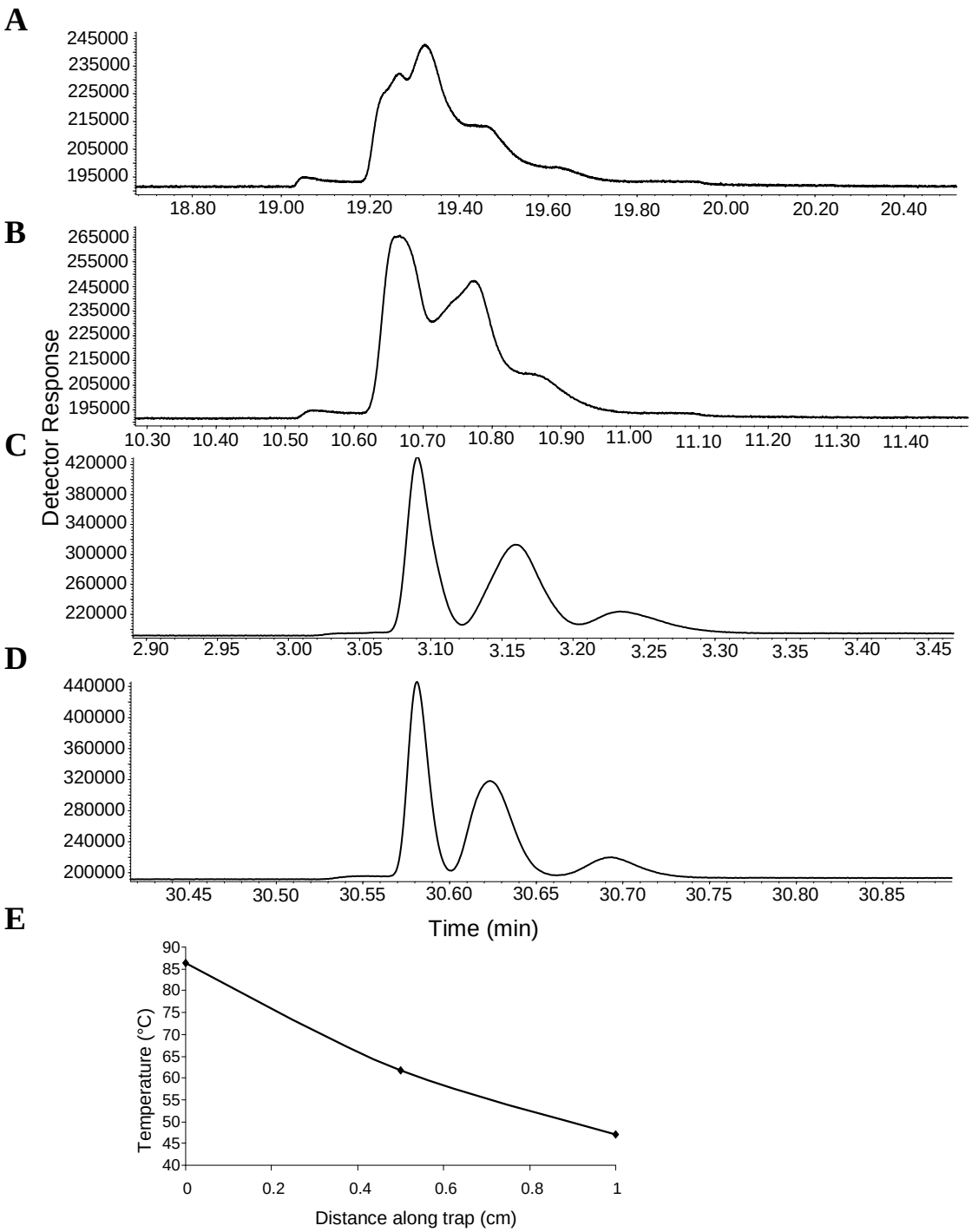

Figure 5.3. Focusing effect of the negative temperature gradient. Analytes that are focused are nitrobenzene, naphthalene, and 3-nitrotoluene. For all chromatograms (A-D), a 1 m x 0.25 mm cyanopropyl-PDMS sol-gel column was used with a flow rate of 1.21 mL/min. A continuous sample was introduced into the gradient for 30 s. The analyte was allowed to focus in the gradient for (A) 30 s, (B) 1 min, (C) 2 min, and (D) 3 min. The gradient used is shown in (E) which ranged from a high temperature of 86°C to a low temperature of 47°C. The desorption temperature was 200°C.

The shape of the negative temperature gradient has an influence on the separation and focusing of the analytes. For example, steep negative temperature gradients tend to focus the analytes more than shallower gradients, due to the higher temperature difference between the front and the rear of the peak. However, the separation power of a steeper gradient is less than that compared to a shallower gradient. Two chromatograms obtained using different gradients generated using the nickel sleeve and heat exchanger apparatus (Figure 5.1) are shown in Figure 5.4. The temperature gradient can be adjusted by controlling the flow and temperature of nitrogen through the heat exchanger tubing. The nitrogen gas can be chilled by placing coiled tubing inside a Dewar containing liquid nitrogen before entering the heat exchanger. Chilling the nitrogen decreases the lower temperature of the gradient. However, the nitrogen gas warms up quickly after being in the heat exchanger tubing and, as a result, a negative temperature gradient with a flat upper gradient that rapidly decreases in temperature is formed. Figure 5.4A shows the separation of the 3 analyte mixture in a temperature gradient ranging from 110°C-27°C that was generated using nitrogen gas at a flow rate of 4 L/min that was chilled with liquid nitrogen prior to entering the negative temperature device.

This separation was compared to another gradient that was established without chilling the nitrogen gas, which produced a shallower temperature gradient as shown in Figure 5.4B. The resolution values between nitrobenzene and naphthalene in Figure 5.4A and 5.4B are 0.91 and 1.31, respectively. The higher resolution of the first two compounds (Figure 5.4B) is a result of the shallower gradient. However, the resolution values for naphthalene and 3-nitrotoluene are 1.01 and 0.89 for Figures 5.4A and 5.4B, respectively. This can be explained by the shape of the gradient. The gradient in Figure 5.4A has a shallow slope at the higher temperature, which decreases rapidly. If analytes are slowed down in this region of the gradient, they are better

resolved than in a steeper gradient. Contreras explained the separation power between two types of gradients: a concave down and concave up. The concave down gradient has a shallower slope at higher temperature, which becomes steeper at lower temperature. In the concave down gradient, the slope is steeper at higher temperature and shallower at lower temperature. Contreras showed that better separation is achieved for heavier compounds in the concave down gradient, and better separation is achieved for more volatile compounds in the concave up gradient.[6] Hence, different negative temperature profiles can lead to different focusing and separation capabilities.

The separation power of the negative temperature gradient is unique compared to traditional focusing techniques (cryotraps and sorbent traps). When analytes are subjected to a negative temperature gradient, they slow down and focus at different locations within the gradient depending on their relative volatilities. Although the separation power may not be higher than traditional gas chromatographic techniques,[6, 9] a gradient can be used to separate analytes while trapping, which shortens the overall analytical method.

A second method was also utilized to generate a negative temperature gradient. By wrapping a copper sleeve with resistive heating wire while gradually increasing the spacing between the loops, a gradient was generated. In this work, a linear gradient was desired and the resistively heated wire was wrapped by hand to generate the gradient. By constructing the gradient in this manner, a wider, linear temperature gradient was established. Figure 5.5 shows a chromatogram and the gradient used to separate and focus the analytes in this gradient. The resolution between nitrotoluene and naphthalene was 1.06 and the resolution between naphthalene and 3-nitrotoluene was 1.28. The linear gradient provided good separation of all three analytes.

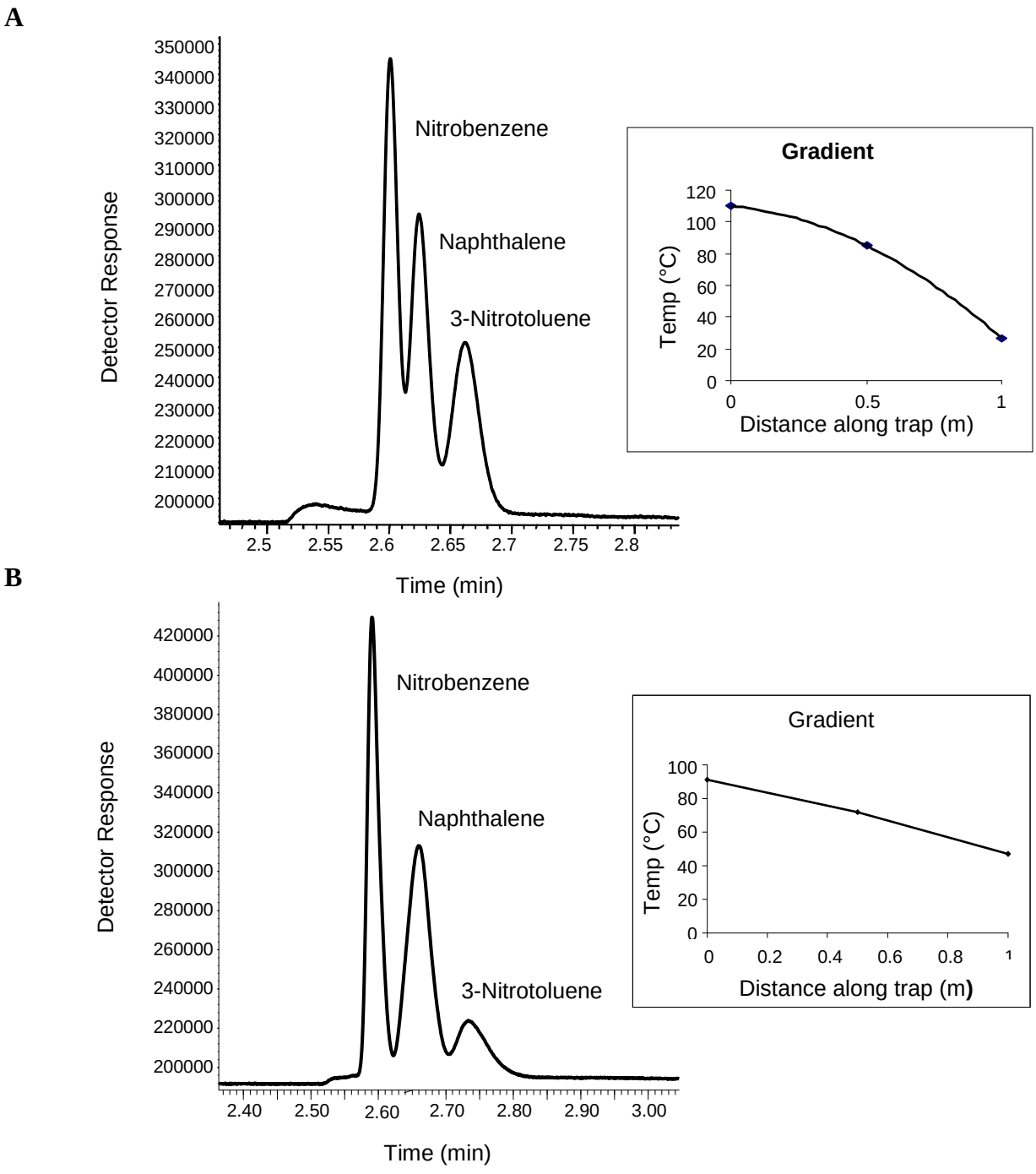

Figure 5.4. (A) Separation and focusing of the 3 analyte mixture using liquid nitrogen to chill nitrogen gas to form the gradient. The gradient ranged form 110°C down to 27°C. (B) Separation of the 3 analyte mixture using nitrogen gas to form the gradient. The highest temperature in the gradient was 91°C and was reduced down to 47°C. For both chromatograms, the sampling time was 30 s, the focusing time was 2 min and the flow was 1.21 mL/min. The trap was a 1 m x 0.25 mm i.d. cyanopropyl-PDMS sol-gel column, and the peaks were desorbed at a temperature of 200°C.

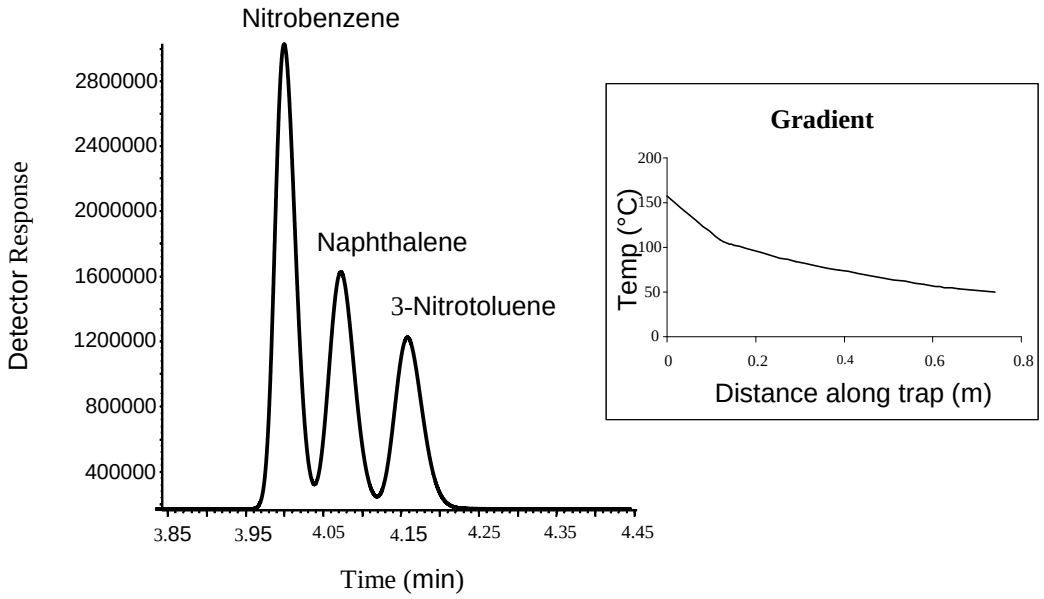

Figure 5.5. Separation and focusing of the 3 analyte mixture using a gradient generated from wrapping resistive heating wire around a copper sleeve. The gradient ranged from 157°C to 53°C. The sampling and focusing times were 30 s and 3 min, respectively. The flow was 1.01 mL/min. The trap was a 1 m x 0.25 mm i.d. cyanopropyl-PDMS sol-gel column, and the peaks were desorbed at a temperature of 160°C.

As can be seen in Figure 5.2B, desorption of the analytes from the gradient involved the use of another resistively heated wire wrapped around the first. The drawback to this setup is it takes longer to desorb the analytes compared to the gradient with the nickel sleeve and heat exchanger, because the desorption wire is not in direct contact with the sleeve. I tried wrapping the resistively heated wire around a low thermal mass nickel sleeve to generate the gradient and desorb the analytes by directly heating the nickel sleeve. However, since the nickel sleeve had low thermal mass, cold spots were generated where the resistively heated wire was wrapped, deteriorating the separation of the analytes. An advantage of the gradient that is formed with the resistively heated wire is that it is simple and requires little equipment. The setup can be easily applied to systems in the field, since all that is needed is a power source to generate the gradient and desorb the trapped compounds.

A

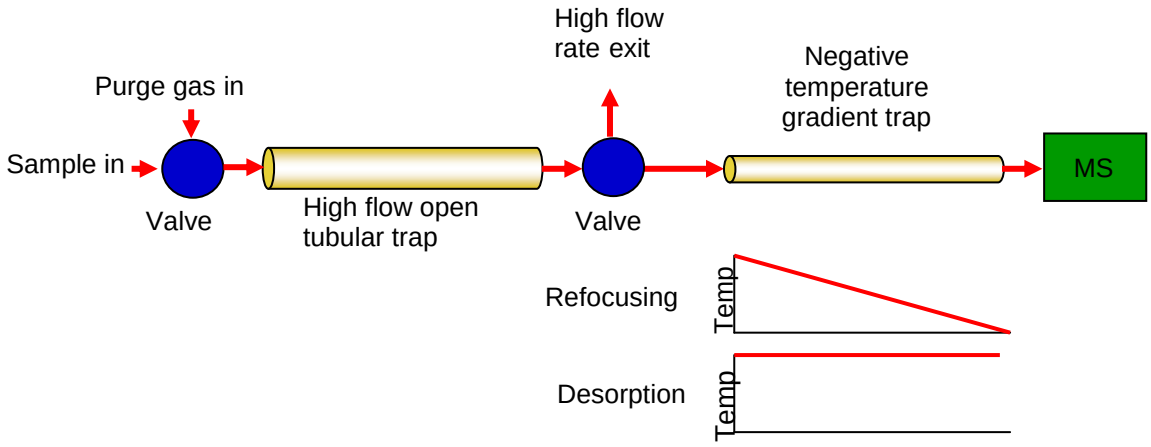

B

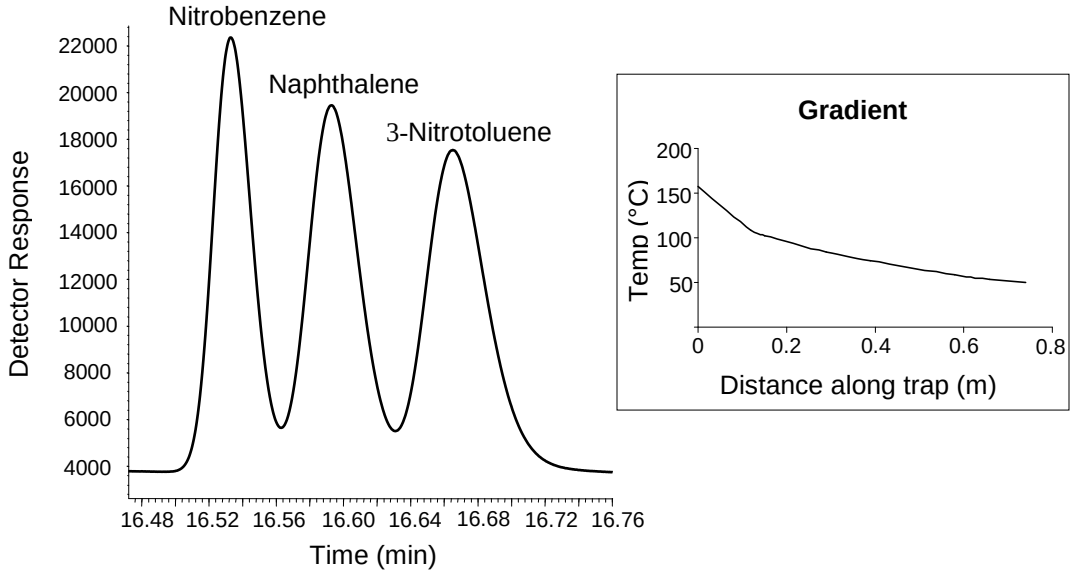

Figure 5.6. (A) Schematic of sampling with a two-trap system. Analytes that are desorbed from the first trap are focused and separated on the second trap in the negative temperature gradient. (B) Chromatogram from sampling from a high flow rate trap and focusing on a second trap with a negative temperature gradient. The high flow rate trap was a sol-gel cyanopropyl-PDMS open tubular trap with dimensions of 1 m x 0.53 mm i.d. Sample was collected and trapped on the first trap for 10 min at a flow rate of 101 mL/min. Analytes were desorbed from first trap, separated and focused in the negative temperature gradient at a flow rate of 1.04 mL/min. The gradient ranged from 157°C and was reduced to 53°C. The focusing time was 5 min. The second trap was 1 m x 0.25 mm i.d. cyanopropyl-PDMS sol-gel column, and the peaks were desorbed at a temperature of 160°C.

A negative temperature gradient can be used as a secondary trap to focus and separate analytes from a high flow rate first trap. Figure 5.6A shows a schematic of a potential 2-trap system, where the first trap can trap analytes at high flow rates. After trapping at high flow rates, the flow is then decreased and directed towards a second trap containing a negative temperature gradient where the analytes are desorbed from the first trap and allowed to focus and separate on the second trap. In this work, a 1 m x 0.530 mm i.d. sol-gel cyanopropyl-PDMS open tubular trap was used as a first trap to accumulate a continuous sample of the 3 analyte mixture for 10 min at a flow rate of 101 mL/min. The flow rate was then decreased to 1.04 mL/min and the analytes were desorbed from the first trap and focused in the second trap, which contained a gradient using the resistively heated wires. The chromatogram obtained is shown in Figure 5.6B. As is observed, the peaks are narrow and well separated, indicating that a negative temperature gradient can be used as a focusing trap and also as a means of separating analytes.

5.4 Conclusions

It was demonstrated in this chapter that a trap subjected to a negative temperature gradient can simultaneously trap, concentrate and focus analytes. The focusing effect can clearly be seen (Figure 5.3) even for shallow temperature gradients. Two different gradient generating devices were constructed to show the focusing effect with slightly different gradient profiles. It was determined that sharp temperature gradients allow for sharper focused peaks compared to shallower gradients, whereas, shallower gradients allow for greater separation between analytes. The device that used resistive heating wire to generate the gradient can be easily applied in the field. Furthermore, it was demonstrated that a negative temperature gradient can be used as a second trap to focus analytes from a first trap. The advantage of using a negative temperature

gradient instead of a common secondary trap (cryotrap or sorbent trap) is that there is separation between analytes with different volatilities. This provides the possibility to separate during trapping, which shorten the overall analysis time by combining the two steps together.

5.5 References

1. Kaiser, R., Reversion Gas Chromatography: A Method for Determination of Traces of Volatile Substances in Gas in the ppb. Range. *Fresenius' Z. Anal. Chem.* **1968,** *236*, 168-170.
2. Kaiser, R. E., Enriching Volatile Compounds by a Temperature Gradient Tube. *Anal. Chem.* **1973,** *45*, 965-967.
3. Drozd, J.; Novak, J.; Rijks, J. A., Quantitative and Qualitative Head-Space Analysis of Parts Per Billion Amounts of Hydrocarbons in Water. A Study of Model Systems by Capillary-Column Gas Chromatography with Splitless Sample Injection. *J. Chromatogr.* **1978,** *158*, 471-482.
4. Rijks, J. A.; Drozd, J.; Novak, J., Versatile All-Glass Splitless Sample-Introduction System for Trace Analysis by Capillary Gas Chromatography. *J. Chromatogr.* **1979,** *186*, 167-181.
5. Reglero, G.; Herraiz, T.; Herraiz, M., Direct Headspace Sampling with on-Column Thermal Focusing in Capillary Gas Chromatography. *J. Chromatogr. Sci.* **1990,** *28*, 221-4.
6. Contreras, J. A. Axial Temperature Gradients in Gas Chromatography. Brigham Young University, Provo, UT 2010.
7. Chong, S. L.; Wang, D.; Hayes, J. D.; Wilhite, B. W.; Malik, A., Sol-Gel Coating Technology for the Preparation of Solid-Phase Microextraction Fibers of Enhanced Thermal Stability. *Anal. Chem.* **1997,** *69*, 3889-3898.
8. Kulkarni, S.; Fang, L.; Alhooshani, K.; Malik, A., Sol-Gel Immobilized Cyano-Polydimethylsiloxane Coating for Capillary Microextraction of Aqueous Trace Analytes Ranging from Polycyclic Aromatic Hydrocarbons to Free Fatty Acids. *J. Chromatogr. A* **2006,** *1124*, 205-216.
9. Blumberg, L. M., Outline of a Theory of Focusing in Linear Chromatography. *Anal. Chem.* **1992,** *64*, 2459-2460.

6 Conclusions and Suggested Work

6.1 Conclusions

In this work, new methods and techniques were developed for fast vapor analysis of VOCs and semi-VOCs for use with portable GC-MS instrumentation. There is an increasing need for portable instrumentation in order to quickly identify and quantitate analytes in the field. The miniaturization of GC-MS is increasing in importance due to its reliability in identifying unknown analytes. The portable GC-toroidal ion trap MS described in this work is a man-portable instrument with dimensions of 47 x 36 x 18 cm and weight of 13 kg (28 lbs). Everything that is needed to operate the instrument is self-contained within these dimensions, including batteries, carrier gas, and data analysis tools. The instrument is simple to use in the field. It only has a 3 min startup time and a 5 min analysis time, which includes time for column cool down. The system has a mass range from 50-442 amu and less than unit mass resolution. The detection limit is 200 pg for methyl salicylate (chemical agent simulant).

Portable instrumentation can also be beneficial for laboratory use when a small footprint is required. The portable MS system (GC removed) was used to identify and quantitate analytes in 5 gas streams from a swatch permeation test system. Swatch testing is performed to determine the amount of analyte that permeates across protective materials that are used to make gloves, boots, masks, suits, etc. The results from swatch testing help determine how long protective equipment is safe when exposed to certain analytes. The system described in this work allows for simultaneous, automated, near-real-time testing of up to 5 swatch samples. The swatches are placed in a temperature controlled swatch test cell fixture where they can be challenged with

either a vapor or liquid challenge. The analyte that permeates through the swatch is swept into a multi-position valve with helium. The valve diverts one sample stream at a time to the MS for analysis. The automated system proved to provide reliable and reproducible data that is compliant with the ASTM F739 method.

It is important to identify vapor hazards, especially if levels are present that can cause immediate danger to life and health. It is often required to detect analytes at trace levels quickly. For example, a concentration of 10 ppt of VX can be harmful. Hence, there is a need to quickly identify trace analytes in air. In this work, open tubular traps were used for high flow trapping of VOCs and Semi-VOCs. Open tubular traps provide less restriction compared to packed traps, which allows for higher flow rates. However, open tubular traps provide low retention, which can be increased by increasing the film thickness and porosity of the trapping film, increasing the length of the trap, and bundling capillaries in parallel. Thick film PDMS open tubular traps showed good retention for semi-VOCs, while a Carboxen open tubular trap showed excellent retention, even for VOCS. Coupling multiple capillaries together allowed for sampling at high flows, while keeping the flow in each individual capillary at a reasonable rate to facilitate trapping. In this work, it was demonstrated that analytes could be trapped at high flow rates, and subsequently re-focused on another trap.

A method using a negative temperature gradient was used to simultaneously focus and separate analytes. In a negative temperature gradient, the analytes are focused because the front of the peak is at a lower temperature than the rear of the peak and, as a result, moves slower, which allows the peak to be focused. Since there is a temperature gradient, analytes with different volatilities will slow down and focus at different temperatures within the gradient. By

using a negative temperature gradient, focusing and separation can occur simultaneously, which can eliminate a separation step downstream, shortening the overall analysis.

6.2 Suggested Work

6.2.1 Swatch permeation testing

In Chapter 3, a swatch permeation test cell fixture was described that provided near-real-time permeation data from multiple samples that is compliant with the ASTM F739 method. Future direction of this project includes satisfying the requirements from the National Fire Protection Association (NFPA) which specifies a flow of 1 L/min of air at 80% relative humidity underneath the swatch. In the current system, helium at a flow of 14 mL/min was used to sweep the bottom of the swatch. Additional improvements should also be made to the system to improve performance. These improvements are illustrated in Figure 6.1. Since the MS signals were not as stable as desired at high concentrations, an FID should be used for quantitation. FIDs are robust and have a wide linear range, which would facilitate the quantitation of analytes over several orders of magnitude. MS detection should still be used for identification of degradation products and/or interferences.

For more precise flow control, the sweeping gas for all sample streams should be independently controlled. In the system described in Chapter 3, the flow was regulated before splitting to the five sample streams. The five sample streams were fed into a multi-position valve with one selection stream and a common outlet for all other streams. Hence, the flow of a single stream could not be measured unless that stream was selected by the multi-position valve. To ensure flow control, modifications should also include a multi-position valve with throughput for each port (each port has a waste). Carryover for the more persistent TICs could be eliminated

using a higher purge flow through the sample. If the FID is used as the main detection system, total purge flows up to 50 mL/min could be used. Increasing the temperature for the valves and transfer line would also help eliminate carryover. This could be accomplished by placing the components in an oven.

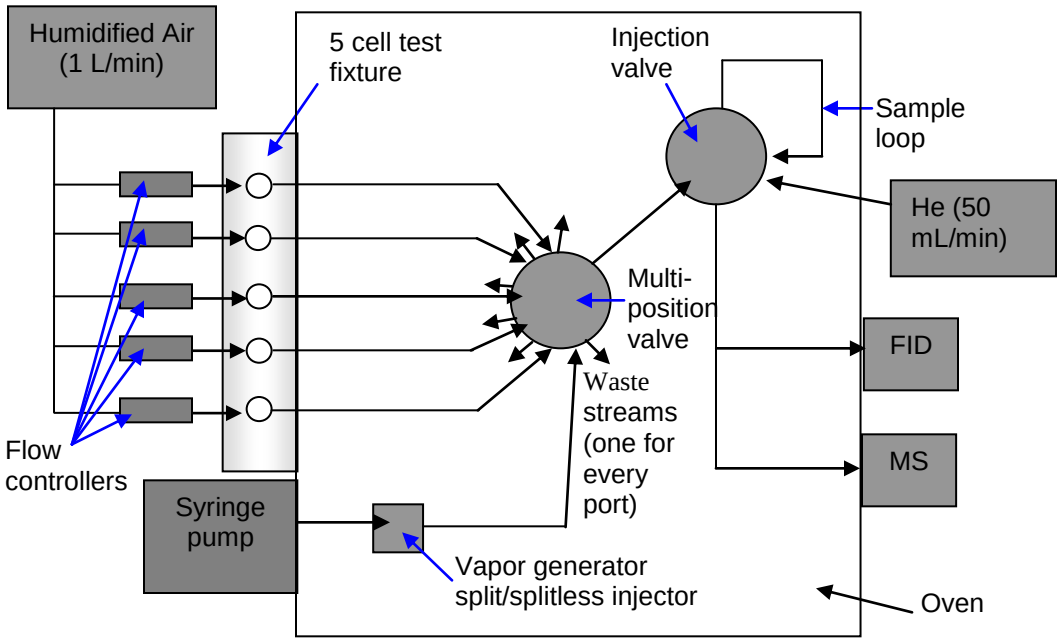

Figure 6.1. Block diagram of permeation testing system with modifications.

6.2.2 Water sorption in open tubular traps

In Chapter 4, it was demonstrated that high flow sampling can be accomplished using multi-capillary open tubular traps. However, no detailed analysis of the effects of water vapor from high humidity samples was performed. Future work should include characterizing the sorption of water from high humidity samples. A thermal conductivity detector (TCD) could be used to detect water that is sorbed in traps. If it became evident that water sorption is

problematic, then several steps could be taken to reduce the amount of water that is transferred to the GC-MS system. This includes using a dry purge prior to desorption,[1] slightly heating the trap during a dry purge,[2-4] or using a drying trap, such as anhydrous lithium chloride upstream from the high flow trap.[5] An FID could be used to determine if there is any loss of VOCs during purge cycles.

6.2.3 Multi-phase open tubular traps

In Chapter 4, it was determined that using a thick film PDMS open tubular trap provided good retention for semi-VOCs, however, fast breakthrough times occurred for VOCs. Carboxen open tubular traps showed excellent retention of all compounds; however, long desorption times were needed to desorb semi-VOCs. A multi-phase capillary trap, similar to the multi-bed packed sorbent tubes, could be made using different phases. Figure 6.2A shows a schematic of a single capillary containing a PDMS phase and Carboxen phase in series. Semi-VOCs would be trapped on the PDMS, and VOCs that breakthrough the PDMS film would be trapped on the Carboxen phase. Figure 6.2B shows a multi-capillary system containing two phases. The direction of the flow for trapping and desorption is also indicated in the figure. Back-flushing the trap would prevent the semi-VOCs from adsorbing onto the Carboxen layer.

Constructing the multi-capillary two-phase system would require coupling two bundled traps with different phases. The method used to prepare the multi-capillary bundle included sealing the ends inside a small ¼" tube. To prepare a bundle with two phases, two multi-capillary traps could be coupled together using one ¼" o.d. tube.

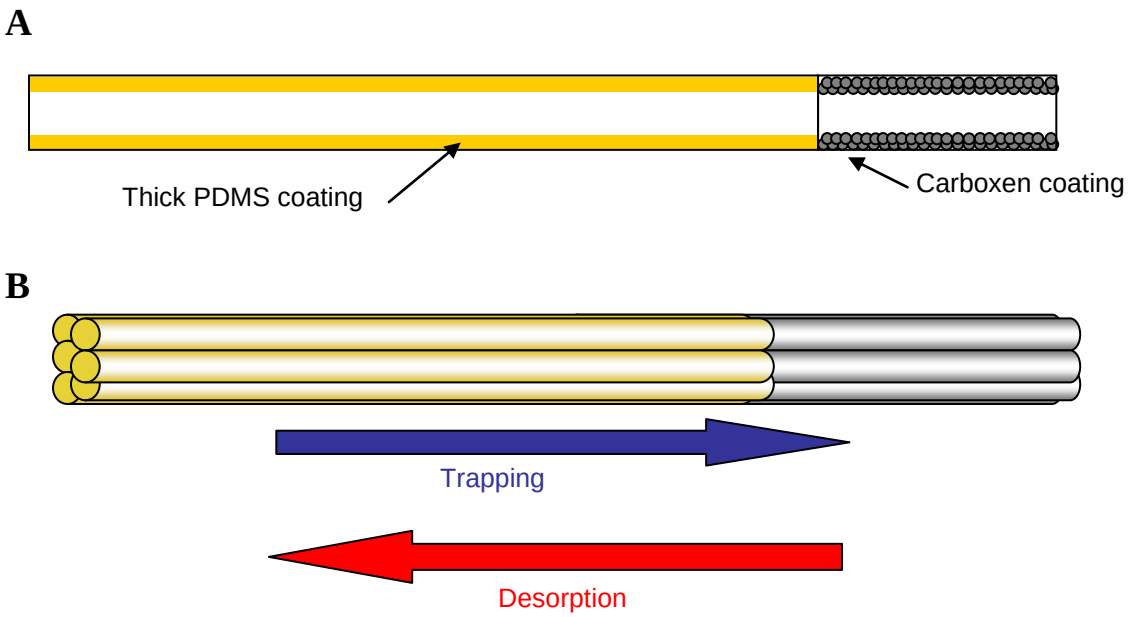

Figure 6.2. (A) Single two-phase open tubular trap consisting of thick film PDMS and Carboxen sections in series. (B) Multicapillary bundle consisting of two phases. The direction of flow is reversed when desorbing.

6.2.4 Interfacing high flow open tubular air sampling to portable GC-MS

The high flow open tubular traps must be coupled to the portable GC-MS system described in Chapter 2 in order to perform fast air sampling in the field. Figure 6.3 shows a schematic of the high flow rate sampling and desorption process. The high flow sampling system could be separated from the GC-MS system (Figure 6.3A) to provide the flexibility of sampling at different locations from where the analysis would be performed. However, after sampling, the first trap would need to be coupled to a second microtrap located at the inlet to the GC to allow the analytes to re-focus before being introduced into the GC-MS system (Figure 6.3B).

Figure 6.4 shows a proposed method to couple the high flow sampling and re-focusing devices to the portable GC-MS. Figure 6.4A shows a sampling module that contains a sample

pump to draw air into the trap at high flow rates. The module also contains a purge gas cartridge that can be used for desorption from the high flow trap. The purge gas could also be supplied by the carrier gas supply for the GC-MS system, but would decrease the number of analyses that would be performed using a single helium cartridge. The sampling module could then be coupled to a focusing module mounted on the GC-MS system (Figure 6.4B). The purge gas would enter the high flow trap to desorb and back-flush the analytes into the focusing trap. The high flow trap could be desorbed at moderately high flow since a vent would be placed after the focusing trap. The analytes would then be desorbed from the focusing trap and into the GC-MS system through the injection port using carrier gas.

A

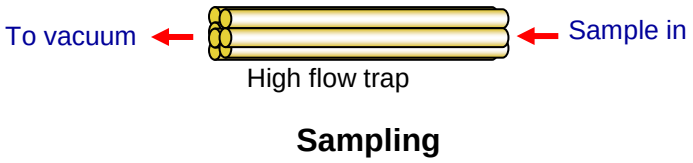

B

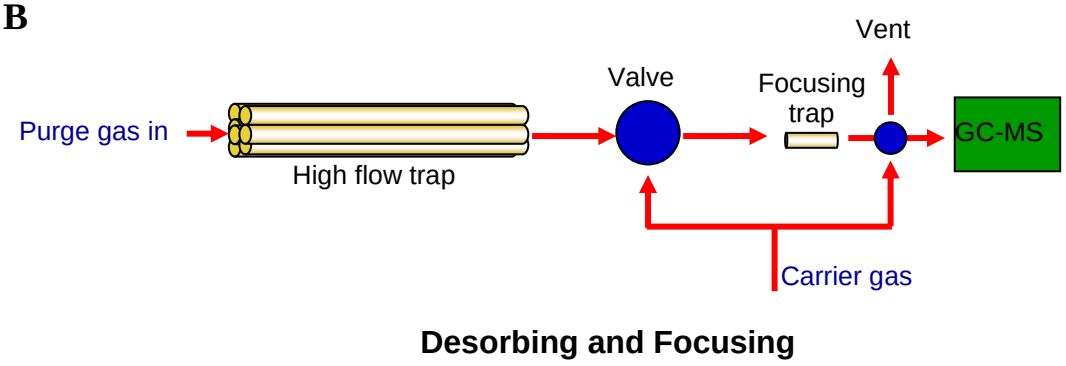

Figure 6.3. Schematic of trapping at high flows in the field with portable GC-MS instrumentation. (A) Sampling at high flows is separate from the GC-MS system. (B) Schematic of desorption, focusing, and injection into the GC-MS system.

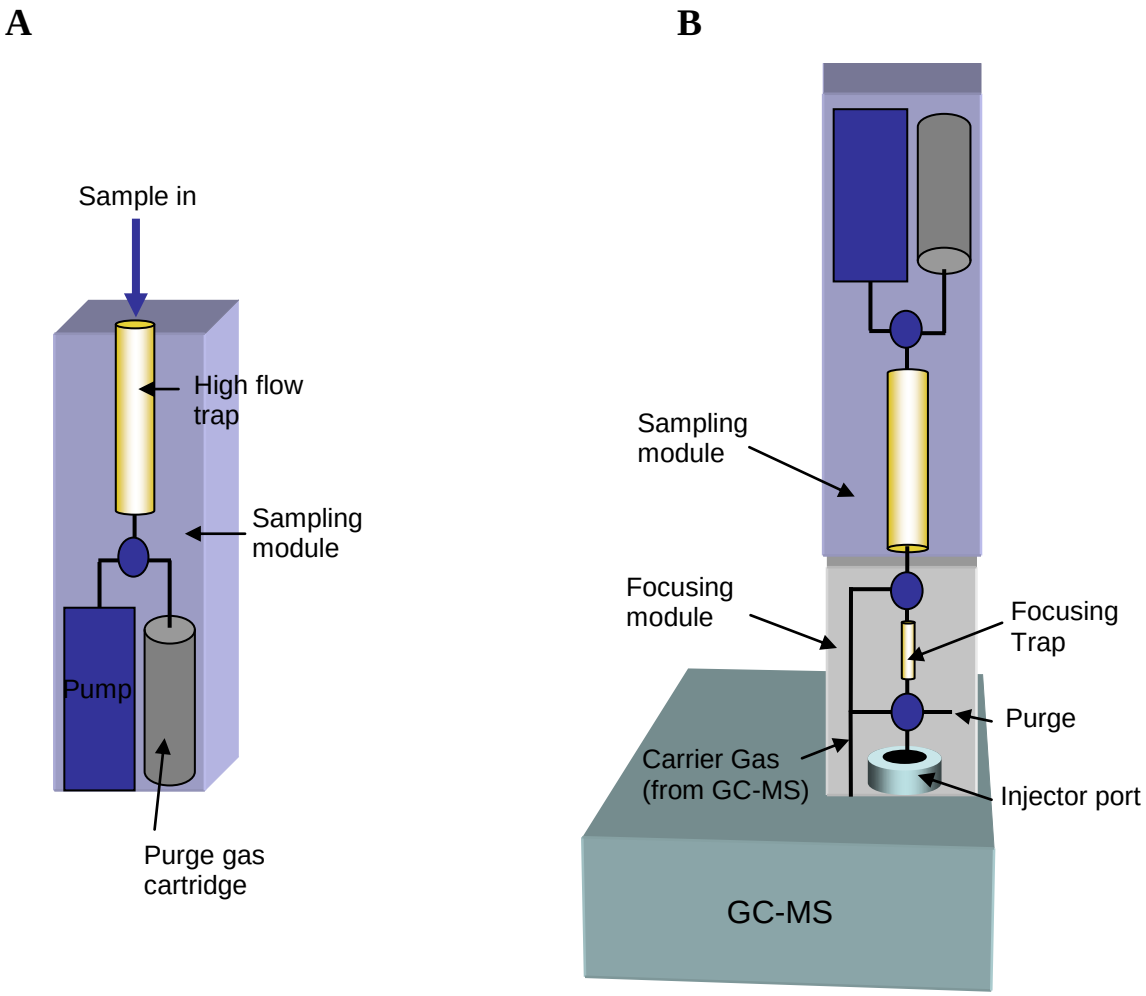

]Figure 6.4. (A) Schematic of a proposed sampling module consisting of a high flow trap, pump and purge gas supply for desorption. The sampling module could be removed from the GC-MS system during sampling. The pump would draw air at high flow rate into the trap where analytes are concentrated. (B) Schematic of the coupling of the sampling module, focusing module, and GC-MS system. The analytes would be desorbed from the high flow trap into the focusing trap using the purge gas supply that is in the sampling module. The focusing trap would then be desorbed, injecting a sharp band into the GC-MS system for subsequent analysis.

6.2.5 On-line sampling using a negative temperature gradient

In Chapter 5, a trap that was subjected to a negative temperature gradient was utilized in order to focus and separate analytes simultaneously. Since separation and focusing occurs at the

same time, this technique could be used for continuous on-line air sampling applications, eliminating the separation step. This would shorten the overall analysis time. The gradient could be prepared using resistively heated wire as discussed in Chapter 5, which would permit an easy transition of the gradient system to the field.

Different temperature gradient profiles lead to different focusing and separation possibilities, as demonstrated in Chapter 5 and in more detail by Contreras.[6] As a result, a custom gradient could be constructed to selectively focus and concentrate a particular analyte. Figure 6.5 demonstrates this concept. In this example, the middle peak is the analyte of interest, which is separated from the other peaks in a less steep section of the gradient. No additional separation step would be needed. Thus, fast on-line vapor analysis for selected analytes could be performed.

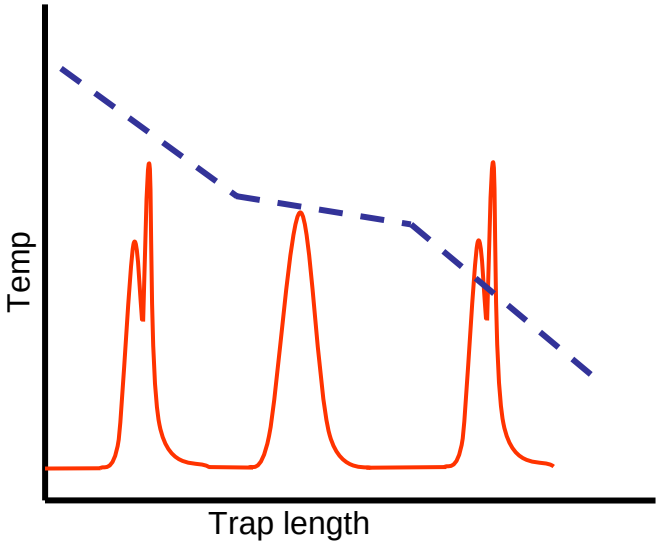

Figure 6.5. Schematic of a custom temperature gradient which could selectively separate and focus a specific analyte.

6.3 References

1. Gawlowski, J.; Gierczak, T.; Pietruszynska, E.; Gawrys, M.; Niedzielski, J., Dry Purge for the Removal of Water from the Solid Sorbents Used to Sample Volatile Organic Compounds from the Atmospheric Air. *Analyst* **2000,** *125*, 2112-2117.
2. Helmig, D.; Vierling, L., Water-Adsorption Capacity of the Solid Adsorbents Tenax-TA, Tenax-GR, Carbotrap, Carbotrap-C, Carbosieve-SIII, and Carboxen-569 and Water Management-Techniques for the Atmospheric Sampling of Volatile Organic Trace Gases. *Anal. Chem.* **1995,** *67*, 4380-4386.
3. Woolfenden, E., Monitoring Vocs in Air Using Sorbent Tubes Followed by Thermal Desorption-Capillary GC Analysis: Summary of Data and Practical Guidelines. *J. Air Waste Manage. Assoc.* **1997,** *47*, 20-36.
4. Gawrys, M.; Fastyn, P.; Gawlowski, J.; Gierczak, T.; Niedzielski, J., Prevention of Water Vapour Adsorption by Carbon Molecular Sieves in Sampling Humid Gases. *J. Chromatogr. A* **2001,** *933*, 107-116.
5. Pettersson, J.; Roeraade, J., Method for Analysis of Polar Volatile Trace Components in Aqueous Samples by Gas Chromatography. *Anal. Chem.* **2005,** *77*, 3365-3371.
6. Contreras, J. A. Axial Temperature Gradients in Gas Chromatography. Brigham Young University, Provo,UT 2010.